Geostatistical Modelling of Zarghat Magnesite Deposit, Saudi Arabia

by

Mohammad Houssain Makkawi

A Thesis Presented to the

FACULTY OF THE COLLEGE OF GRADUATE STUDIES

KING FAHD UNIVERSITY OF PETROLEUM & MINERALS

DHAHRAN, SAUDI ARABIA

In Partial Fulfillment of the
Requirements for the Degree of

MASTER OF SCIENCE

In

EARTH SCIENCES

August, 1991

Order Number 1354092

Geostatistical modelling of Zarghat magnesite deposit, Saudi Arabia

Makkawi, Mohammad Houssain, M.S.

King Fahd University of Petroleum and Minerals (Saudi Arabia), 1991

U·M·I
300 N. Zeeb Rd.
Ann Arbor, MI 48106

GEOSTATISTICAL MODELLING
OF
ZARGHAT MAGNESITE DEPOSIT
SAUDI ARABIA

BY

MOHAMMAD HOUSSAIN MAKKAWI

A Thesis Presented to the

FACULTY OF THE COLLEGE OF GRADUATE STUDIES

KING FAHD UNIVERSITY OF PETROLEUM & MINERALS

DHAHRAN, SAUDI ARABIA

In Partial Fulfillment of the
Requirements for the Degree of

MASTER OF SCIENCE
In

EARTH SCIENCES

August 1991

KING FAHD

UNIVERSITY OF PETROLEUM AND MINERALS

DHAHRAN, SAUDI ARABIA

College of Graduate Studies

This thesis, written by Mr. Mohammad Houssain Makkawi under the direction of his Thesis Committee, and approved by all its members, has been presented to and accepted by the Dean, College of Graduate Studies, in partial fulfillment of the requirements for the degree of Master of Science in Earth Sciences.

Dean, College of Graduate Studies

Date: 5-8-91

4/8/91

Department Chairman
Dr. Abdul-Wahab Abokhudair

Thesis Committee

30.07.1991

Chairman, Dr. Ali Sahin

1/8/1991

Member, Dr. Saiful-Islam Saif

30/7/91

Member, Dr. Munir Ahmad

This thesis is dedicated to my beloved father, mother and wife.

ACKNOWLEDGEMENT

I would like to express my deep thanks and appreciation to Dr. Ali Sahin, my thesis supervisor, for his valuable advices and constructive discussions throughout all phases of this research, critical reading and correcting of the manuscript as well as following up the research plan.

Special thanks are also due to Dr. Saiful-Islam Saif (Earth Sciences Department) and Prof. Munir Ahmad (Mathematics Department), my thesis committee members, for their critical reading of the manuscript and valuable suggestions. I, also, wish to thank both Dr. Mustafa Al-Ukayli and Dr. Abdul-Wahab Abo-Khudair the former and current chairmen of the Department of Earth Science for their moral support, continuous encouragement and providing the necessary research facilities.

A word of appreciation is due to Prof. Z. R. El-Naggar, who suggested this field of study, for his helpful support. A special word of thanks is extended for both Mr. M. Al-Ahmadi and Mr. A. Rameezuldeen (King Abdul-Aziz University) for providing the basic data used in the research.

Thanks are also recorded here to Mr. Ali Abdul-Latif and Mr. Amin R. Ghaleb who helped me during the computation stages of this work. My thanks are also due to Mr. Ahmad Al-Shaikh, Mr. Mutlaq Al-Mutlaq and Mr. Abdul Wahab Zaki for their help in plotting geologic maps using computer intergraph system.

My great appreciation is due to my two colleagues: Mr. Mustafa Hariri, who helped me during data-feeding stage, and Mr. Walid Abdul-Ghani, who provided me with some important references. My thanks are also recorded here to Mr. Amin Desai, of the Research Institute, for typing the manuscript and to my family for their moral support throughout all phases of this work.

Finally, acknowledgement is due to King Fahd University of Petroleum and Minerals for providing academic, computing and research facilities without which this work would be next to impossible.

TABLE OF CONTENTS

LIST OF TABLES

LIST OF FIGURES

LIST OF APPENDICES

بسم الله الرحمن الرحيم

النموذج الجيوإحصائي لمترسب الماجنيزيت في منطقة زرغط بالمملكة العربية السعودية

خلاصـــة الرسالـــة

يوجد مـترسب الماجنيـزيت في منطقـة زرغط الواقـعـة في الجـزء الشمالي الغربي من الدرع العربي مكونا الجزء العلوي من "مجموعة الجبالة" التي تمثل احدث صخور الدرع العربي .

وقـد دلت نتـائج التـحليل الإحصائي لنسب التركيز المئوية لكل من متغيري أكسيد الماغنسيوم وأكسيد الكالسيوم – والتي جمعت من ٥١ بئرا حفرت في التل الرئيسي من المترسب – على ان هذه النسب موزعة توزيعا لوغاريثميا ، لذلك أقترح إستخدام لوغاريثماتها للحصول على أفضل التقديرات .

وقد صممـــت نماذج كروية مركبة لتتـطابق مـع دوال التبـاين البيانيـــة (السيميفاريوجرام) للوغاريثمات المتغيرين . وقد تم تحديد التقديرات المحلية اللوغاريثمية مع معدلات إنحرافها المعياري لكتل أكسيد الماغنسيوم بتقسيم المترسب الى مكعبات ذات أبعاد ٢٥م × ٢٥م × ١م بإستخدام طريقة كريجنج . وكنتيجة لإستخدام هذه الطريقة وُجد ان معدلات الإنحراف المعياري منخفضة بشكل عام مما يؤكد صحة التقديرات . وتم رسم العلاقة بين لوغاريثم درجة تركيز أكسيد الماغنسيوم وكميته بإستخدام التقديرات المحلية لكتله ووجد أن مخزونه هو حوالي ٢ر٣ مليون طن.

ونظرا للعلاقة القوية بين المتغيرين ، تم إستخدام طريقة التقدير المشتـرك (كوكريجنج) لإيجاد قيم بعض العينات ووجد بأن هذه الطريقة تعطي نتائج أفضل من نتائج طريقة التقدير العادية.

ABSTRACT

Zarghat magnesite deposit, located in the northeastern part of the Arabian Shield, occurs in the upper part of Jibalah Group, the youngest rocks of the Shield.

The sampling distributions of CaO% and MgO% values, derived from 51 vertical drill-holes located in the Central Hill deposit, are characterized by lognormal behavior suggesting that more accurate evaluation can be achieved using logarithmic values.

Th compound spherical models have appropriately fitted to the experimental semivariogram of both CaO% and MgO% logarithmic values. The kriged estimates and the corresponding relative kriging standard deviations of the logarithms of MgO% were determined for blocks of 25m x 25m x 1m dimensions. The relative kriging standard deviations are generally lower, implying the reliability of kriged estimates. The grade-tonnage relationship, based on kriged estimates, indicates the existence of 3.2 million tonnes.

Finally, considering strong linear correlation between CaO% and MgO%, point co-kriging was used to estimate known sample values. The results indicate that co-kriging produces better estimate than kriging.

CHAPTER 1

INTRODUCTION

1.1 General information

Zarghat area is located at about 250 km NE of Al-Madina in the northern part of the Arabian Shield. It is easily accessible by road from Al-Madina or Hail as it lies close to Al-Madina/Hail highway (Figure 1.1). The magnesite deposit in the area is located at about 5 km from Zarghat village in the South-east direction, with 26°30`N latitude and 40°35`E longitude as shown in Figure 1.2.

The deposit is found in the form of three small hills referred to as the Central Hill, East-southeast Hill and West-northwest Hill. Besides these hills, a minor occurrence in the form of a lens has also been reported in the South (Figure 1.3).

The Central Hill is the largest among all occurrences and contains about 3 million tons of magnesite with a grade ranging from 38% to 48% MgO (Brosset, 1976). Most of the magnesite in the Central Hill is considered to be of good quality with a typical white color. A recent study by Celik (1990) has indicated that the benefication of the ore from the Central Hill by calcination yields a concentration with high MgO (>99%) and low silica contents (less than 1%). These results are encouraging and may provide enough motivation for the mining companies to exploit the deposit in the future.

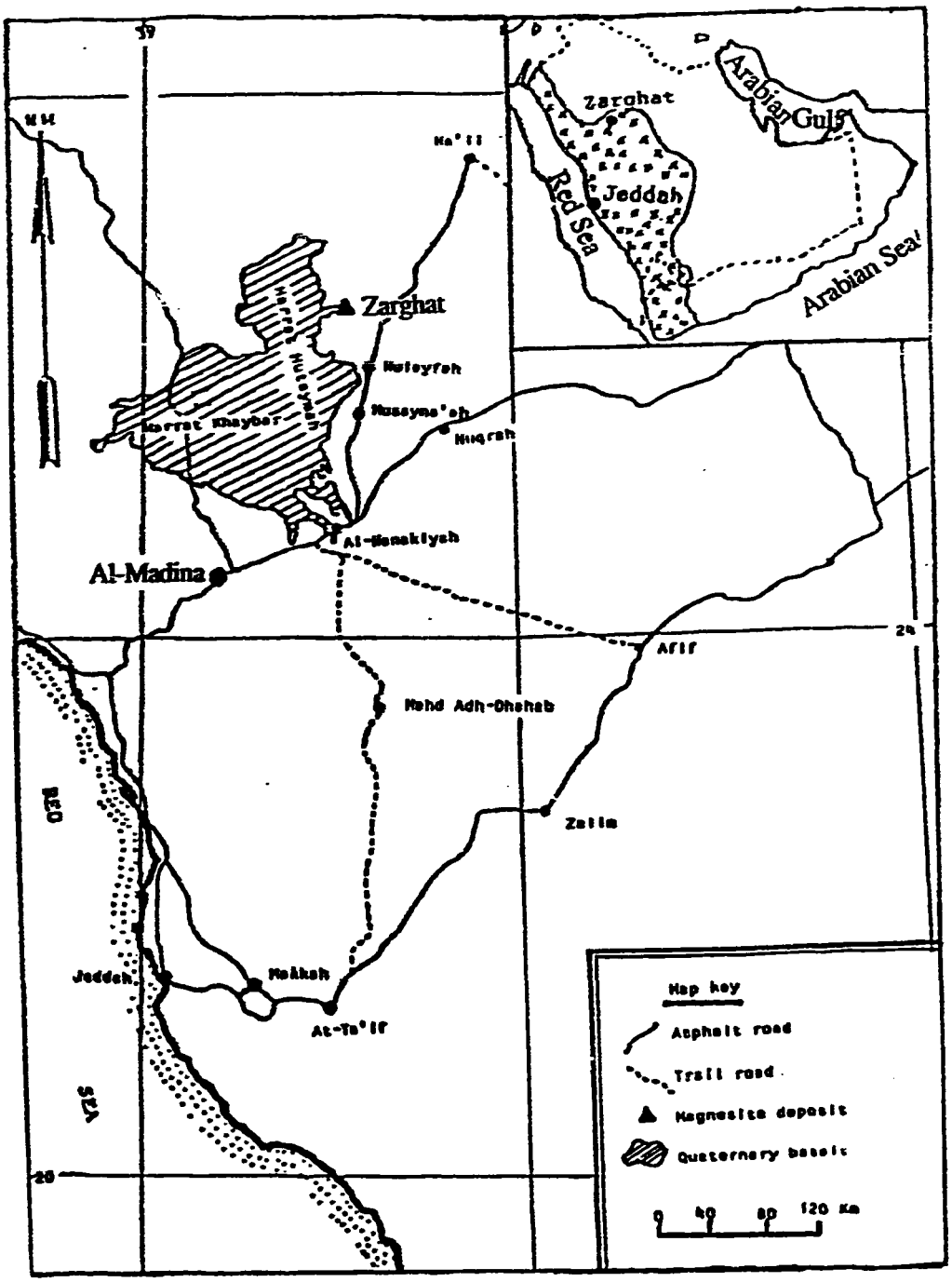

Fig. 1.1. Location map of Zarghat area (After Brosset, 1970)

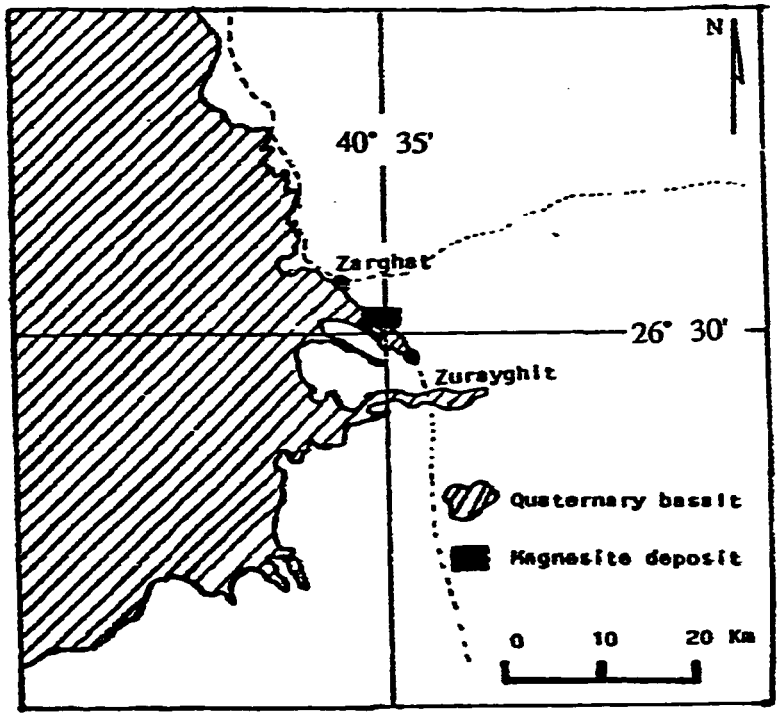

Fig. 1.2: Location map of the deposit (After Brosset, 1978)

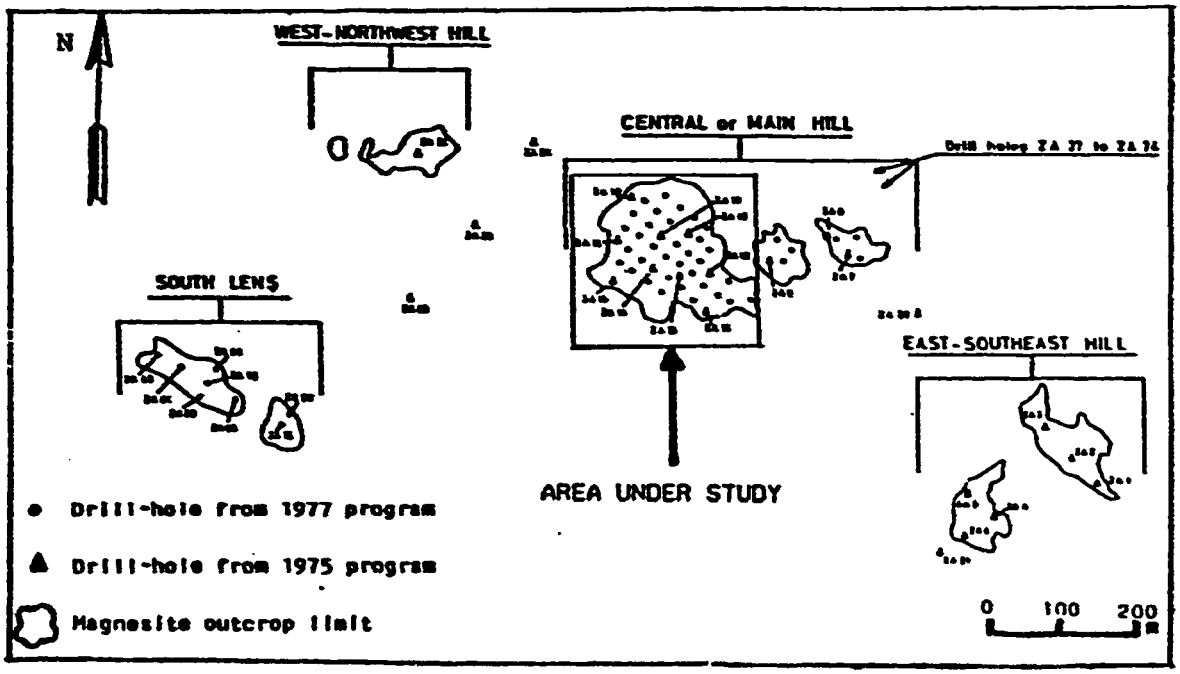

Fig. 1.3: Sketch map of Zarghat magnesite deposit main outcrops (After Brosset, 1978)

1.2 Economic importance of magnesite

Magnesite ($MgCO_3$) is considered to be one of the most important minerals because of its widespread usage in industry. It is used in the extraction of MgO and Mg by either electrolytic or calcination processes. MgO is referred to as the dead-burned magnesite that has been calcined at a high temperature and contains less than 1% CO_2 (Klein and Hurlbut, 1985). Brief descriptions of these substances can be found in Morris (1981) and Zim and Shafer (1957).

MgO has many industrial uses, some of which are mentioned by Jensen and Bateman (1981) as follows:

1) Production of electric insulation and semiconductor devices.

2) Production of high-temperature refractory bricks that are used as linings in furnaces of cement and steel factories.

3) Chemical and paper industries.

As for the magnesium, Greenfield (1972) and Petrucci (1977) have mentioned several industrial uses listed below:

1) Manufacturing aircraft, missiles, rockets and motor vehicles parts.

2) Production of fuel element cans in nuclear reactors.

3) As a reducing agent in certain metallurgical and chemical processes.

4) Production of incendiary bombs.

According to the catalog of "The Economics of Magnesium Metal" (1982), the main magnesite-producing countries in the world are U.S.A., U.S.S.R., U.K., Austria, Brazil, Canada and Australia. The same catalog lists the main consumer countries as follows: U.S.A., U.K., Germany, Canada and Japan.

1.3 Previous studies

Several studies were reported on Zarghat magnesite deposit since 1962. Most of these studies have, however, concentrated on the geological, mineralogical and structural aspects of the deposit. These studies are summarized below in historical order.

In 1962, Khar investigated Zarghat area and reported the existence of magnesite deposit. Three years later, in 1965 Feugueur recommended the sampling and assaying for MgO in the area to delineate the extent and the nature of the deposit. He reported his observations and recommendations in an open-file report (1966).

These preliminary investigations were followed by a brief survey and sampling by Berton in 1968. As a result of this survey, Berton constructed a geological map of the main out-crops at a scale of 1:5000 and recommended diamond drilling to delineate the structure of the deposit. A more detailed geologic and topographic map, at a scale of 1:1000, for the main outcrops was prepared by Brosset in 1970. He reported the existence of one million metric ton of magnesite and recommended diamond drilling to determine the thickness and quality of mineralization at depth. On the basis of the previous studies, Delfour (1970) published his report entitled"Preliminary Data on the Zarghat Magnesite Prospect".

Between 1975 and 1977, Bureau de Recherches Géologique et Minières (BRGM) conducted a preliminary and exploratory drilling programs in order to determine the extent, shape and quality of the deposit. The preliminary reserve estimation, based on the data derived from this drilling program, indicated the existence of three million tons of magnesite. More details about these drilling programs are given in Chapter 3.

In 1985, Ghaleb presented his master thesis entitled "the geological, mineralogical and geostatistical studies on Zarghat magnesite deposit". However, due to insufficient data, which included 199 samples from 9 vertical drill holes, he concentrated only to semivariogram modelling in geostatistical part of his thesis.

Besides a recent study by Celik (1990) which was referred earlier, two other studies were published about the deposit in recent years. Saif and Ghaleb (1987) published a paper entitled "Geology and Origin of Zarghat Magnesite Deposit, Saudi Arabia", whereas Sahin and others (1988) a paper entitled "Spatial Distribution in Zarghat Magnesite Deposit of

Saudi Arabia". The latter study reported the presence of some lateral variations in grade within the deposit and based on the strong negative linear correlation observed between MgO % and CaO %, suggested the consideration of co-kriging technique in the local estimation of the deposit.

1.4 Scope of the present study

This study which is based on 1239 samples derived from 51 vertical drill-holes concentrates mainly on the geostatistical modelling of the deposit and includes the following main topics:

1) Review of the geology of Zarghat area.

2) Description of available data sets and methods of data preparation.

3) The statistical analysis of data with the objective of determining types of distributions and the basic statistical parameters including the correlation coefficients between MgO% and CaO%.

4) The computation and modelling of semivariograms and cross-semivariogram functions leading to geostatistical parameters required in subsequent local estimations.

5) The application of geostatistical method of simple linear kriging to estimate the block and some point values within the deposit.

6) The application of geostatistical method of co-kriging to estimate some point values mentioned in previous item and to compare the results with the corresponding results derived from kriging.

7) The derivation of grade-tonnage relationship for the deposit.

To carry out this study, computer software packages such as GEOSTAT (1984) and SAS (1986) available at the Data Processing Center (DPC) of King Fahd University of Petroleum and Minerals (KFUPM) as well as several FORTRAN programs written in the department for specific purposes (Sahin, 1983) have been used.

CHAPTER 2

GEOLOGICAL REVIEW

2.1 General geology of the Arabian Shield

The Arabian Shield consists of Precambrian crystalline basement rocks that have been affected by several phases of complex foldings, faultings and metamorphism. It occupies an area of about 650,000 sq. km. in the western part of the Arabian Peninsula. This area is equal to roughly one-third of the total area of the peninsula and surrounded from its northern, eastern and southern sides by the sedimentary cover rocks that are bedded uniformly and dipping gently towards northeast, east and southeast. The sedimentary rocks, which represent the entire Phanerozoic era, form large curved belts flanking the eastern margin of the Shield. However, the Shield is bounded on the western side by Cenozoic formations in the Red Sea coastal plain. The alkalic basalt flows, which are Tertiary and Quaternary in age, form several lava fields on the shield, extending roughly parallel to the Red Sea coast (Saint-Mark, 1978).

Hadley and Schmidt (1980) suggested that the Shield was formed by the successive accretions of newly formed crusts between 1000 and 600 m.y. ago. This has resulted in the formation of ophilitic belts especially in the central and eastern parts of the Shield. Three distinct depositional phases (lithostratigraphic sequences) of sedimentary rocks have been

distinguished in the Arabian Shield as shown in Table 2.1. The three phases are further subdivided into groups. Carbonate rocks are abundant in all groups of the three phases except the Shammar Group in phase III. Volcanic rocks, on the other hand, are observed in all three phases. The rocks of Phase I and II have been metamorphosed to greenschist and amphibolite facies, whereas the rocks of Phase III are unmetamorphosed. The sedimentary rocks of phase I and phase II have been deposited in basins with generally N-S trend and those of phase III in basins with E-W trend.

2.2 Geology of Zarghat area and magnesite deposit

Zarghat magnesite deposit occurs in a small sedimentary basin of the Jibalah (Jubaylah) Group which is considered to be Late Proterozoic to Early Cambrian in age (Brosset, 1970). Detailed field studies indicated that Jibalah Group occurs in the northwestern and eastern parts of the Arabian Shield. In the northwestern part, the group consists of the graben-type sediments, such as carbonates, that were interstratified by alkalic, intermediate and basic volcanic rocks in addition to well developed andesites. This part was affected by faults and folds having a nortwest trend during the orogenic-epeirogenic event before the deposition of Cambro-Ordovician sandstones. In the eastern part, the group comprises essentially sandstones, shales and conglomerates (Brown and Jakson, 1978, Calves and others 1984, Hadley, 1974). The lithostratigraphic sequence, structure and mineralization in Zarghat area have been summarized in the following sections.

TABLE 2.1: Distribution of the Sedimentary depositional phases in the Arabian Shield (after Hadley and Schmidt, 1980; and Stoeser, 1985)

Phases	Age	Groups
III	550 - 610 ma	Jubaylah (Jibalah) Shammar
II	610 - 800 ma	Murdama (includes Fatima) Halaban Ablah
I	800 - 950 ma	Jeddah Bahah Baish

2.2.1 Lithostratigraphic sequence

According to Brosset (1978), Zarghat sedimentary basin is an elongated structure with dimensions of 4.5x2.5 km. It consists of carbonate rocks and underlying andesite unit of Jibalah Group as shown in (Figure 2.1). These units are described (from base to top) as follows:

1) Andesite unit

This unit consists mostly of brown to gray amygdaloidal andesite with some feldspathic microlites. Red-brown calcareous sandstone and weathered polygenic conglomerate are, also, observed in places.

2) Carbonate succession

The carbonate sequence contains (from base to top) cherty limestone, dolomitic limestone, bedded dolomite and magnesite.

a) Cherty limestone and dolomitic limestone

These rocks form the lower part of the carbonate succession. The cherty limestone is well developed and exposed throughout the basin. It is brown in color and has been interbedded with thin layers of brown argillaceous sandstone and some green to yellow siltstone. Several lenses of dark brown dolomitic limestone are observed in places.

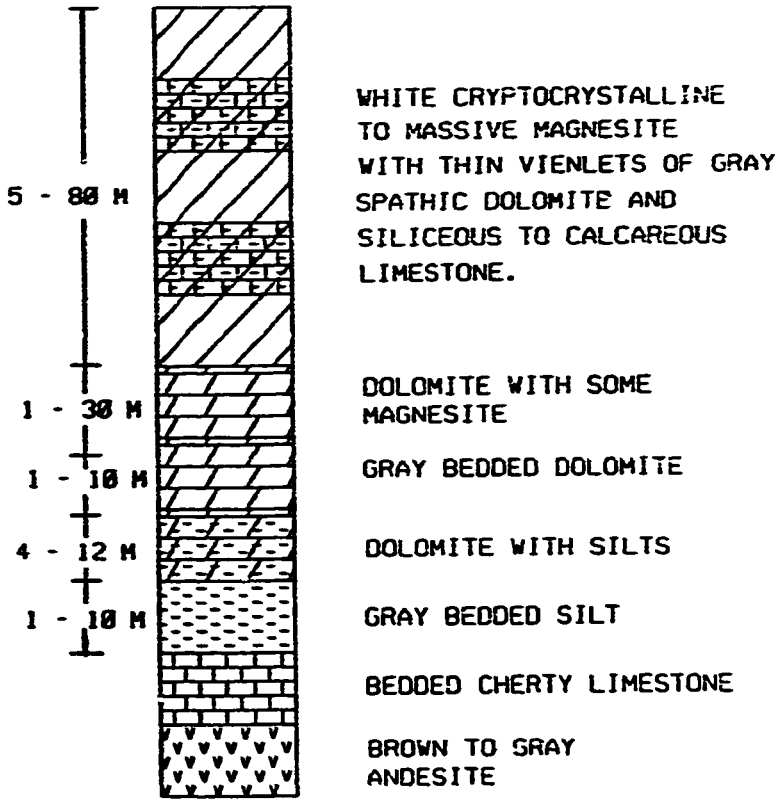

Fig. 2.1: Generalized lithostratigraphic section of Jibalah Group in Zarghat sedimentary basin (after Brosset,1978).

b) Bedded dolomite

This unit, which comprises the middle part of the succession, is exposed at the base of the small hills consisting of magnesite. Although the contact between the beded dolomite and the magnesite is quite clear, several magnesite lenses have been observed within bedded dolomite near its top (Saif and Ghaleb, 1987).

c) Magnesite

Magnesite forms the uppermost part of the succession and is observed in three small hills referred to as Central, West-northwest and East-southeast hills as shown in Figure 1.3. These hills are located along a line of 1.5 km length having WNW-ESE trend. Dolomite veins of different colors, sizes and patterns, which are considered to be one of the important features of the deposit, were observed in all magnesite occurences (Saif and Ghaleb, 1987).

2.2.2 Structure

Several structural events can be observed in the area as reported by Ghaleb (1985) and Brosset (1978). These are summarized in the following paragraphs.

The strata of Jibalah Group make a triangular synclinal basin. The strikes of beds in the northern part of this basin range from NW to NE and the corresponding dip angles vary

from 60° to 40° towards SW and SE. The beds in the southeastern part, on the other hand, strike NW with various dips ranging from 45° SW to almost vertical.

A major fault trending NW passes through the area as shown in Figure 2.2. It has brought the rhyolite of Fatima Group against the andesite of Jibalah Group. One large and two smaller faults branch out from the major fault extending in NE and SW directions respectively. In addition, two faults trending SE are observed towards the southern part of the basin. Four sets of major joints and irregular fractures are common in the area, particularly in the magnesite body that has been highly fragmented and brecciated.

2.2.3 Mineralization

The mineralization, as represented in the form of three hills and other smaller lenses of magnesite and dolomitic magnesite, occurs as hard, dense and massive bodies which are highly fractured, fragmented and brecciated. The magnesite appears to be gray or pale brown colored on weathered surfaces, but white in sub-surface samples (Saif and Ghaleb, 1987).

The Central Hill is the largest among all occurrences and constitutes about 3 million tons of magnesite. The erosion has segmented it into three parts exposing the underlying dolomites and dolomitic limestones along narrow valleys. The lateral dimensions of the Central Hill is about 450 m x 200 m with its top lying about 16 m above the plain

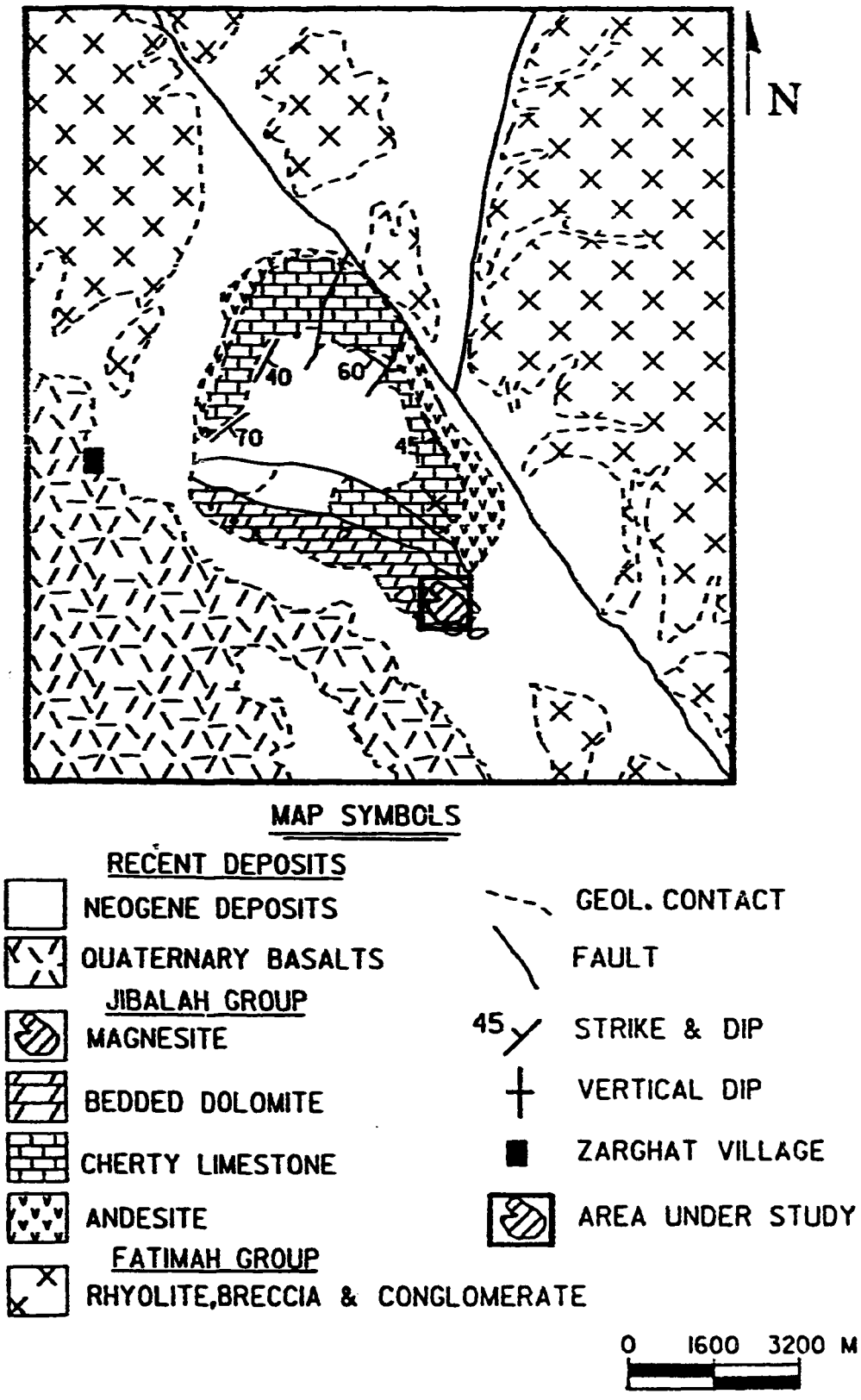

Fig. 2.2: Simplified geologic map for Zarghat area (after Brosset, 1976)

Figure 2.3). The drill-holes intersecting magnesite in the Central Hill have revealed a thickness ranging from about 5 to 50 m as illustrated in Figure 2.4.

The East-southeast Hill is composed of two smaller hills separated by narrow valleys which have exposed underlying outcrops of dolomites and dolomitic limestones. The lateral dimensions of this hill is about 200 m x 200 m with 4 to 5 m height above the plain. The West-northwest Hill, on the other hand, has about 150 m x 50 m lateral dimensions and 8 m height.

Dolomite veins of various colors, thicknesses and patterns commonly interesect the magnesite bodies in the area. These veins vary in color from brown to pale gray and in thickness from about one meter to micro-veinlets. Some veins exhibit branching, cross-cutting and dendritic patterns. Larger veins commonly enclose scattered fragments and blocks of magnesite.

2.2.4 Origin of the deposit

Several models have been proposed about the origins of magnesite deposits. The model, which appears to be suitable to Zarghat deposit (Saif & Ghalib, 1987), is summarized in the following paragraphs.

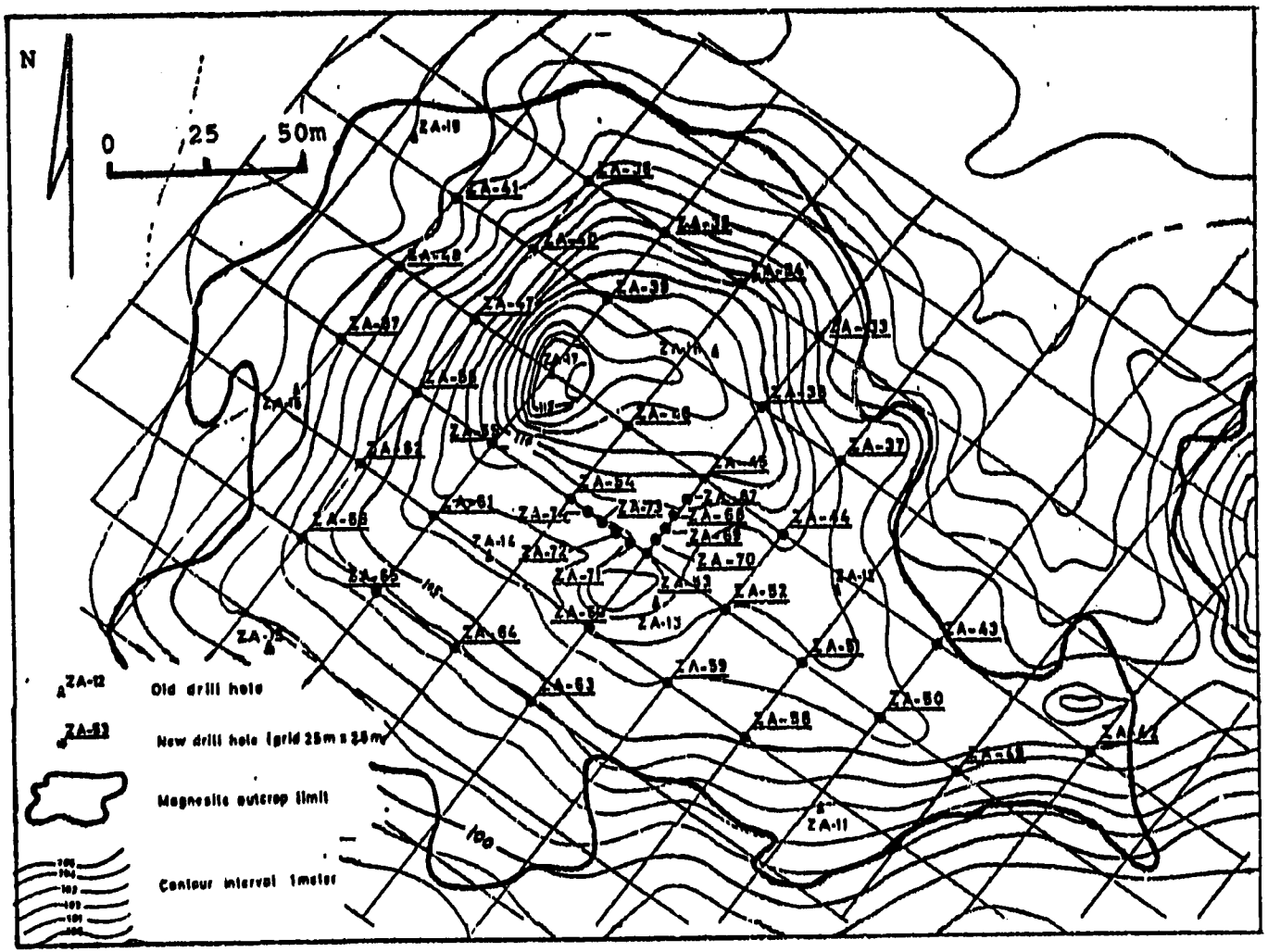

Fig. 2.3: Topographic map for the largest portion of the Central Hill (after Brosset, 1978)

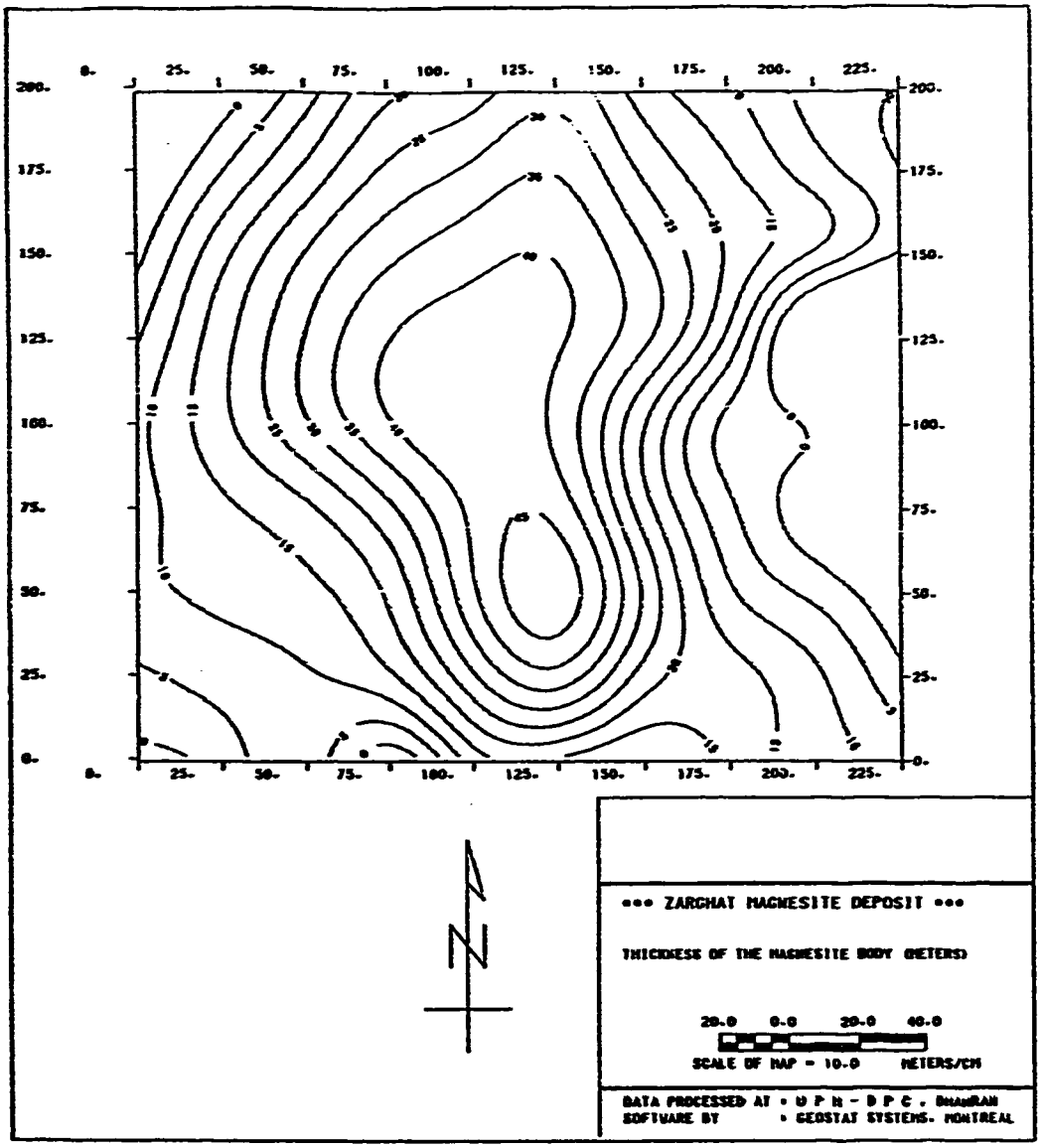

Fig. 2.4: Isopach map indicating the thickness of magnesite deposit in the largest portion of the Central Hill

Zarghat magnesite is of sedimentary type that has been formed after bedded dolomite during a normal sequence of carbonate deposition (Ghaleb, 1985). This conclusion is suported by the field observations made on the stratigraphic sequence, the contact between magnesite and bedded dolomite and the crypto-to micro-crystalline texture of deposit. The absence of related igneous body or hydrothermal activity, as well as the absence of hydrothermal minerals and replacement textures within the deposit may provide further evidence for this conclusion.

It has, also, been suggested that magnesite was precipitated originally as an assemblage of hydromagnesite or nesquahonite ($Mg\ CO_3.3H_2O$) under high pH conditions in a restricted marine environment. After deposition, this assemblage was dehydrated into magnesite ($MgCO_3$) due to higher temperature and pressure resulting from the burial.

Dolomite veinlets were probably deposited within the orebody by the expelled solutions. These solutions, which were derived during the dehydration process of hydromagnesite, dissolved early formed $CaCO_3$ and $MgCO_3$ and redeposited them as dolomite [$CaMg(CO_3)_2$] with minor calcite. The fractures, crevices and brecciated zones, which were filled by dolomitic veins, were probably produced due to shrinkage in the orebody resulting from the dehydration process.

It was noted that the temperatures during the diagenesis and dehydration phases were not high enough to transform fine-grained magnesite into coarser grained deposit, as it was suggested by Tewari (1973).

CHAPTER 3

DATA SET DESCRIPTION

3.1 Drilling programs

The geological investigations on Zarghat area were conducted by BRGM between 1962 and 1978. Earlier studies have indicated the necessity of conducting a preliminary drilling program in the area in order to explore the size and the quality of the magnesite deposit (Brosset, 1976). This preliminary drilling program was conducted in 1975 and followed by the exploratory drilling program in 1977 to determine the extent, shape and the quality of the deposit (Brosset, 1978).

3.2 Distribution of drill-holes

Out of a total of 90 vertical drill-holes drilled in the whole area during the above mentioned drilling programs, 60 drill-holes were located in the Central Hill. The data for this study were derived from 51 drill-holes located in the largest portion of the Central Hill as illustrated in Figure 3.1. Among these, the drill-holes numbered ZA 11 to ZA 19 were completed during the preliminary drilling and ZA 33 to ZA 74 during the exploratory drilling programs. These two drilling programs provided a total of 1239 samples.

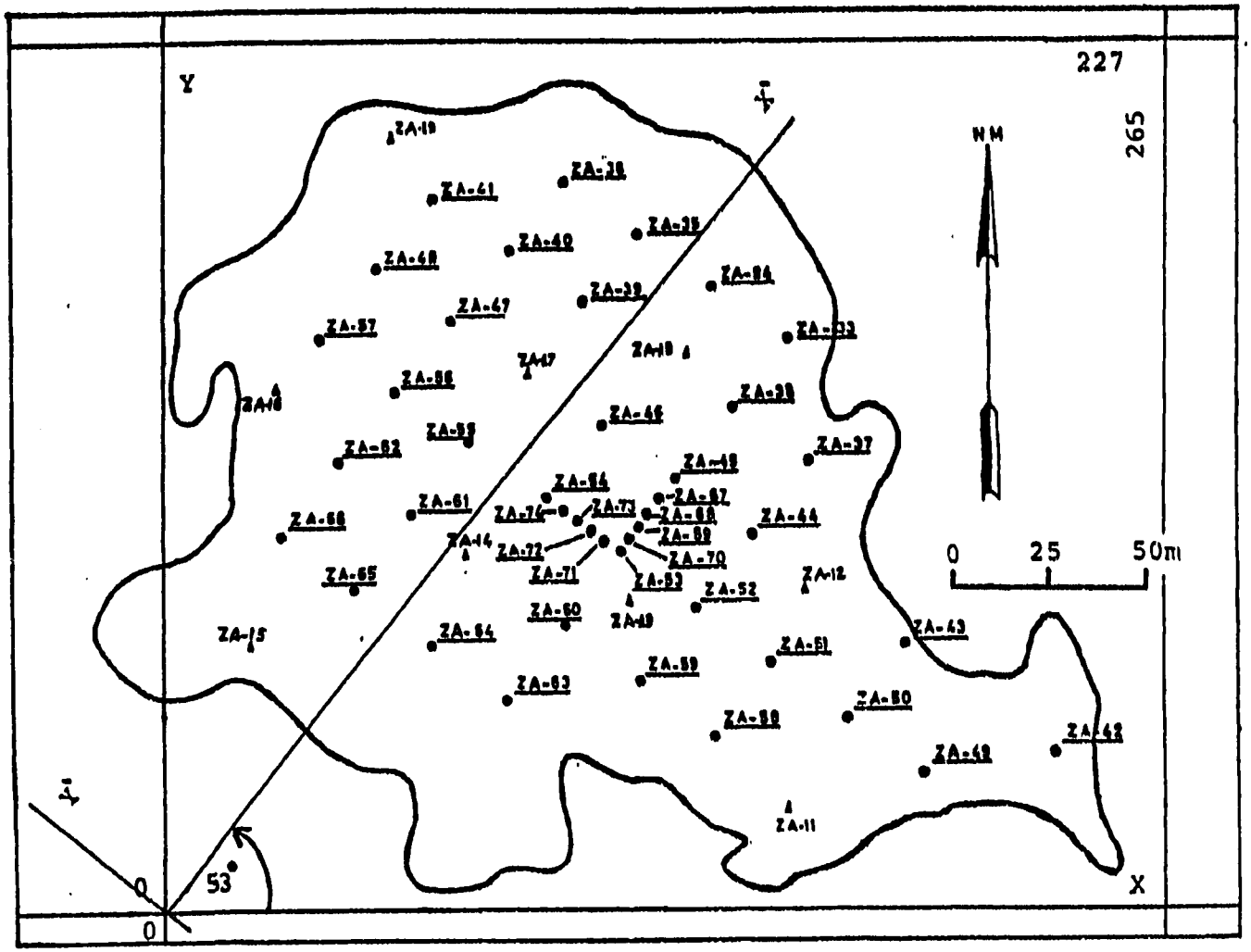

Fig. 3.1: Base map indicating the location of the drill-holes in the Central Hill

According to their spacing the drill-holes can be grouped in two sets as follows:

1) The first set consisting of 43 drill-holes (from ZA 11 to ZA 19 and from ZA 33 to ZA 66) can be fitted to almost a Regular Grid with 25m x 25m dimensions covering the largest portion of the Central Hill. One axis of this grid is oriented in N 37° E direction. The main purpose of drilling of this set was to determine the quality, extent and economic feasibility of the deposit.

2) The second set consisting of eight in-fill drill-holes with 5m spacing. Four of these holes (ZA 67 to ZA 70) were drilled along a line in NE direction between ZA 53 and ZA 45; and the other four (ZA 71 to ZA 74) were drilled along a line in NW direction between ZA 53 and ZA 54. Each of these drill-holes has been terminated at 6m depth from the top (i.e. each one has only 6 samples having 1 m thickness). The purpose of this in-fill drillings was to determine the behaviour of the regionalized variables at distances smaller than 25m and to define the lateral continuity of the deposit (Brosset, 1978).

3.3 Chemical analysis of samples

The sampling along drill-holes has been carried out at a uniform interval of 1 m. Samples were sent to BRGM laboratory in Jeddah for chemical analysis which included the determination of the crude magnesite using the atomic absorption for CaO, Al_2O_3 and Fe_2O_3; the volumetric analysis for MgO; the gravimetric analysis for the insoluble residue

and the ignition loss. The results of the above-mentioned analysis and the calculated theoretical percentages for calcined magnesite were recorded in drill-hole log sheets in BRGM reports (Brosset,1976 and 1978).

3.4 Preparation of data sets

Data set preparation is the first step to be completed before any statistical and geostatistical analysis. The preparation of data sets for this study is summarized as follows:

1) X and Y coordinates as well as the elevation of collar (i.e. Z-coordinate) for each drill-hole were determined from the drill-hole location and topographic maps. These values, which were measured in meters, are recorded in Table 3.1 together with the depths from the collar to the top and bottom of the deposit and the thickness of deposit in each hole.

2) A master data file, which included the survey data (coordinates, azimuth and inclination angles), the depths from the collar to the top and bottom of each sample and the assay values for the variables, was prepared. Since all the drill-holes are vertical, the azimuth and inclination angles were recorded to be 0.0° and -90.0° respectively. The assay values included both the crude and calcined values of MgO% and CaO%. An excerpt from this master file with some descriptions is given in Appendix A.

TABLE 3.1: SURVEY DATA OF ZARGHAT MAGNESITE DEPOSIT

HOLE	X(m)	Y(m)	Z(m)	Top (m)*		Bottom(m)*	Thickness (m)**
ZA-11	164.288	25.419	102.8	0.0	-	5.0	5.0
ZA-12	168.723	81.547	106.9	0.0	-	25.0	25.0
ZA-13	122.491	78.817	108.3	0.0	-	44.0	44.0
ZA-14	79.500	90.930	106.2	0.0	-	15.0	15.0
ZA-15	22.860	67.728	100.5	0.0	-	11.0	11.0
ZA-16	29.684	135.115	99.7	0.0	-	10.0	10.0
ZA-17	95.877	138.698	115.3	0.0	-	43.0	43.0
ZA-18	137.845	144.157	111.7	0.0	-	40.0	40.0
ZA-19	60.051	201.479	99.2	0.0	-	8.0	8.0
ZA-33	164.288	147.910	106.0	0.0	-	39.0	39.0
ZA-34	144.669	161.729	109.0	0.0	-	45.0	45.0
ZA-35	124.709	175.718	107.0	0.0	-	37.0	37.0
ZA-36	105.260	189.707	104.0	0.0	-	32.0	32.0
ZA-37	169.747	114.814	107.0	0.0	-	12.0	12.0
ZA-38	149.957	129.315	110.5	0.0	-	39.0	39.0
ZA-39	110.378	157.976	111.3	3.0	-	44.0	41.0
ZA-40	90.759	171.112	105.6	1.0	-	34.0	33.0
ZA-41	70.970	184.760	100.7	1.0	-	22.0	21.0
ZA-42	234.234	39.238	104.7	0.0	-	7.0	7.0
ZA-43	194.824	68.069	105.6	4.0	-	15.0	11.0
ZA-44	155.246	96.048	108.3	0.0	-	46.0	46.0
ZA-45	135.115	110.890	109.9	0.0	-	45.0	45.0
ZA-46	115.667	124.879	111.6	0.0	-	50.0	50.0
ZA-47	75.917	153.199	106.1	0.0	-	30.0	30.0
ZA-48	56.127	166.847	101.1	0.0	-	22.0	22.0
ZA-49	199.602	34.461	104.2	1.0	-	28.0	27.0
ZA-50	179.642	48.621	106.3	3.0	-	15.0	12.0
ZA-51	160.193	63.293	106.8	0.0	-	53.0	53.0
ZA-52	140-063	77.111	107.0	0.0	-	51.0	51.0
ZA-53	120.444	91.783	108.5	0.0	-	39.0	39.0
ZA-54	100.825	105.601	108.0	0.0	-	34.0	34.0
ZA-55	80.182	120.273	109.0	0.0	-	34.0	34.0
ZA-56	60.734	133.921	105.0	0.0	-	29.0	29.0
ZA-57	41.285	148.251	100.8	0.0	-	13.0	13.0
ZA-58	145.181	44.015	105.2	0.0	-	41.0	41.0
ZA-59	125.903	58.345	105.9	0.0	-	40.0	40.0
ZA-60	105.431	72.334	107.2	0.0	-	25.0	25.0
ZA-61	65.340	101.166	106.4	0.0	-	18.0	18.0
ZA-62	46.233	114.814	103.6	0.0	-	18.0	18.0
ZA-63	90.077	53.568	103.8	1.0	-	10.0	9.0
ZA-64	70.458	67.387	104.0	0.0	-	15.0	15.0
ZA-65	50.327	81.888	103.7	0.0	-	12.0	12.0
ZA-66	31.220	95.877	102.7	3.0	-	13.0	10.0
ZA-67	130.680	105.260	109.3	0.0	-	6.0	6.0
ZA-68	127.268	101.166	108.8	0.0	-	6.0	6.0
ZA-69	125.050	98.095	108.7	0.0	-	6.0	6.0
ZA-70	122.491	95.024	108.6	0.0	-	6.0	6.0
ZA-71	116.008	94.171	108.0	0.0	-	6.0	6.0
ZA-72	112.596	96.901	107.8	0.0	-	6.0	6.0
ZA-73	108.843	99.630	107.9	0.0	-	6.0	6.0
ZA-74	105.260	102.189	108.0	0.0	-	6.0	6.0

* Depth to top and bottom of deposit from the collar.

** Thickness of deposit.

3) The master data file was processed using the program COMPOS of the GEOSTAT package (1984). The objective of this step was to arrange the data in a format suitable for processing using other programs.

4) The output obtained from the compositing program was processed using a simple FORTRAN program written with the objective of rotating coordinates and determining the common logarithms of assay values. The original X and Y axes were rotated 53° counter clockwise direction and the coordinates of samples with reference to the new axes parallel to Regular Grid sides were determined. The purpose of this rotation was to simplify the computation of semivariograms and cross-semivariograms. The transformation of the real assay values of both crude CaO% and crude MgO% into common logarithmic values was, also, necessary as it will be explained in the following Chapter. An excerpt from the output resulted from this step is presented in Appendix B.

CHAPTER 4

PRELIMINARY STATISTICAL ANALYSIS

4.1 Introduction

Calculating certain quantities (i.e. statistical parameters) representing the geological variables under consideration is the common practice in any statistical analysis. These statistics provide valuable information about the deposit in all stages of exploration and exploitation programs. Besides these statistics, histograms and cumulative frequency plots are valuable tools in determining the type of sampling distribution for variables and the correlation diagrams for determining the relationship between pairs of variables. Detailed presentations of the statistical analysis of geological data can be found in Cheeney (1983), David (1988), Davis (1986), Koch and Link (1980) and Marsal (1987)

Using the available data for both crude and calcined CaO% and MgO% assay values, a preliminary statistical analysis for Zarghat magnesite deposit have been carried out. The results of this analysis are presented, in detail in the following sections.

4.2 Statistical parameters

The preliminary statistical analysis has been carried out using 1128 samples out of the complete set of 1239 samples. The filtering of the number of samples was recommended due to the presence of some abnormally very high and very low values of both CaO% and MgO% in the set. This may be due to the presence of samples that are located near the edges of the deposit. This automatic filtering of the abnormal samples resulted in a significant reduction in the values of the statistical variances for both variables. Detailed discussions about the problems of outliers and related solutions can be found in Hawkins (1980).

Summary statistics for the whole deposit and for the individual drill-holes are listed in Tables 4.1 and 4.2 respectively. The following conclusions can be drawn from these statistics:

1) The comparison of the variances of the variables for pairs of drill-holes using F-tests indicates that variations exist in most parts of the deposit at $\alpha = 0.05$.

2) It has been observed that both CaO% and MgO% values have considerably higher variations in drill holes located near the boundary of the deposit (Figure 4.1). Beside this, the same drill-holes have relatively higher CaO% and lower MgO% mean values. Therefore, it is logical to conclude that the locations intersected by these drill-holes may have been more intensely affected by dolomite veins described in Chapter 2.

TABLE 4.1: Summary statistics for the whole deposit

Variables	Number of Sample	Mean ($\bar{X}$)	Variance (S^2)	Min.	Max.	Range	Sum	Correlation Coefficients (r)
CaO % (Crude)	1128	1.38	2.26	0.15	7.03	6.88	1558	-0.89
MgO % (Crude)	1128	46.27	2.22	41.78	47.75	5.97	52189.92	
CaO % (Calcined)	1128	2.86	10.88	0.20	46.40	46.20	3231.09	-0.85
MgO % (Calcined)	1128	96.02	16.45	74.77	99.94	25.17	108306.47	

TABLE 4.2: Summary statistics for individual drill holes

D.H. #	Number of Samples	CRUDE					CALCINED				
		CaO %		MgO %			CaO %		MgO %		
		$\bar{X}$	S^2	$\bar{X}$	S^2	r	$\bar{X}$	S^2	$\bar{X}$	S^2	r
ZA-11	5	1.97	0.51	45.25	1.32	-0.93	4.00	2.04	92.70	9.95	-0.77
ZA-12	25	0.57	0.08	47.18	0.20	-0.84	1.17	0.35	98.09	0.59	-0.89
ZA-13	42	2.21	2.46	45.16	1.68	-0.91	4.59	10.46	94.31	10.72	-0.93
ZA-14	15	1.46	1.41	46.32	1.82	-0.93	3.00	5.94	95.91	10.03	-0.95
ZA-15	11	3.74	2.87	43.75	2.99	-0.98	11.31	46.16	89.26	20.25	-0.35
ZA-16	9	3.51	4.83	44.72	3.95	-0.99	7.12	19.50	91.38	22.57	-0.99
ZA-17	42	0.43	0.43	47.27	0.45	-0.93	0.87	1.71	98.35	3.85	-0.97
ZA-18	39	1.07	1.02	46.84	0.88	-0.95	2.19	4.11	97.24	5.86	-0.96
ZA-19	8	1.29	3.72	46.39	3.23	-1.00	2.54	16.19	96.74	19.65	-0.99
ZA-33	36	2.96	5.35	44.56	3.91	-0.82	5.84	20.61	88.54	31.47	-0.70
ZA-34	39	1.45	3.16	45.13	4.96	-0.89	2.93	12.72	93.33	45.94	-0.78
ZA-35	37	0.82	1.13	46.14	2.05	-0.76	1.69	4.53	96.06	22.04	-0.60
ZA-36	21	1.07	1.25	46.92	1.48	-0.92	2.17	4.85	96.98	15.63	-0.97
ZA-37	12	3.48	6.28	44.70	5.26	-0.99	6.95	24.38	92.05	35.00	-0.98
ZA-38	38	0.95	1.61	46.84	1.05	-0.96	1.96	6.60	97.20	10.04	-0.88
ZA-39	39	0.85	1.26	46.39	0.84	-0.95	1.79	5.37	97.68	5.38	-0.99
ZA-40	32	1.52	3.51	46.31	2.20	-0.97	3.07	13.95	95.97	16.52	-0.99
ZA-41	20	2.35	4.11	46.22	2.67	-0.94	4.75	16.11	94.81	21.37	-0.98
ZA-42	5	2.33	1.57	44.97	2.02	-0.95	4.85	6.75	94.00	11.54	-0.95
ZA-43	11	4.19	0.93	42.91	0.44	-0.96	8.57	3.65	87.86	4.37	-0.87
ZA-44	45	0.69	0.25	46.64	0.21	-0.68	1.45	1.07	97.92	1.18	-0.95
ZA-45	45	0.59	0.14	47.38	0.11	-0.79	1.23	0.60	98.51	0.68	-0.93
ZA-46	50	0.54	0.39	47.29	0.55	-0.88	1.12	1.69	98.75	2.06	-0.99
ZA-47	29	0.86	0.78	47.14	0.50	-0.87	1.73	3.26	97.71	3.87	-0.96
ZA-48	17	0.98	0.91	47.10	1.15	-0.90	1.98	3.50	97.03	13.81	-0.94
ZA-49	22	1.96	2.07	45.64	2.42	-0.96	4.03	8.36	94.42	13.00	-0.89
ZA-50	10	1.92	5.61	45.76	5.25	-1.00	3.92	22.96	94.78	32.82	-1.00
ZA-51	53	1.14	0.30	46.33	0.41	-0.90	2.38	1.26	96.77	2.71	-0.94
ZA-52	51	0.53	0.24	47.22	0.18	-0.75	1.10	1.03	98.25	1.53	-0.97
ZA-53	39	1.39	1.72	46.43	1.60	-0.89	2.88	7.14	96.62	8.50	-0.99
ZA-54	34	1.19	0.60	46.58	0.74	-0.90	2.49	2.49	96.50	5.90	-0.86
ZA-55	30	0.55	0.89	46.87	1.78	-0.70	1.13	3.62	97.84	8.10	-0.97
ZA-56	29	1.24	2.15	46.18	2.53	-0.91	2.61	9.31	96.86	11.41	-0.99
ZA-57	12	1.80	2.82	46.37	1.27	-0.99	3.69	11.09	95.93	11.16	-1.00
ZA-58	40	2.92	2.10	45.01	1.33	-0.92	6.03	8.50	92.83	8.94	-0.98
ZA-59	39	2.16	2.98	45.47	2.41	-0.94	4.32	12.31	94.63	13.64	-0.97
ZA-60	22	0.86	0.55	46.62	1.00	-0.90	1.81	2.31	97.11	5.35	-0.91
ZA-61	18	1.29	2.31	46.15	2.32	-0.99	2.70	9.49	96.52	15.15	-0.99
ZA-62	15	2.08	1.29	45.57	1.01	-0.97	4.32	5.42	94.72	7.20	-0.98
ZA-63	8	2.74	2.59	45.79	2.13	-0.99	5.60	10.58	93.99	12.47	-1.00
ZA-64	15	2.10	2.59	45.76	1.28	-0.97	4.18	10.95	94.84	13.43	-0.95
ZA-65	11	3.05	3.57	45.03	1.86	-0.97	6.26	14.55	92.87	13.15	-0.99
ZA-66	8	0.49	0.01	47.42	0.07	-0.36	1.02	0.05	98.85	0.05	-1.00
ZA-67	6	0.35	0.01	47.29	0.01	-0.71	0.73	0.03	99.14	0.03	-1.00
ZA-68	6	0.26	0.01	47.39	0.02	0.26	0.58	0.03	99.29	0.03	-1.00
ZA-69	6	0.35	0.01	47.25	0.08	-0.29	0.73	0.06	99.14	0.06	-1.00
ZA-70	6	0.62	0.04	47.05	0.04	-0.98	1.29	0.19	98.58	0.19	-1.00
ZA-71	6	0.27	0.01	47.27	0.13	-0.72	0.56	0.06	99.31	0.06	-1.00
ZA-72	6	0.28	0.08	47.24	0.07	-0.03	0.58	0.34	99.29	0.34	-1.00
ZA-73	6	0.15	0.00	47.39	0.02	0.33	0.31	0.00	99.57	0.00	-0.99
ZA-74	6	0.35	0.04	47.16	0.09	-0.40	0.74	0.17	99.04	0.14	-0.97

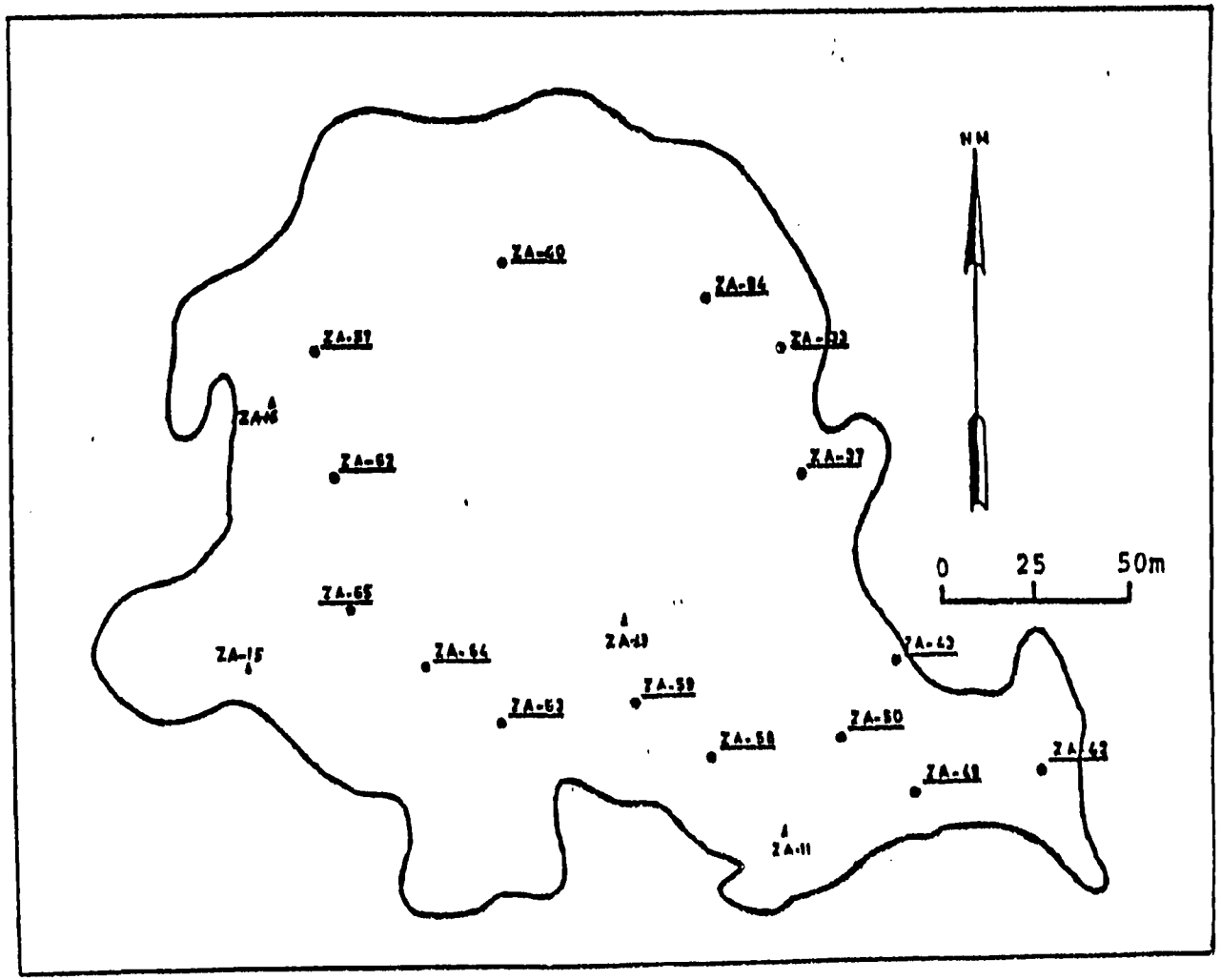

Fig. 4.1 : Drill-holes with higher CaO% and lower MgO% mean values (indicating locations more intensely affected by dolomite viens).

4.3 Histograms and frequency distributions

The histograms for CaO% and MgO% values are illustrated in Figure 4.2 to Figure 4.5. The histograms for both crude and calcined CaO% values show strong positive skew suggesting lognormal distribution with a high proportion of lower values. However, the histograms for both crude and calcined MgO% values show strong negative skew suggesting lognormal distribution having high proportion of higher values.

4.4 Cumulative frequency plots

To confirm the lognormality of the distributions, the cumulative frequency percentages for both crude CaO% and MgO% distributions were plotted against sample values on a 2-cycle logarithmic-probability graph papers and illustrated in Figures 4.6 and 4.7 respectively.

The resulting plots indicate the lognormal nature of distributions for both variables. These plots have revealed higher than expected proportion of low grade values. The excess of low grade values may be explained by the presence of randomly distributed poorly mineralized zones, such as the zones more intensely affected by dolomite veins, within the deposit. Similar types of distributions with the excess of low values have been reported from other deposits (Rendu, 1984).

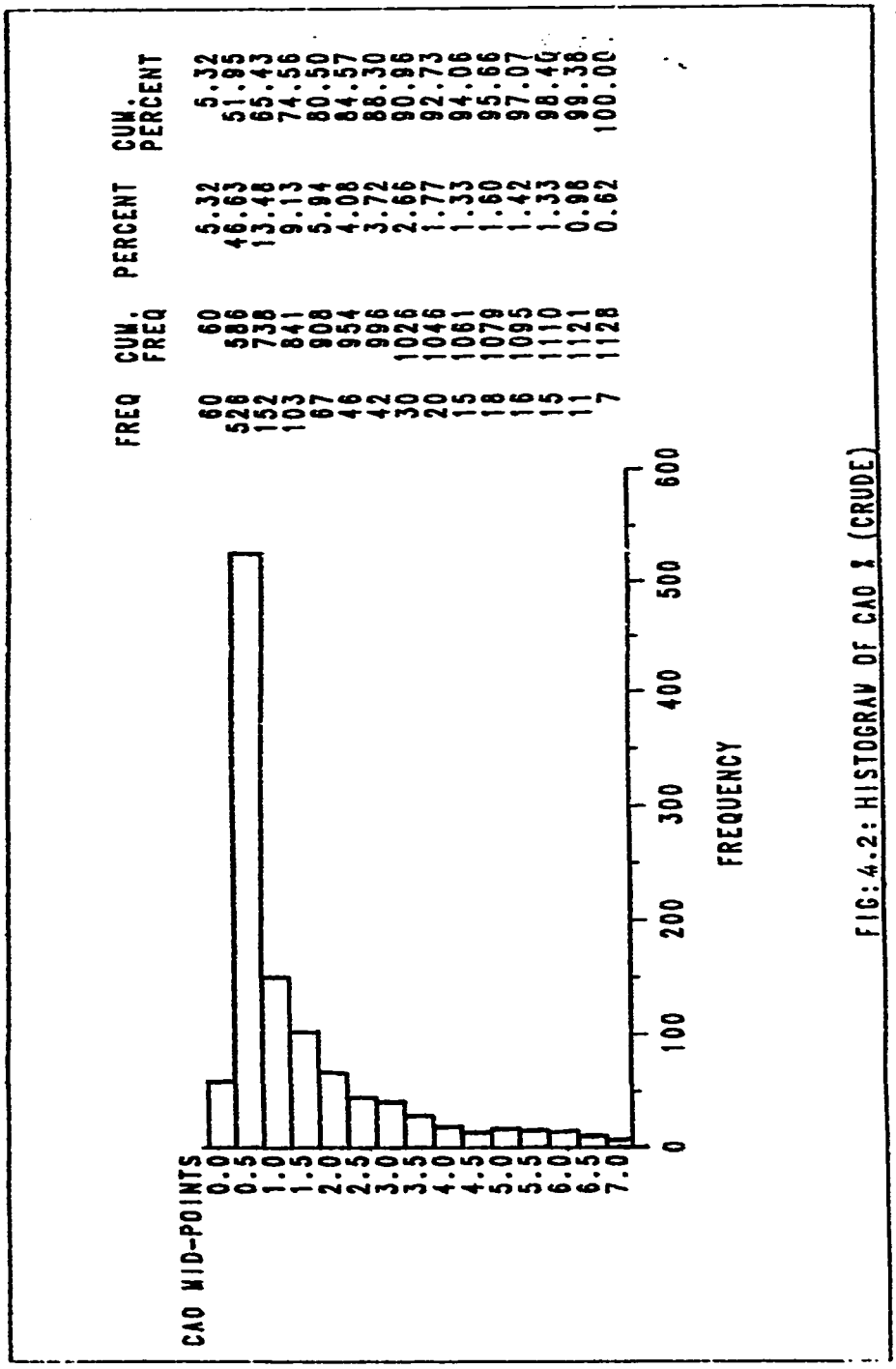

FIG:4.2: HISTOGRAM OF CAO 1 (CRUDE)

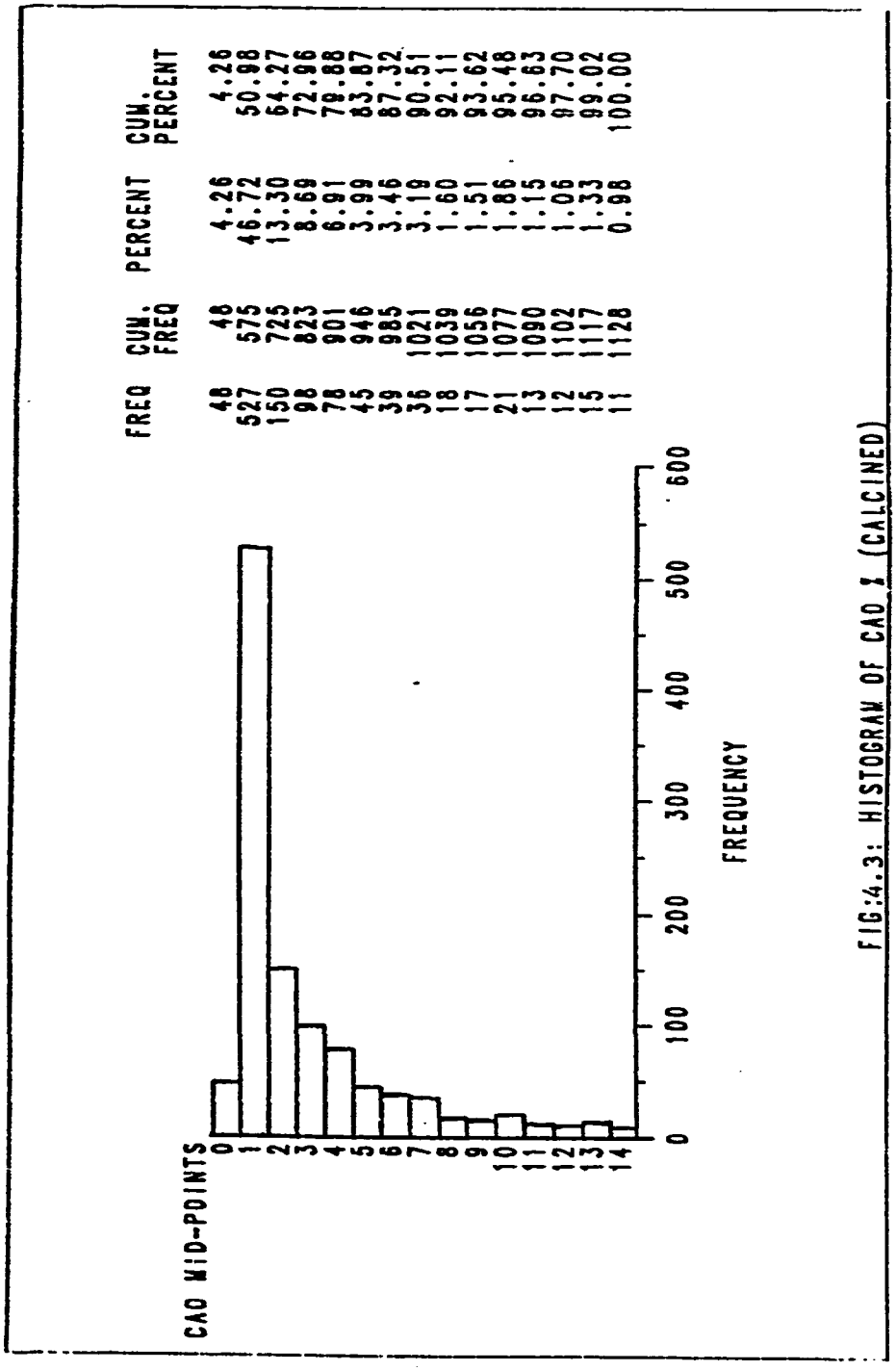

FIG:4.3: HISTOGRAM OF CAO % (CALCINED)

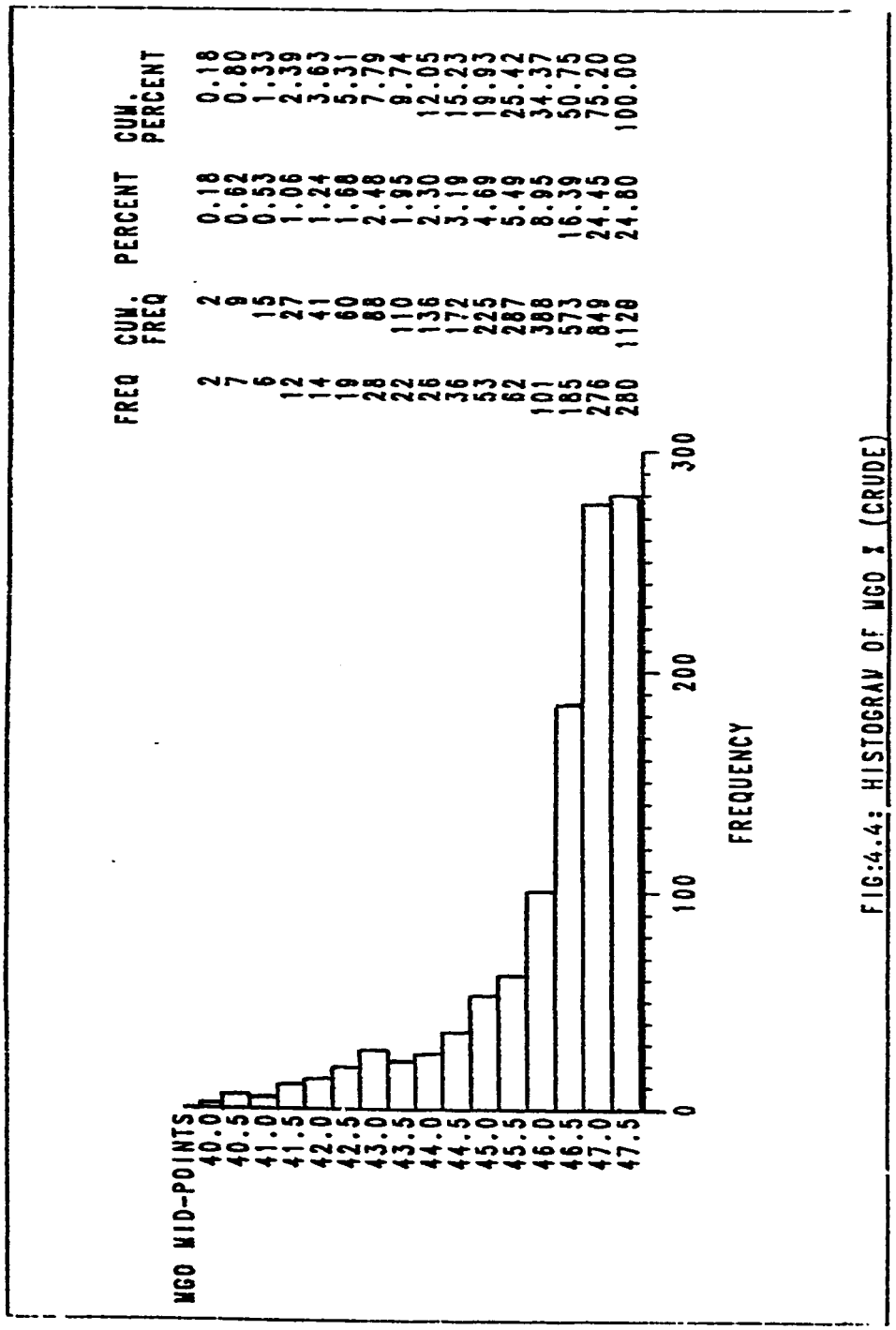

FIG:4.4: HISTOGRAM OF MGO % (CRUDE)

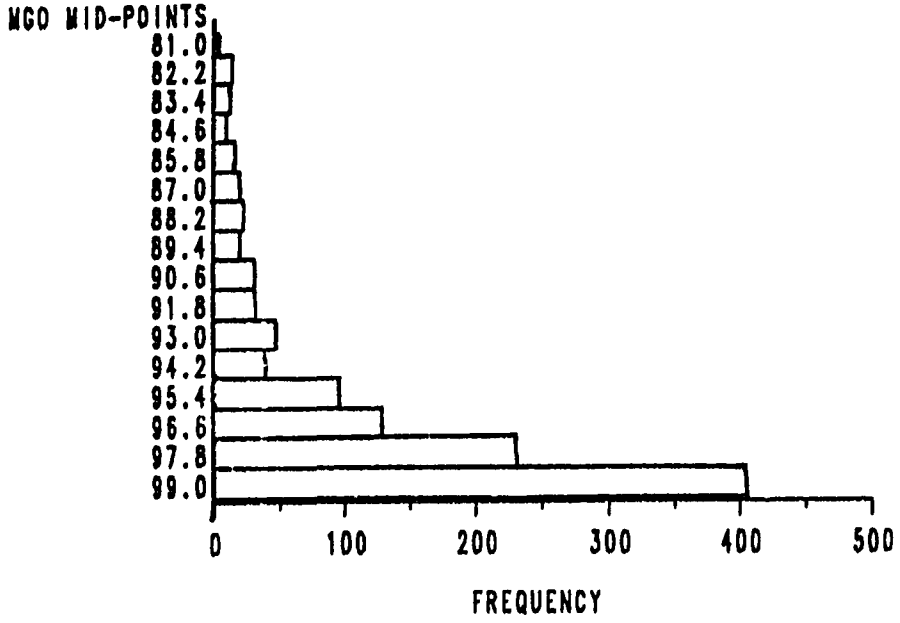

FREQ	CUM. FREQ	PERCENT	CUM. PERCENT
3	3	0.27	0.27
14	17	1.24	1.51
13	30	1.15	2.66
10	40	0.89	3.54
17	57	1.51	5.05
20	77	1.77	6.82
23	100	2.04	8.86
20	120	1.77	10.63
31	151	2.75	13.37
32	183	2.83	16.21
47	230	4.16	20.37
39	269	3.45	23.83
96	365	8.50	32.33
128	493	11.34	43.67
231	724	20.46	64.13
405	1128	35.87	100.00

FIG: 4.5:HISTOGRAM OF MGO % (CALCINED)

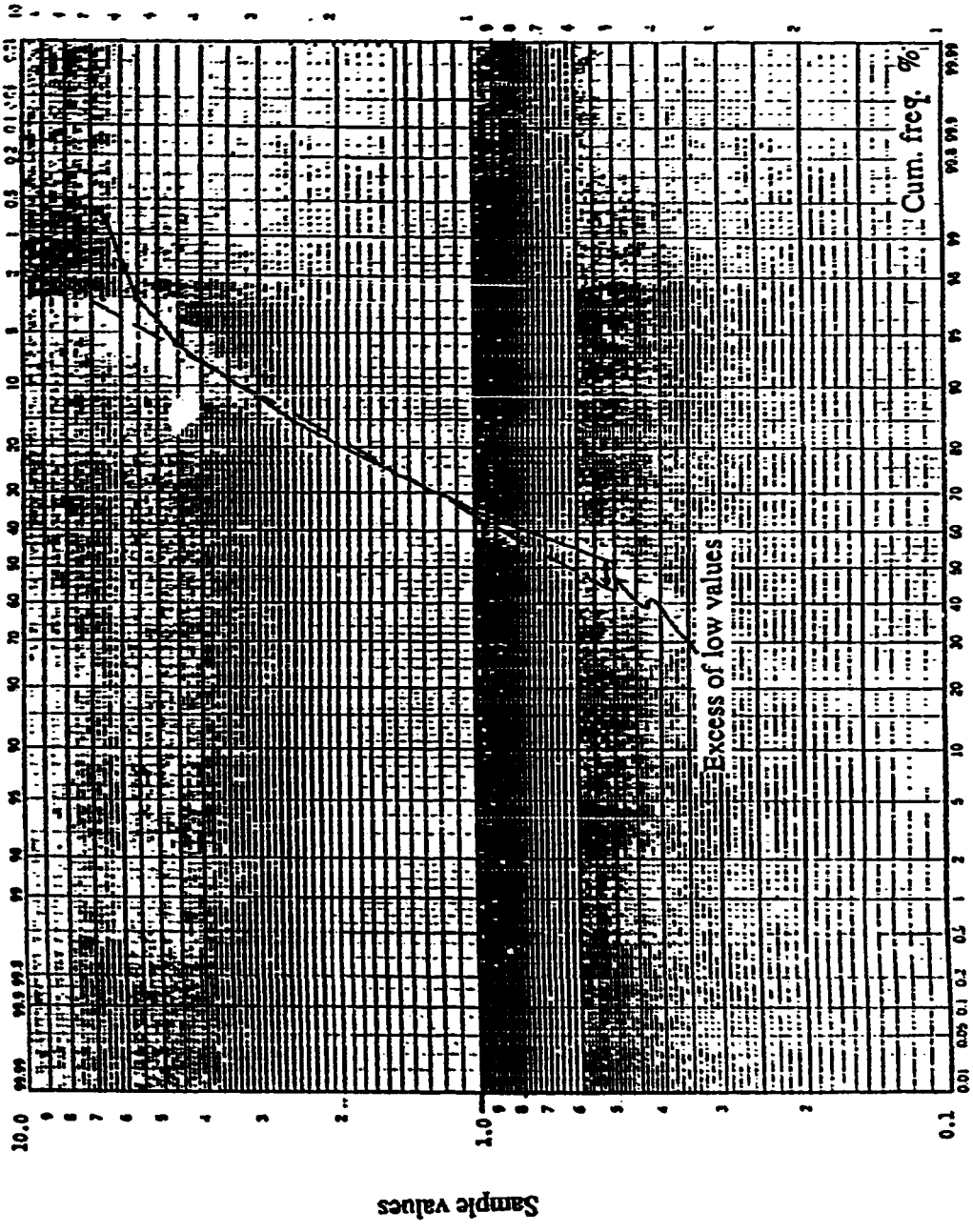

Fig. 4.6 : Percentage cumulative frequency plot for crude CaO% values.

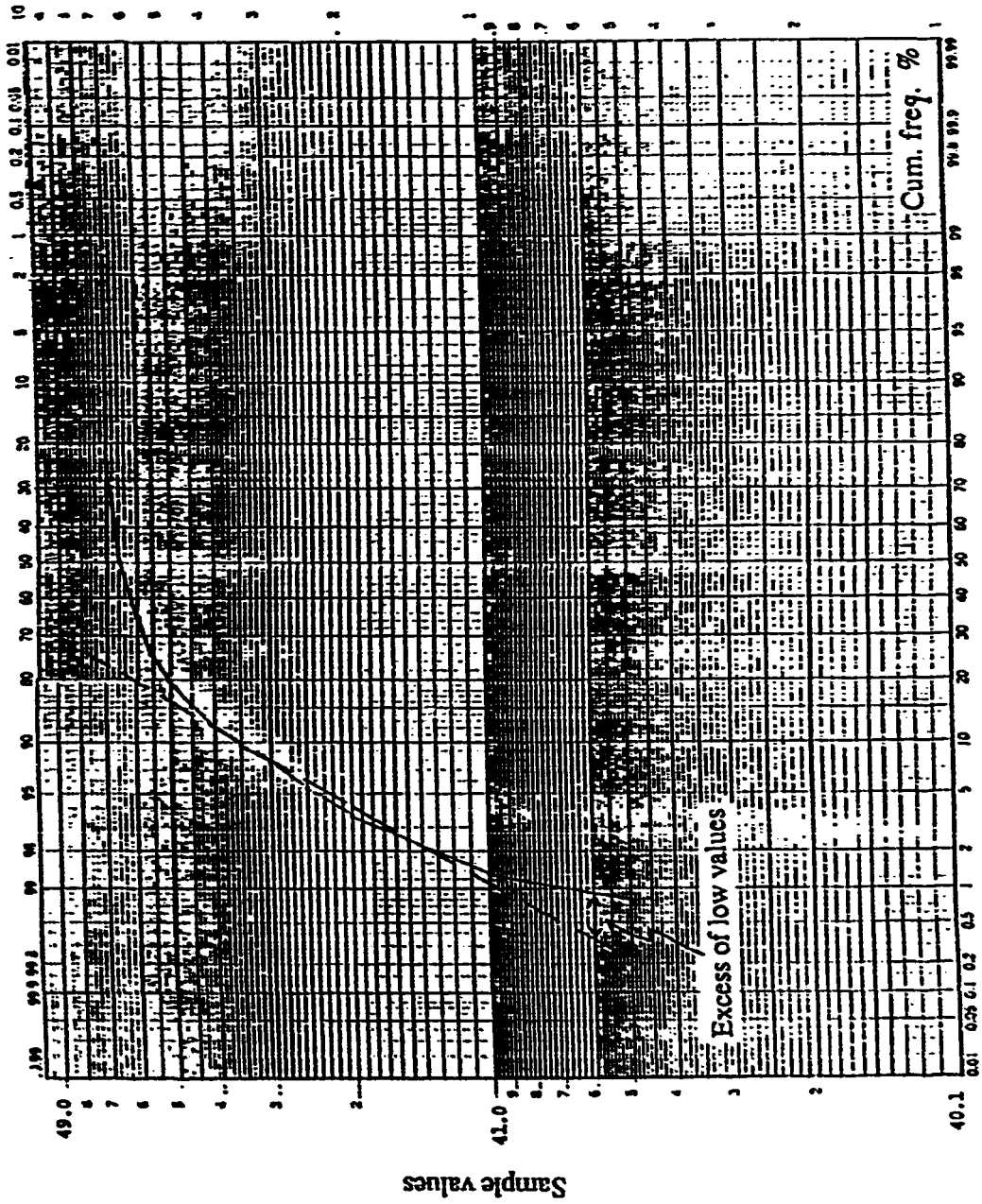

Fig. 4.7 : Percentage cumulative frequency plot for crude MgO% values.

4.5 Correlation diagrams

The correlation diagram is a valuable tool to reveal the statistical relationship and dependency between two variables. In practice, it is commonly used to predict the values of one variable from the values of another (David, 1977).

The correlation diagrams between MgO% and CaO% values (both crude and calcined) are illustrated in Figure 4.8 and 4.9. The following conclusions have been drawn from these diagrams:

1) There is an inverse relationship between the variables with most of the samples having higher MgO% and lower CaO% values which indicate high quality of the ore.

2) The Pearson's linear correlation coefficients between crude values of MgO% and CaO% was found to be -0.89 and the same coefficient between the calcined values to be -0.85. This negative correlation, which can be explained by the process of enrichment of Mg at the expense of Ca during the diagenesis of the orebody, suggests the suitability of Co-kriging in the local estimation of the deposit.

The correlation diagrams between the calcined and the crude values of individual variables (MgO% and CaO%) were, also, constructed and illustrated in Figures 4.10 and 4.11. A significant positive correlation with the coefficient value equal to + 0.97 was observed in both cases. It can be concluded that close similarities exist between crude and

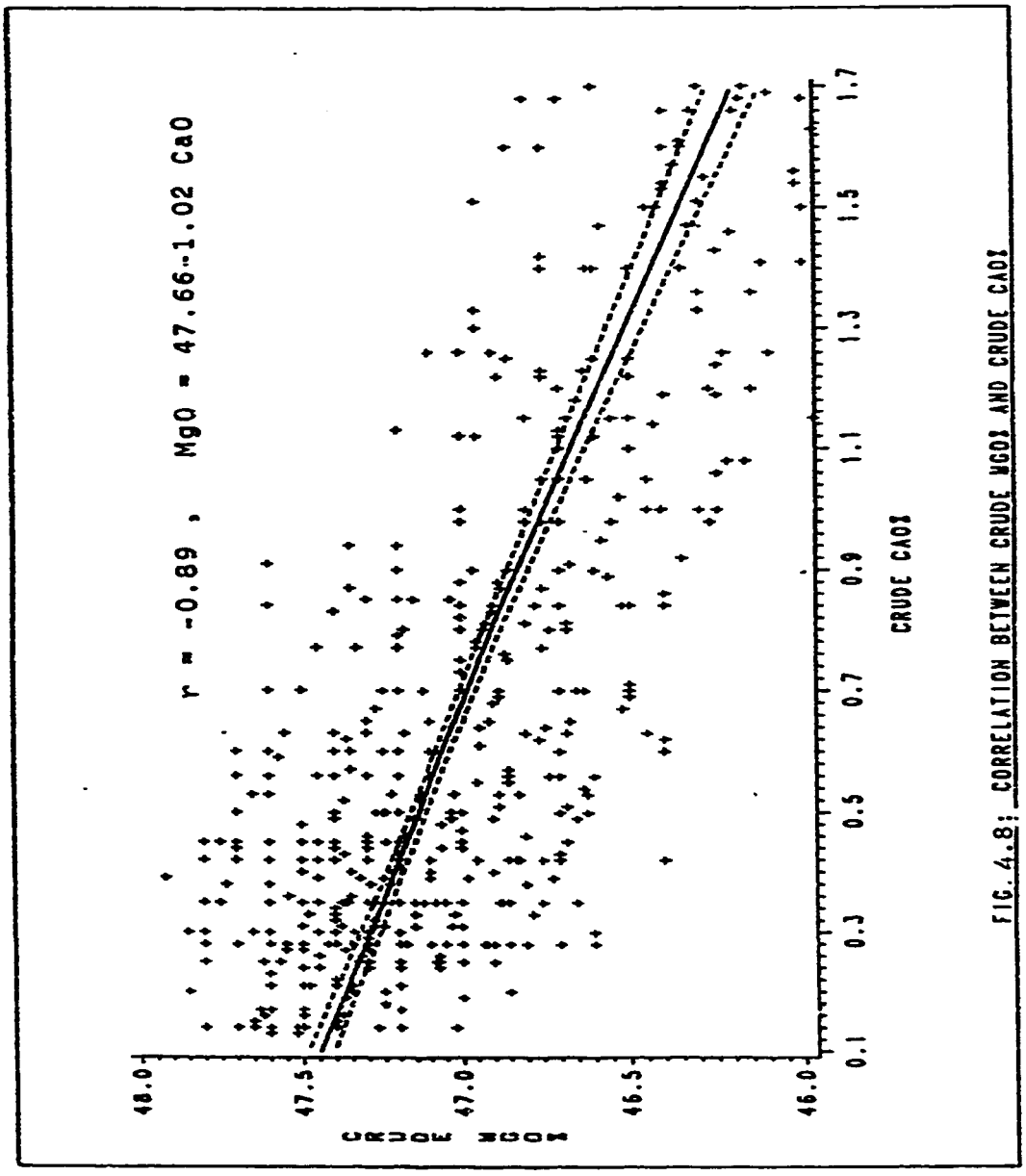

FIG. 4.8: CORRELATION BETWEEN CRUDE MGO% AND CRUDE CAO%

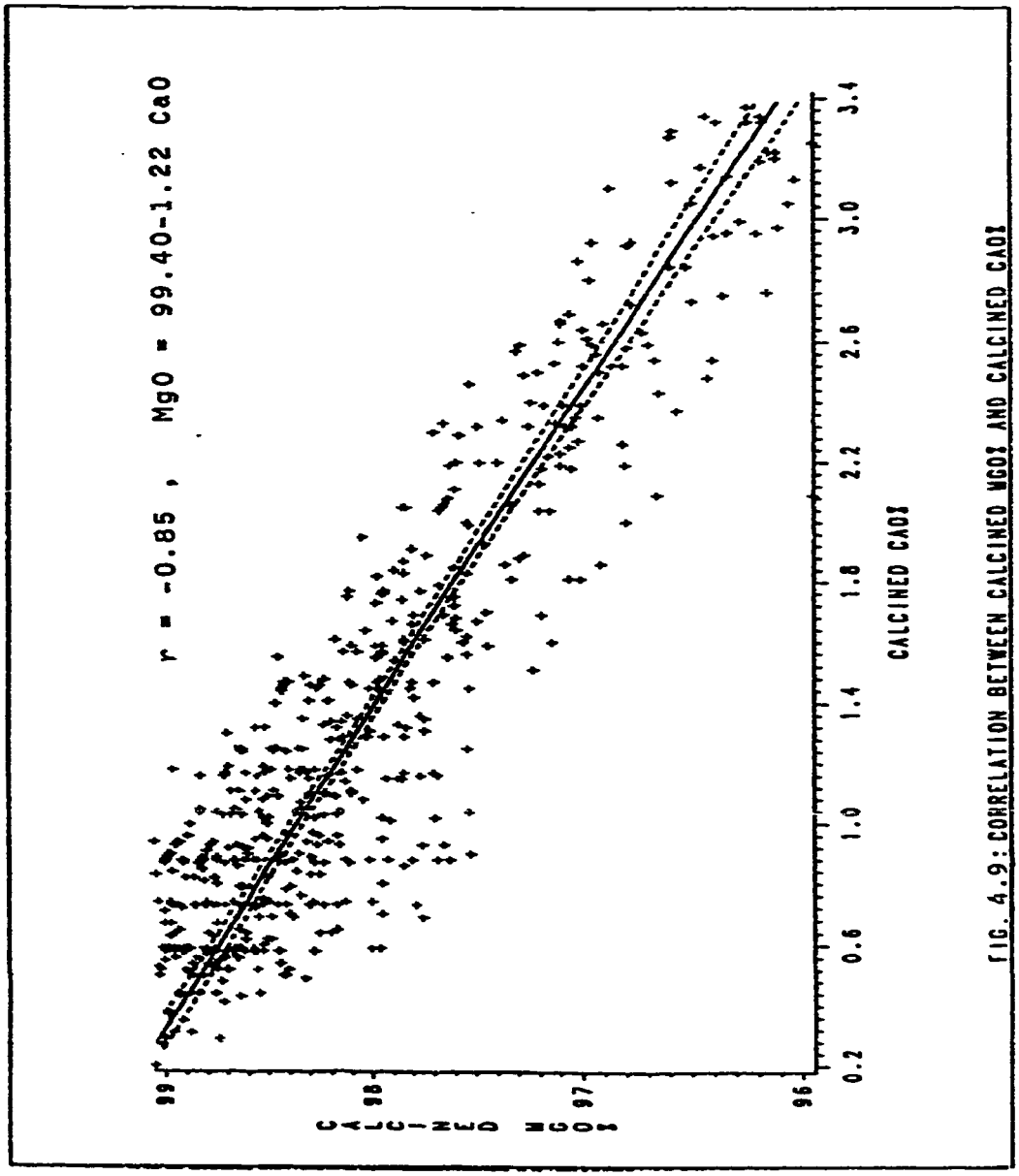

FIG. 4.9: CORRELATION BETWEEN CALCINED MGO% AND CALCINED CAO%

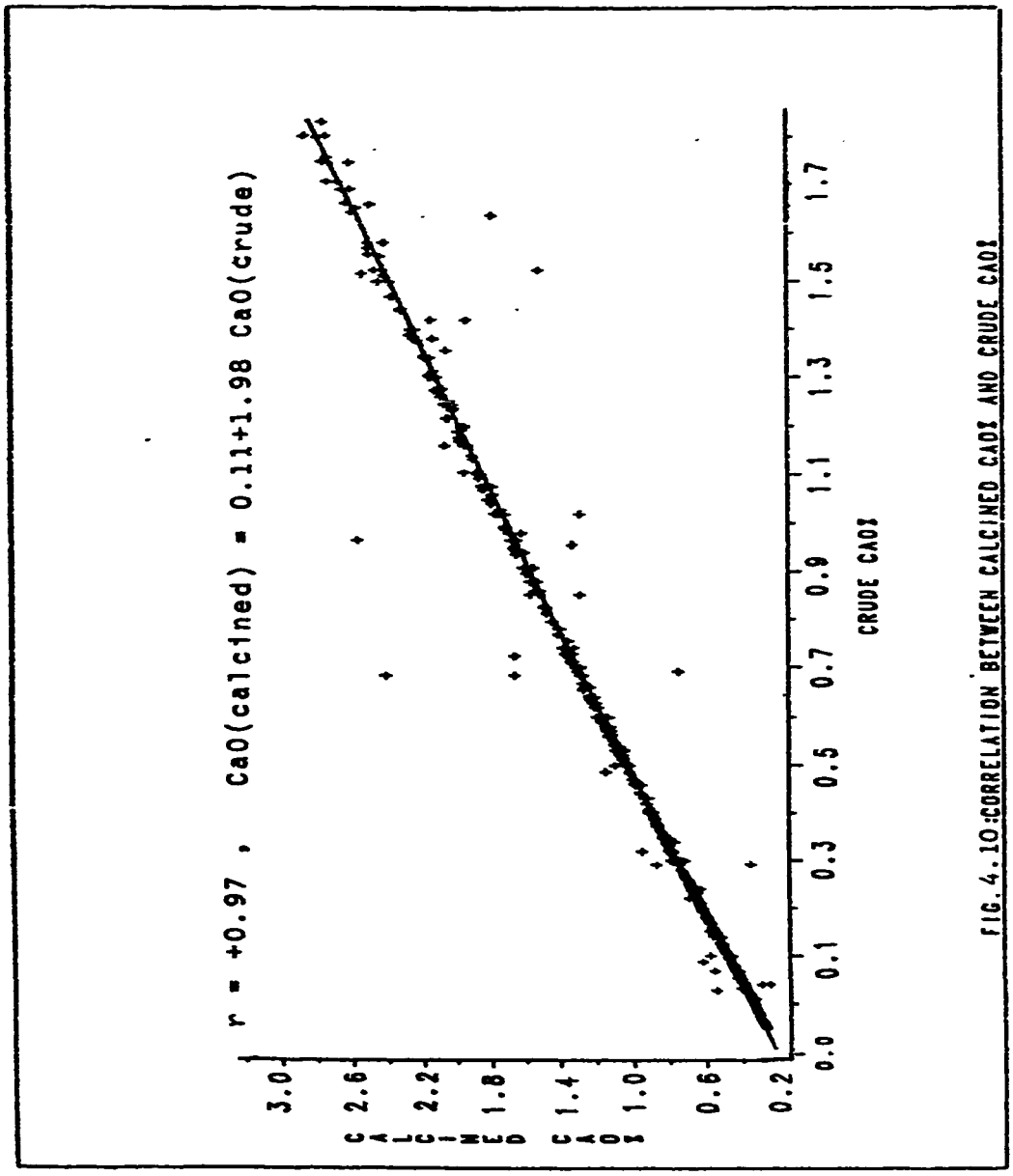

FIG. 4.10:CORRELATION BETWEEN CALCINED CaO% AND CRUDE CaO%

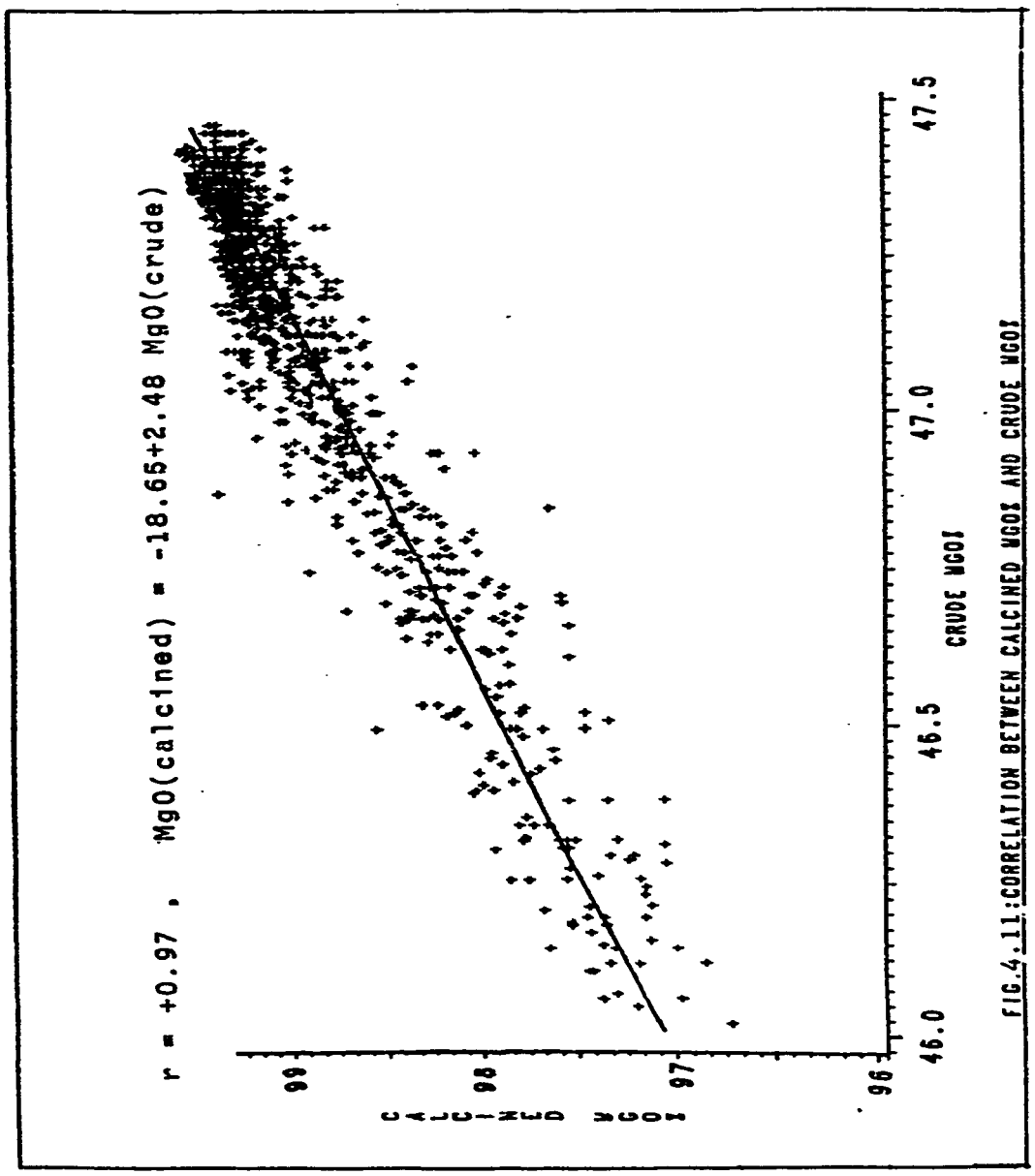

FIG.4.11:CORRELATION BETWEEN CALCINED MGOI AND CRUDE MGOI

calcined values of each sample. Therefore, the crude values for variables will be used in the subsequent geostatistical modelling.

To determine the adequacy of the linear regression models fitted in the correlation diagrams, it is necessary to calculate the coefficient of determination (R^2) for each model. Table 4.3 illustrates the model together with its related coefficient of determination for each diagram. Considering the high percentage values of coefficients of determination, it is concluded that the models were satisfactory to confirm the dependency relationships between the variables (i.e. one variable can be predicted on the basis of another using the linear regression model). For more details about R^2 - statistic, the reader is referred to Montgomery (1984).

4.6 Summary and discussions

1) The summary statistics for variables in individual drill-holes indicate that considerable variations exist in different parts of the deposit.

2) The lognormal behaviour of the histograms of sampling distributions suggest that it is appropriate to transform raw data values into the logarithmic ones before semivariogram calculations. Similar type of transformation has been applied in several case studies (Hohn, 1988).

3) Cumulative frequency plots indicate the presence of poorly mineralized zones located within the deposit.

TABLE 4.3: Results of fitted models and related coefficients of determination

Linear regression model	Coefficient of determination (R^2)	Related diagrams
MgO (crude) = 47.66 - 1.02 CaO(crude)	79%	Fig. 4.8
MgO (calcined) = 99.40 - 1.22 CaO(calcined	73%	Fig. 4.9
CaO (calcined) = 0.11 + 1.98 CaO(crude)	94%	Fig. 4.10
MgO (calcined) = - 18.65 + 2.48 MgO(crude)	95%	Fig. 4.11

4) The inverse relationship between the MgO% and CaO% values indicate the enrichment of Mg at the expense of Ca. This relationship, also, suggests the suitability of co-kriging method in the local estimation of the deposit.

CHAPTER 5

SPATIAL DISTRIBUTION OF THE GEOLOGICAL VARIABLES

5.1 Introduction

Geologists have always been aware of the fact that the value of a geological variable (i. e. grade, thickness, accumulation .. etc.) in a given volume (i.e orebody) depends on its position. To be able to take this phenomenon into consideration in the evaluation of geological variables, Professor Matheron has introduced the theory of "Regionalized Variables" in 1962. This theory attempts to describe the behavior of regionalized variables which are numerical functions describing geological phenomena in space (Matheron, 1971).

Geostatistics, which is based on the theory of regionalized variables, provides both quantitative and qualitative information about the geological variables. In comparison with the traditional estimation methods, geostatistics has more sound basis leading to the knowledge of the minimum variance unbiased estimators as well as the estimation errors associated with these estimates. Geostatistics began with the study of mine sampling data three decades ago and rapidly expanded, in recent years, to other fields of Earth Sciences including petroleum geology, hydrogeology, engineering geology and geophysics.

For the details about the theory of regionalized variables and geostatistics, the reader is referred to Armstrong (1989), Blais and Carlier (1968), David (1977), Journal and Huijbregts (1978), Matheron (1963 and 1971), Royle (1980), and Verly and others (1984).

The semivariogram is the basic tool in geostatistics. Therefore, a review about semivariogram including its definition, computation and modelling is given in this chapter. The remaining part of the chapter is devoted to the presentation of the experimental and model semivariograms for Zarghat magnesite deposit. This part, also, includes a simple test for the verification and the adjustment of model parameters.

5.2 Semivariogram

5.2.1 Definitions and importance

The semivariogram is defined as the half of the expected (mean) squared difference between sample values separated by vector h. It can be represented by the following theoretical expression:

$$\gamma(h) = \frac{1}{2} E [Z(x_i) - Z(x_i + h)]^2 \qquad (5.1)$$

The experimental semivariogram is, however, computed using the following mathematical expression:

$$\gamma(h) = \frac{1}{2} \sum_{i=1}^{n} \frac{[Z(x_i) - Z(x_i + h)]^2}{n\,(h)} \qquad (5.2)$$

where $Z(x_i)$ and $Z(x_i + h)$ are the values of variables at point x_i and $x_i + h$ respectively, and $n\,(h)$ is the number of data pairs $[Z(x_i), Z(x_i + h)]$ separated by vector h.

Depending on the value of h, the corresponding values of $\gamma(h)$ are computed and the relationship is expressed in the graphical form. Semivariogram is an important tool in geostatistics as it provides both quantitative and qualitative information about the spatial distribution of the variable under consideration.

5.2.2 Theoretical models of semivariograms

After constructing the experimental semivariogram, it is essential to fit a theoretical model to this semivariogram and to determine its parameters. Model semivariograms can be classified according to the presence or absence of sill in two groups: models with sill and models without sill. These models together with their mathematical expressions and parameters are listed in Tables 5.1 and 5.2. The spherical models have been found to be applicable to most types of mineral deposits as reported in the geostatistical literature.

TABLE 5.1: Theoretical models of semivariograms with sill

Model	Mathematical Expression		Parameters	Related figure
Simple Spherical	$\gamma(h) = C_o + C\left[\frac{3}{2}\frac{h}{a} - \frac{1}{2}\left(\frac{h}{a}\right)^3\right]$	for $h<a$	C_o, C, a	Fig. 5.1
	$\gamma(h) = C_o + C$	for $h \geq a$		
Exponential	$\gamma(h) = C_o + C\,[1 - \exp(-h/a)]$		C_o, C, a	Fig. 5.1
Gaussian	$\gamma(h) = C_o + C\,[1 - \exp(-h^2/a^2)]$		C_o, C, a	Fig. 5.1
Compound Spherical	$\gamma(h) = C_o + C_1\left[\frac{3}{2}\frac{h}{a_1} - \frac{1}{2}\left(\frac{h}{a_1}\right)^3\right] + C_2\left[\frac{3}{2}\frac{h}{a_2} - \frac{1}{2}\left(\frac{h}{a_2}\right)^3\right]$	for $h<a_1$	C_o, C_1, C_2, a_1, a_2	Fig. 5.2
	$\gamma(h) = C_o + C_1 + C_2\left[\frac{3}{2}\frac{h}{a_2} - \frac{1}{2}\left(\frac{h}{a_2}\right)^3\right]$	for $a_1<h<a_2$		
	$\gamma(h) = C_o + C_1 + C_2$	for $h \geq a_2$		

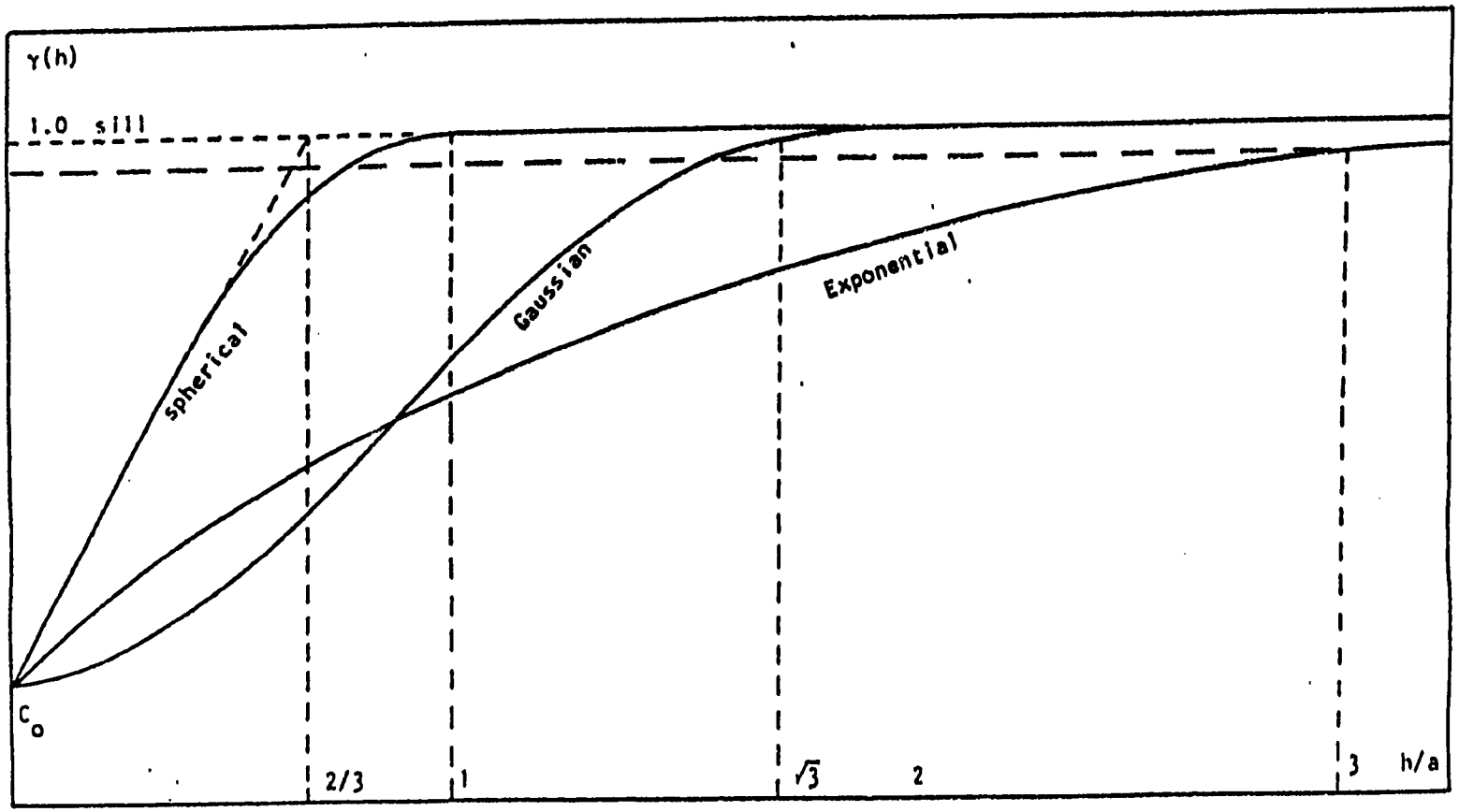

Fig. 5.1: Semivariogrms with sills (after Rendu, 1978).

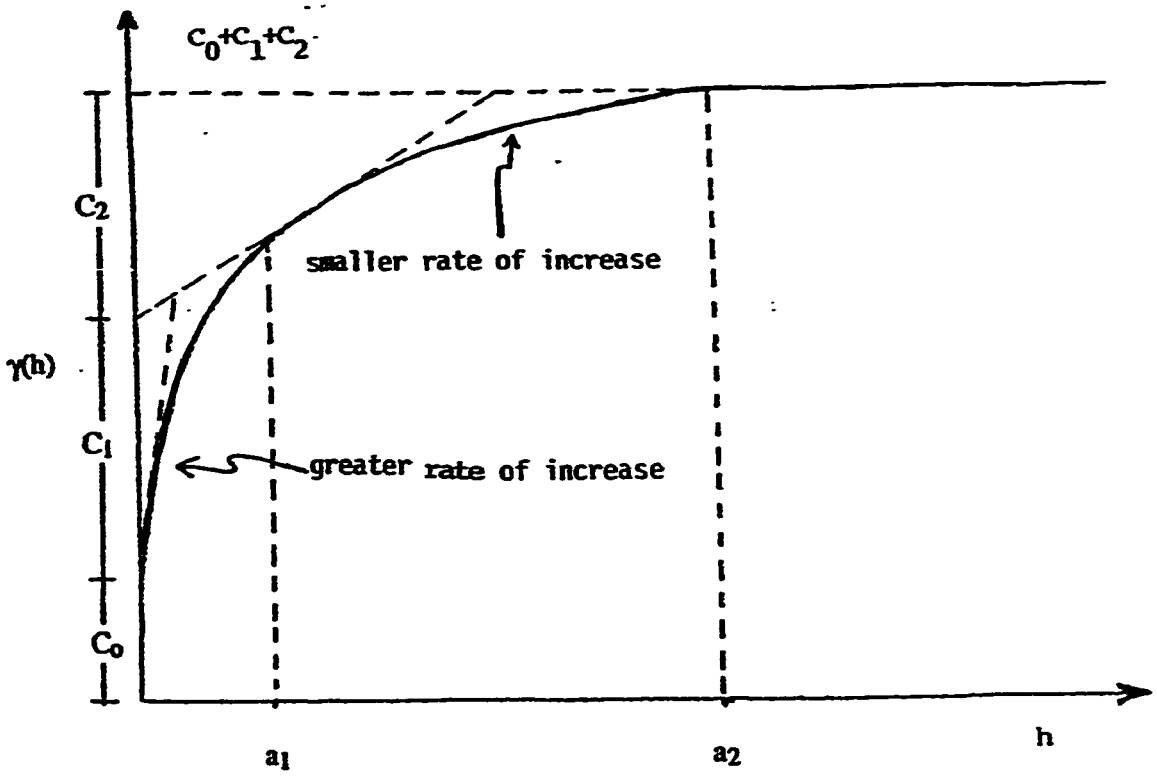

Fig. 5.2 - Compound spherical semivariogram

TABLE 5.2: Theoretical models of semivariograms without sill

Model	Mathematical Expression	Parameters	Related figure
Linear	$\gamma(h) = \omega h\theta$	ω = slope	Fig. 5. 3
De Wijsian	$\gamma(h) = 3\,\alpha\,\mathrm{Ln}\,h$	α = absolute dispersion	Fig. 5.4

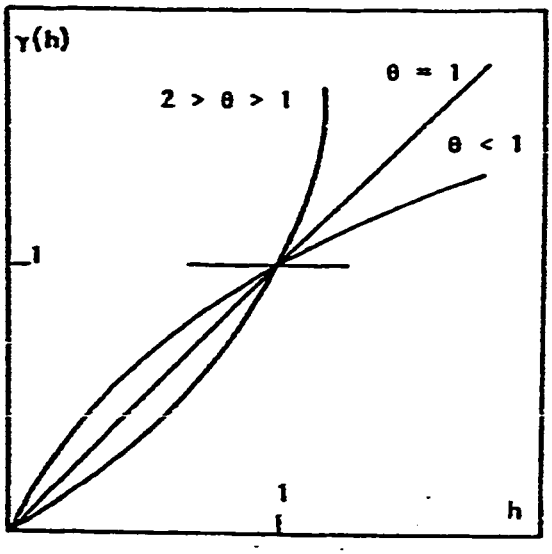

Fig. 5.3 - Linear semivariogram

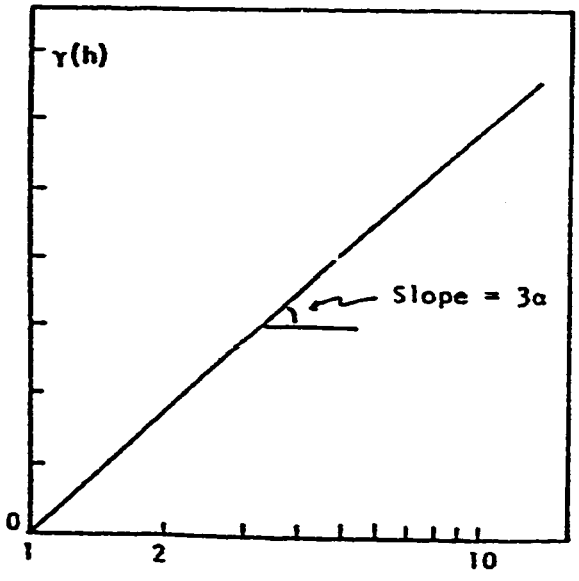

Fig. 5.4 - De Wijsian semivariogram

5.2.3 Semivariogram and geologic characteristics

Since the semivariogram measures the spatial variations of regionalized variable representing a geological phenomenon, it can be used as a descriptor of geological characteristics of this phenomenon. The most important geological characteristics that can be revealed by the semivariogram are:

Continuity: this feature can be considered as a measure of similarity of sample values at smaller distances. It can be detected by the behavior of semivariogram near the origin. Four types of behavior can be distinguished as summarized in Table 5.3.

Zone of influence: this is the zone beyond which the influence of a sample disappears. It corresponds to the distance at which $\gamma(h)$ reaches the sill as shown in Figure 5.6. This distance, which is referred to as the range, represents the average dimensions of the geological structures such as bedding, lenses and basins.

Anisotropies: anisotropy means that the zone of influence and/or sill value vary in different directions. If the semivariograms along various directions are identical, the regionalized variable is said to be isotropic. The semivariograms in different directions, in such case, can be combined to give average semivariogram. Two types of anisotropy may be distinguished. These are geometrical and zonal anisotropies summarized in Table 5.4. The geometrical anisotropy indicates the

TABLE 5.3: Types of continuity

Type	Behavior near the origin	Geologic reason	Examples	Related Figures
Continuous	prabolic	highly continuous phenomena	bed-thickness	Fig. 5.5 (a)
Linear	has oblique tangent	continuous phenomena	base-metal deposits	Fig. 5.5. (b)
Nugget	discontinuous (i.e. $\gamma(h) \neq 0$ at $h = 0$)	phenomena with nugget effect.	gold deposits	Fig. 5.5 (c)
Random	purely random	completely discontinuous phenomena	rarely observed in nature except for some trace elements	Fig. 5.5 (d)

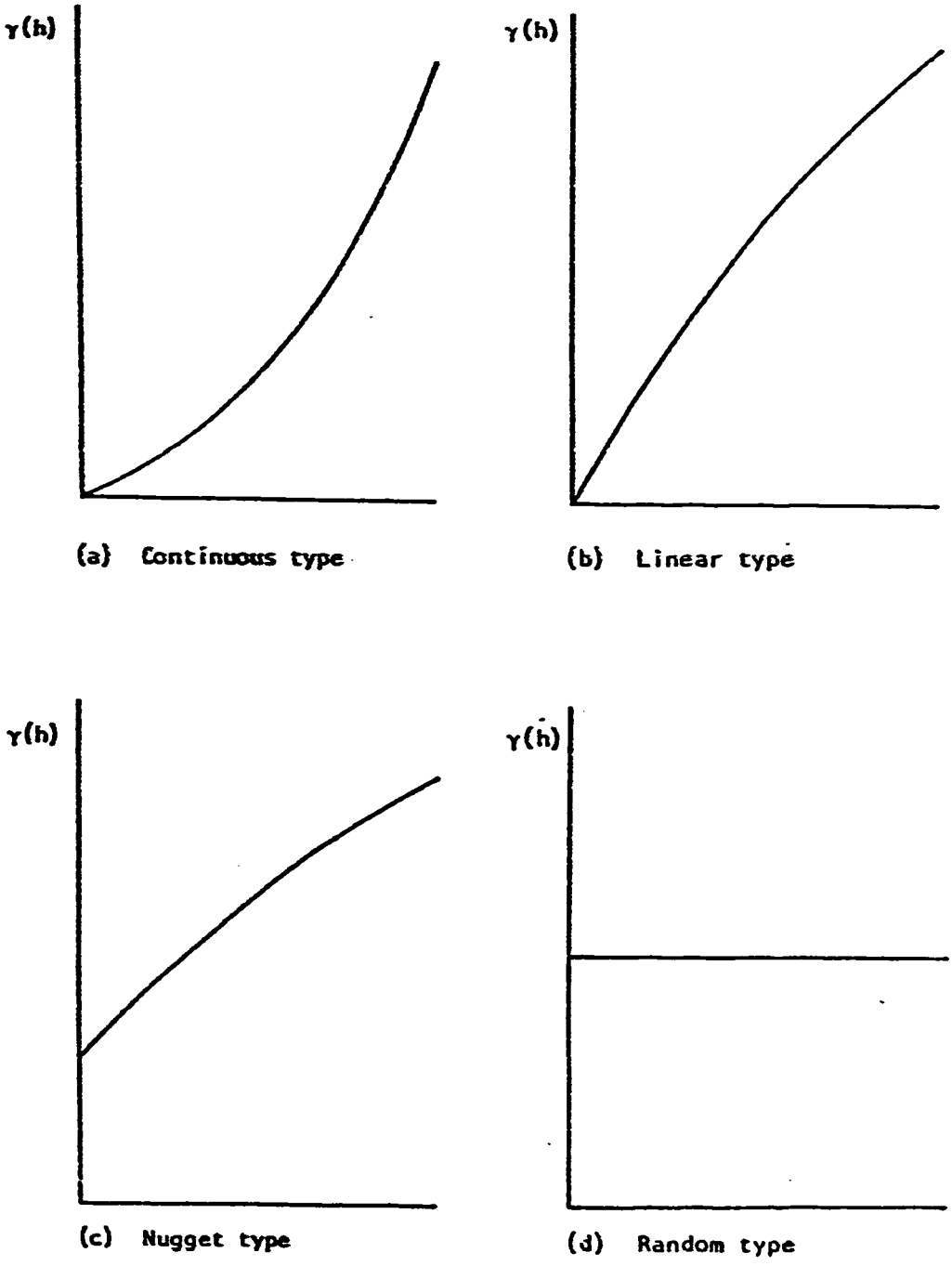

Fig. 5.5 - Types of continuity

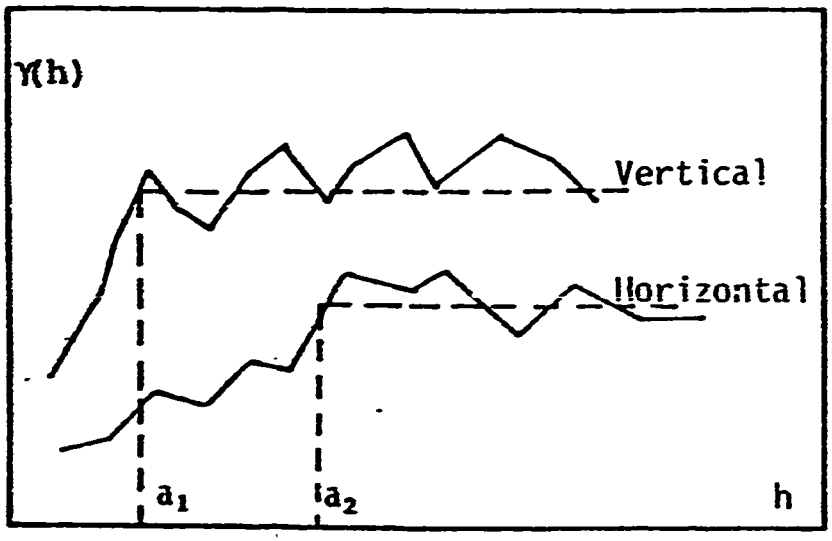

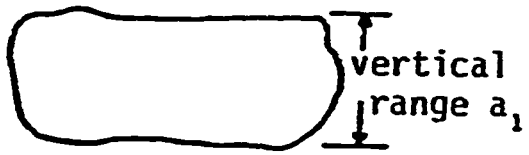

cross-section of the structure

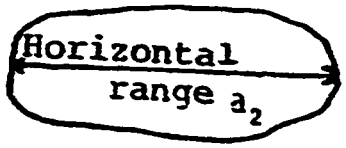

top view of the structure

Fig. 5.6 : Zones of influence and related structures (journel and Huij bregts, 1978)

TABLE 5.4: Types of anisotropies

Type	Diagnostic Characters	Geologic reason	Related figure
Geometrical	different ranges in different directions.	presence of structures that have unequal dimensions such as micro-basins, lenses .... etc.	Fig. 5.7 (a)
Zonal	different sills in different directions	presence of layering or zonation. It is commonly observed in stratiform deposits.	Fig. 5.7 (b)

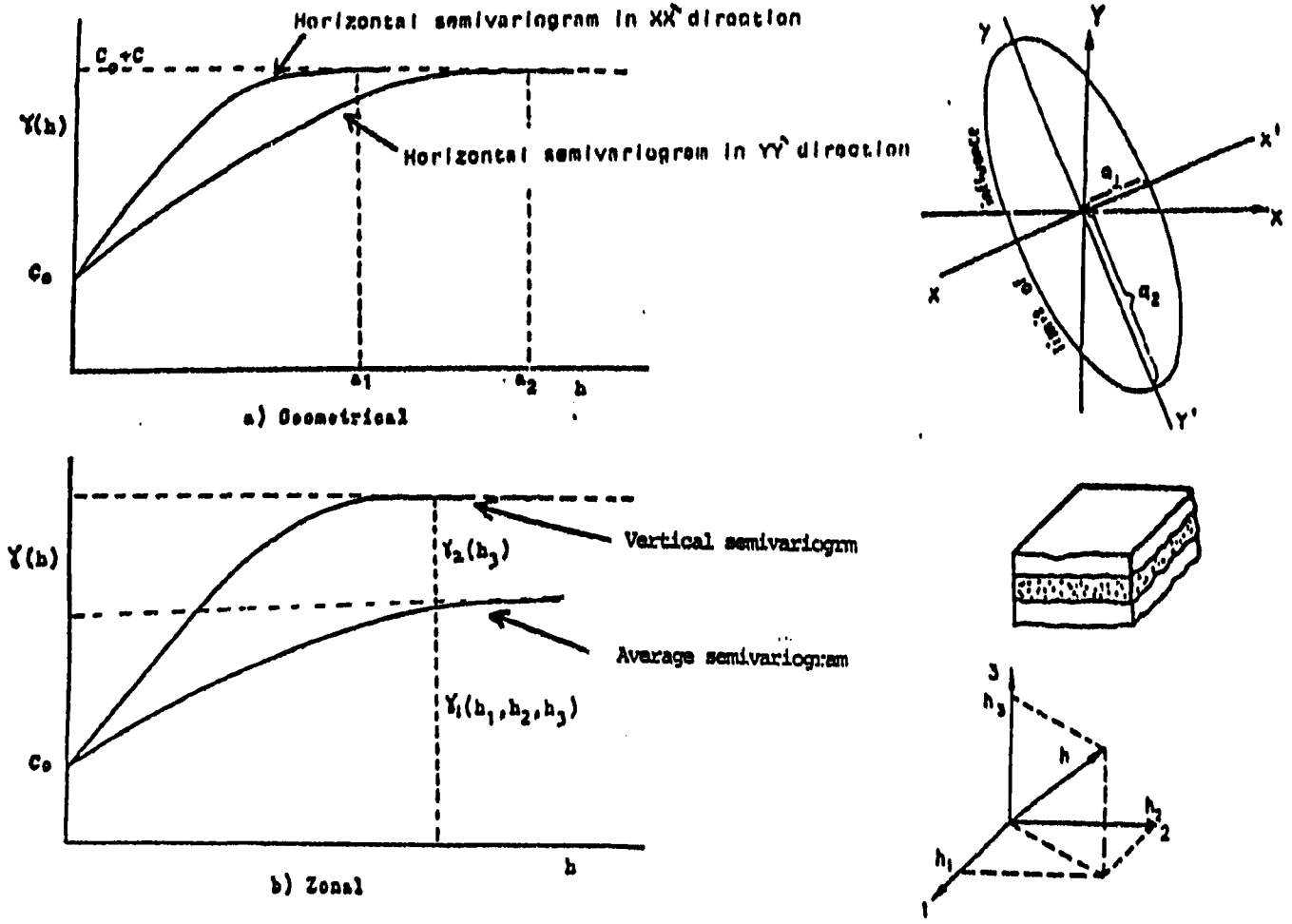

Fig. 5.7 : Types of anisotropies (Rendu, 1978)

presence of structures that have unequal dimensions. The zonal anistropy on the other hand, points to the presence of layering or zonation in the deposit.

5.2.4 Verification of model semivariograms

The verification and necessary adjustment of model semivariograms should be carried out before any application of these models. Since all subsequent interpretations and estimations are based on model parameters, any inaccuracy in these parameters will lead to grave consequences. Therefore, it is necessary to verify the validity of model parameters.

One of the methods used to verify the validity of model parameters is the comparison between observed and estimated dispersion variances of samples within the deposit. This method assumes that the sample support can be approximated by a point (i.e, the fitted model can be approximated by a point model). This assumption is valid when the support of samples is small as compared to the range of semivariogram and acceptable in most cases (Journel and Huijbregts, 1978). The basic steps in the application of this method to a compound spherical model are listed as follows:

1) compute the observed dispersion variance (statistical variance) of samples within the deposit, i.e. S^2 (O/D).

2) find the dispersion variance of samples within a block that has specific dimensions using model parameters. This variance is given by the following expression:

$$\sigma^2 (O/V) = C_o + C_1 [F(H/a_1, L/a_1)] + C_2 [F(H/a_2, L/a_2)] \quad (5.3)$$

where L and H are block dimensions and F(H/a, L/a) is a function read directly from Figure 5.8.

3) find the dispersion variance of blocks within the deposit using the following expression:

$$\sigma^2 (V/D) = C_1 [1-F(H/a_1, L/a_1)] + C_2 [1-F(H/a_2, L/a_2)] \quad (5.4)$$

4) Compute the estimated dispersion variance of samples within the deposit. This variance is equal to the sum of two variances given by the equations 5.3 and 5.4.

$$\sigma^2 (O/D) = \sigma^2 (O/V) + \sigma^2 (V/D) \quad (5.5)$$

5) finally, compare $S^2(O/D)$ with σ^2 (O/D) and derive conclusions about the validity of parameters.

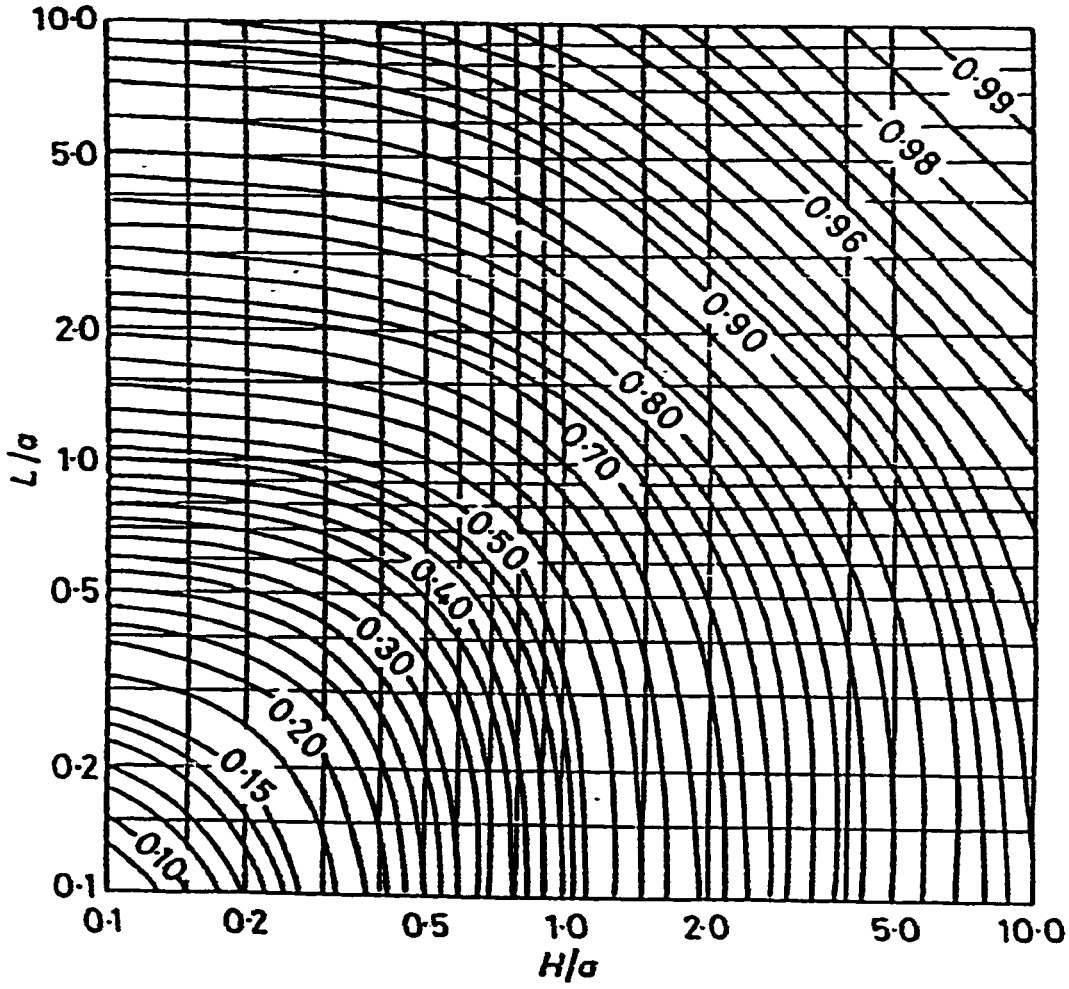

Fig. 5.8 : Two-dimentional F-Function chart (after Sahin and Royle, 1990)

5.3 Semivariogram modelling for Zarghat magnesite deposit

5.3.1 Vertical semivariograms

To determine the spatial behavior in the vertical direction, the vertical semivariograms were computed for the logarithmic values (refer to Section 4.6) of both crude CaO% and crude MgO% along individual drill-holes. Several of these semivariograms, which were computed using the program VARIO3 of GEOSTAT computer package, are shown as examples in Appendix C. These semivariograms exhibit similar behavior suggesting the similarity of geological controls prevailing at the time of deposition. Therefore, they were combined to give the average (isotropic) vertical semivariogram for the whole deposit.

Figures 5.9 and 5.10 illustrate the average vertical experimental semivariograms for CaO (log %) and MgO (log %) respectively. The first points on these semivariograms were estimated with 1053 and 1056 pairs for CaO (log %) and MgO (log %) respectively. The following thirty points, for both semivariograms, have been estimated with pairs ranging from 1012 to 315, indicating the reliability of estimates. The compound spherical models with a short range of about 7m and a long range of about 22m appear to be suitable in both cases. In physical terms, these ranges indicate the presence of two groups of structures: smaller structures with an average thickness of about 7m nested within larger structures that have an average thickness of about 22m

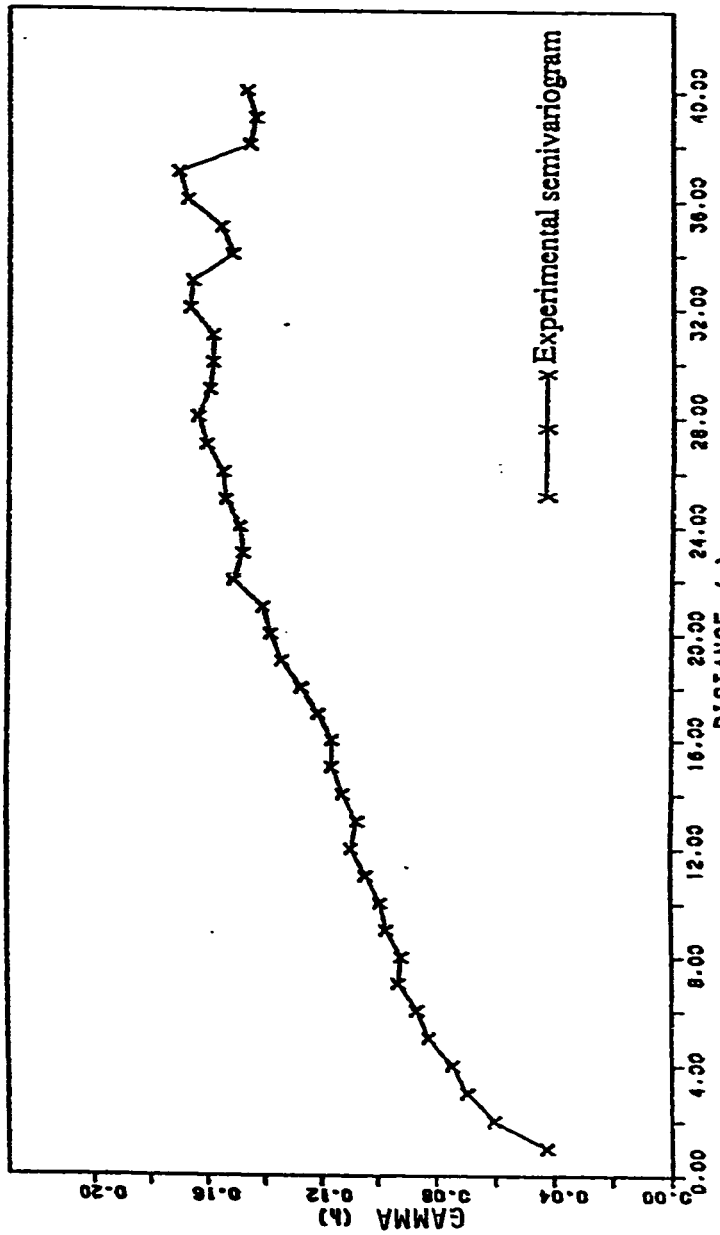

Fig. 5.9 - AVERAGE VERTICAL LOGARITHMIC SEMIVARIOGRAM (1m Lag) for CaO (log%)

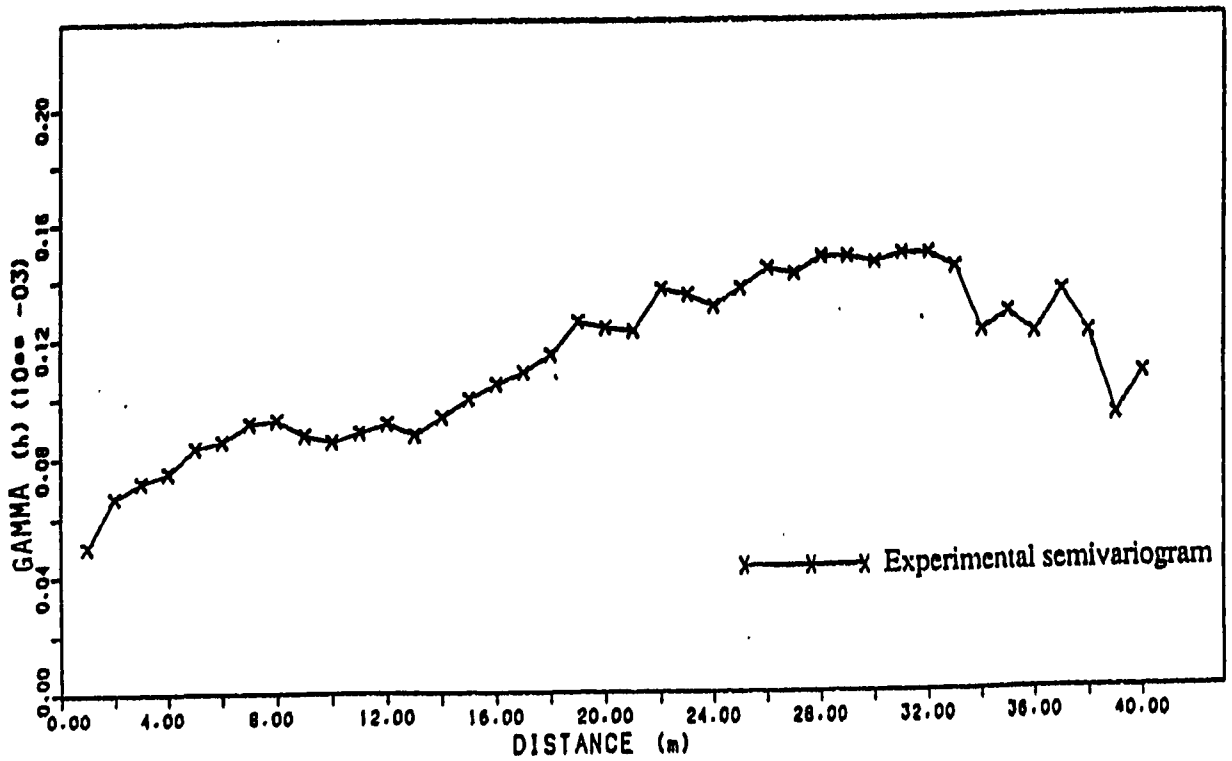

Fig. 5.10 - AVERAGE VERTICAL LOGARITHMIC SEMIVARIOGRAM (1m lag) for MgO (log%)

Although the general behavior of these semivariograms are similar, there are differences in sill values. The sill value of MgO (log%) semivariogram is lower than that of CaO (log %) semivariogram indicating more uniform spatial distribution of MgO within the deposit. Nugget variances can be detected from both CaO (log%) and MgO (log%) semivariograms with values of 0.026 $(\log\%)^2$ and 0.03×10^{-3} $(\log\%)^2$ respectively. These indicate the discontinuity of the semivariograms at their origins, and may reflect the presence of smaller scale structures that can not be detected with 1m sample spacing.

5.3.2 Horizontal semivariograms

The directional semivariograms for each variable in E-W, NE-SW, N-S and NW-SE directions have been constructed with an angle of regularization of 20° and illustrated in Appendix D.

Study of their general behavior indicates that they are similar in many aspects. Therefore, the isotropy assumption in the horizontal direction appears to be valid for the semivariograms of both CaO (log %) and MgO (log %).

The isotropic horizontal semivariograms and their fitted models for CaO (log %) and MgO (log %) are illustrated in Figures 5.11 and 5.12 respectively. The first point on the experimental semivariogram of CaO (log %) has been estimated with 3018 pairs. On the other hand, 2988 pairs were used to estimate the first point on MgO (log %) semivariogram.

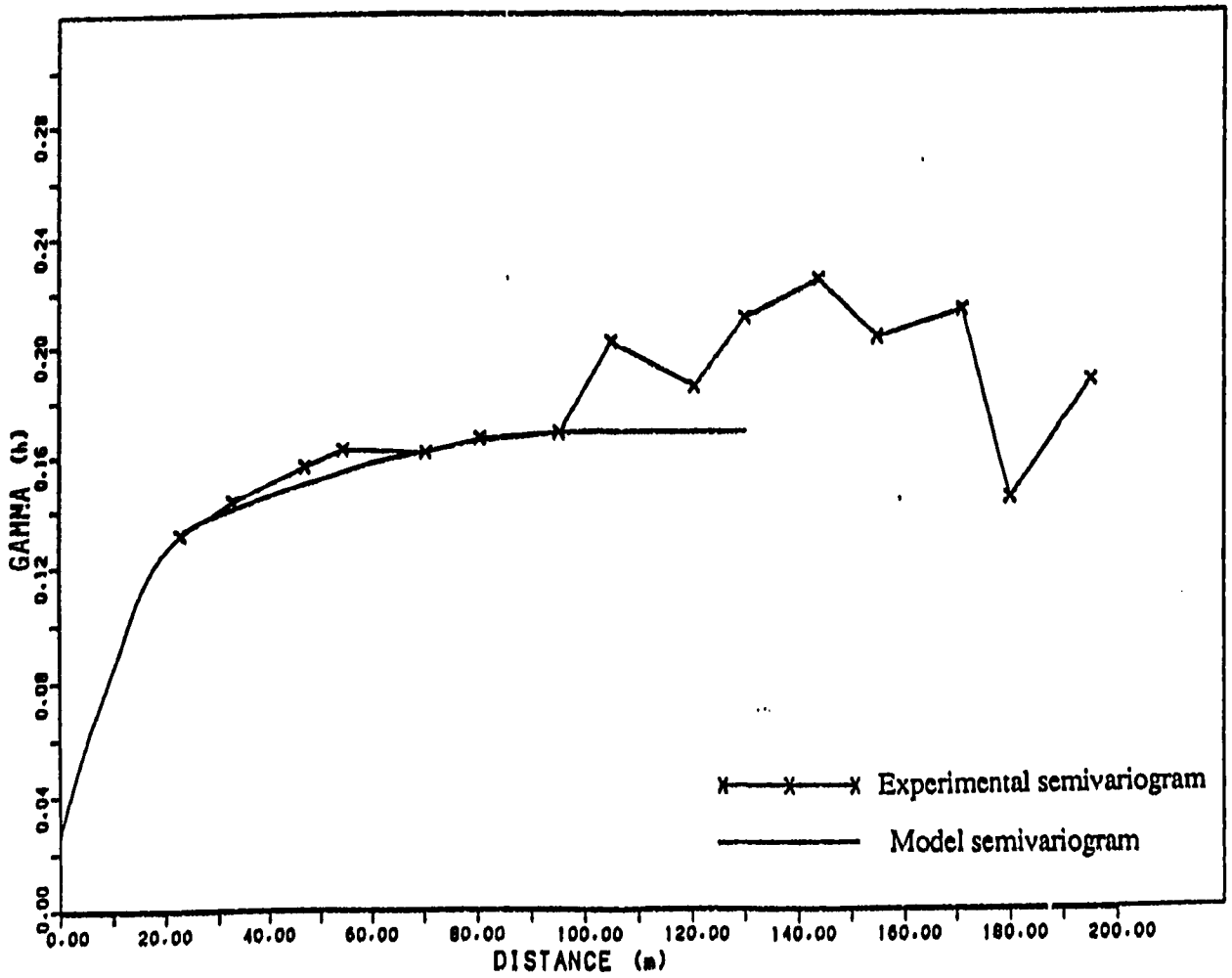

Fig. 5.11: Isotropic horizontal logarithmic semivariogram for CaO (log %)

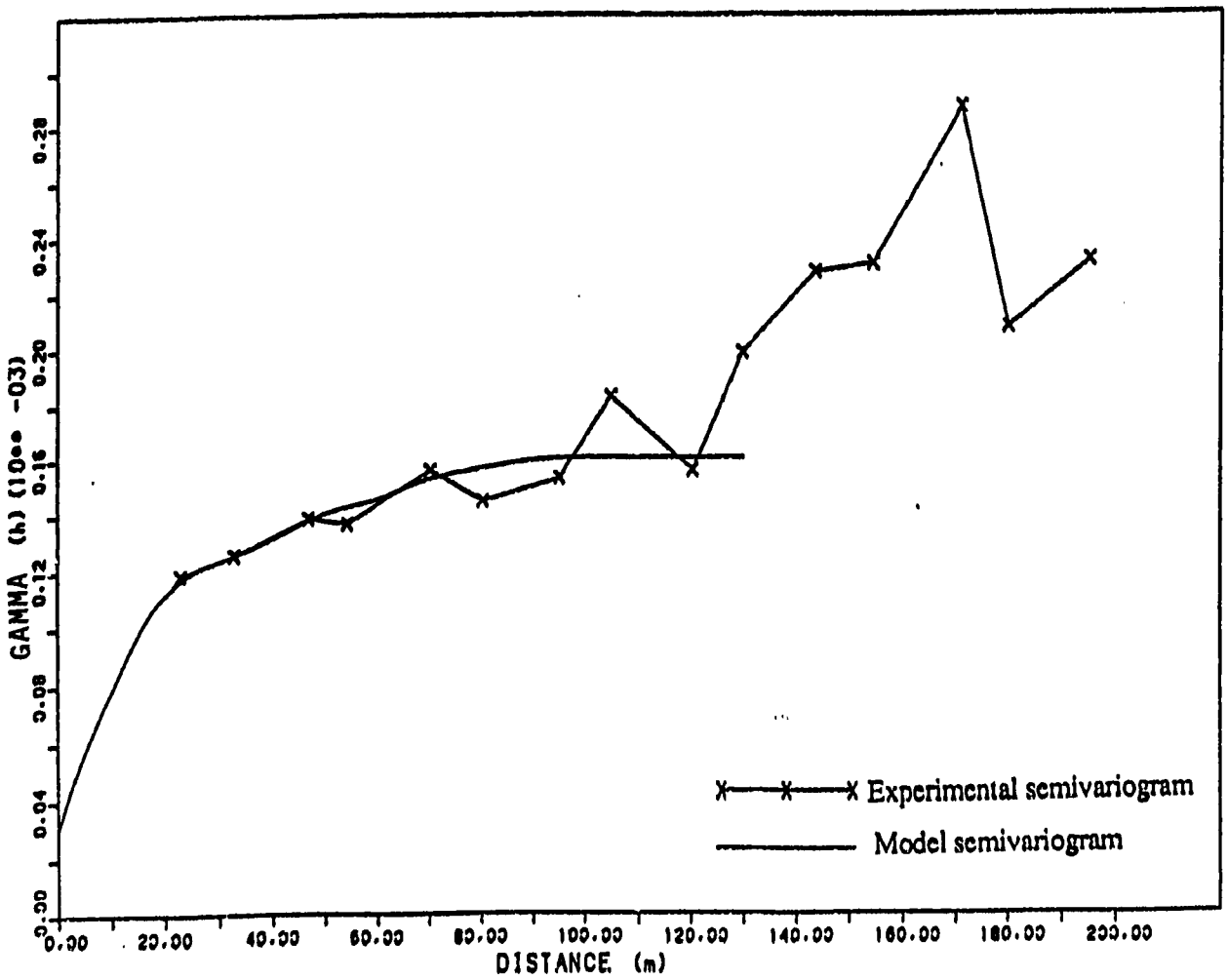

Fig. 5.12: Isotropic horizontal logarithmic semivariogram for MgO (log %)

All other experimental points for both semivariograms were estimated with mostly over 400 pairs ensuring excellent reliability. The compound spherical models were fitted by considering several factors including the general behavior of the semivariogram under consideration, the nugget constant fixed from the corresponding vertical semivariogram as well as the statistical variance of sample values.

The models for both variables exhibit discontinuity at the origin and imply the presence of nested structures characterized by ranges of 25m and 100m respectively. The sill values for both CaO (log %) and MgO (log %) isotropic semivariograms in the horizontal direction are nearly similar to the corresponding sill values which have been determined from the semivariograms in the vertical direction. This is an indication of similar spatial behavior in the horizontal and vertical directions.

The model parameters for both variables are listed in Table 5.5. These parameters will be used in subsequent estimation (kriging) procedures described in the following chapters.

5.3.3 Semivariograms for in-fill drill-holes.

The horizontal semivariograms along NE and NW directions and the average horizontal semivariogram for both directions using the data from in-fill drill-holes were computed and illustrated in Appendix E. These semivariograms reveal the following information:

TABLE 5.5: Parameters for horizontal model semivariograms

Parameters	Variables	
	CaO	MgO
C_o (log%)^2	0.026	0.03 x 10^{-3}
C_1 (log%)^2	0.088	0.065 x 10^{-3}
C_2 (log%)^2	0.054	0.065 x 10^{-3}
a_1 (m)	25	25
a_2 (m)	100	100

1) A structure with about 13 m can be detected from CaO (log %) semivariogram. However, there is no clear evidence of a structure in MgO (log %) semivariograms.

2) The nugget variances for both semivariograms appear to be zero.

It should, however, be pointed out that because of the limited number of samples used in computing these semivariograms and the fact that the in-fill drill-holes have been terminated at depth of 6m as mentioned earlier, the information derived from these semivariograms are not considered reliable.

5.3.4 Verification of model parameters

The models fitted to the experimental semivariograms were tested and verified in order to determine their accuracy. Considering 25m x 25m x 1m blocks in both cases, the method outlined in section 5.2.4 has been applied to the horizontal models of both variables. The results of verification are listed in Table 5.6 and the details of calculations given in Appendix F.

Considering the low percentage differences between the observed and estimated dispersion variances of samples within deposit, it can be concluded that the models accurately represent experimental semivariograms. The values of ratios between the

TABLE 5.6: Results of observed and estimated dispersion variances

Variable	Block dimensions (mxmxm)	σ^2(O/V) (log %)^2	σ^2(V/D) (log %)^2	Estimated σ^2(O/D) (log %)^2	Observed S^2(O/D) (log %)^2	Difference	Ratio
CaO (log %)	25 x 25 x 1	0.094	0.074	0.168	0.177	5%	1.05
MgO (log %)	25 x 25 x 1	0.085 x 10^{-3}	0.075 x 10^{-3}	0.160 x 10^{-3}	0.166x 10^{-3}	3.6%	1.04

corresponding observed and estimated dispersion variances, also, support the same conclusion. The variance ratios are nearly equal to 1 in both cases. This indicates that there is no significant difference between the two variances. Therefore, horizontal models for both CaO (log %) and MgO (log %) are considered to be reliable for use in the subsequent estimations.

5.4 Summary and Discussion

Semivariogram modeling for both variables in Zarghat magnesite deposit led to the following conclusions:

1) Compound spherical models have been fitted to both vertical and horizontal semivariograms.

2) The behavior of the semivariograms near origin indicate nugget type with average continuity. The nugget variances are relatively small as expected from a deposit of sedimentary origin.

3) The nugget variances may be due to the presence of microstructures such as randomly distributed dolomitic veinlets within the deposit in addition to the errors in sampling, assaying and chemical analysis.

4) The presence of smaller and larger structures within the deposit have been indicated by the compound models. Average vertical dimensions of these structures are 7m and 22m and the average horizontal dimensions are 25m and 100m respectively. These structures may be explained by the presence of small depositional basins nested within larger one.

5) Low percentage differences obtained between the observed and estimated dispersion variances of samples indicate that the models accurately represent the experimental semivariograms and will provide sound basis for local estimation.

CHAPTER 6

LOCAL ESTIMATION AND GRADE-TONNAGE RELATIONSHIP

6.1 Introduction

The computation of the optimum estimates of mining blocks in the deposit and the construction of the grade-tonnage relationship based on these estimates are two other objectives of this study. Brief reviews of local estimation and grade-tonnage relationship are given in the following sections. These are followed by presentation and discussions of the results on Zarghat magnesite deposit.

6.2 Local estimation

Several estimation methods have been introduced in order to solve the problem of local estimation. Most of these methods are, however, unable to give unbiased estimates with minimum variances (Royle, 1977). Kriging, which was introduced by Matheron and named after Dr. Krige in early 1960's, is a geostatistical estimation procedure used to obtain local estimates. This method provides unbiased estimates with minimum estimation variances referred to as the kriging variances. The latter is used to measure the reliability of the estimates. The lower the kriging variances the more reliable the estimates and vice versa.

6.2.1 Block kriging

The kriged estimates are obtained by assigning optimal weights to sample values used to estimate (i.e., to krige) block.

Let Z be the true value of the block to be estimated and Z* be its estimated value. If $x_1, x_2, x_3, \ldots\ldots x_n$ are sample values used in estimation, the kriged estimator Z*, is given as the linear combination of these sample values as shown in the following formula:

$$Z^* = \sum_{i=1}^{n} \lambda_i x_i \qquad (6.1)$$

Where λ_i's are the weighting coefficients assigned to the samples. The main problem, in kriging, is to calculate λ_i values which satisfy the following criteria simultaneously:

1. The estimator, Z*, must be unbiased

i. e. $$E[Z - Z^*] = 0 \qquad (6.2)$$

This condition implies that the sum of the weights is equal to unity

i. e. $$\sum_{i=1}^{n} \lambda_i = 1 \qquad (6.3)$$

2. The estimation variance, $E[(Z-Z^*)^2]$, must be minimum. The estimation variance can be expressed as follows:

$$E[(Z-Z^*)^2] = E(Z)^2 - 2E(ZZ^*) + E(Z^*)^2$$

Now, substituting the value of Z^* from equation (6.1) leads to:

$$E[(Z-Z^*)^2] = E(Z)^2 - 2E(Z\sum_i \lambda_i x_i) + E(\sum_i \sum_j \lambda_i \lambda_j x_i x_j)$$

$$= \sigma_Z^2 - 2\sum_i \lambda_i \sigma_{Zx_i} + \sum_i \sum_j \lambda_i \lambda_j \sigma_{x_i x_j} \qquad (6.4)$$

Where σ_Z^2 designates the variance of sample within the block and $\sigma_{x_i x_i}$ the average value of covariance function $\sigma(h)$ when two extremities of the vector h is located at point x_i and x_j respectively.

The above mentioned problem can be restated as the computation of weights (λ_i's) which minimize the estimation variance, $E[(Z-Z^*)^2]$, under the condition that $\sum \lambda_i = 1$. To solve this problem according to the Lagrange principle, the following expansion should be minimized:

$$F = E[(Z-Z^*)^2] - 2\mu(\sum_{i=1}^{n} \lambda_i - 1)$$

$$F = \sigma_Z^2 - 2\sum_i \lambda_i \sigma_{Zx_i} + \sum_i \sum_j \lambda_i \lambda_j \sigma_{x_i x_i} - 2\mu(\sum_i \lambda_i - 1) \qquad (6.5)$$

where μ is additional unknown called the Lagrange multiplier. Thus, the derivatives of equation (6.5) should be taken with respect to all unknowns (i.e λ_i's and μ) and equated to zero:

$$\frac{\delta F}{\delta \Sigma \lambda_i} = -2\sigma_{Zx_i} + 2\sum_j \sigma_{x_i x_i} - 2\mu$$

$$= -\sigma_{Zx_i} + \sum_j \sigma_{x_i x_j} - \mu = 0 \qquad (6.6)$$

and,

$$\frac{\delta F}{\delta \mu} = 2\sum_i \lambda_i - 2$$

$$= \sum_i \lambda_i - 1 = 0 \qquad (6.7)$$

The equations (6.6) and (6.7) are rearranged to give the following linear system of n + 1 equations with n + 1 unknowns referred to as the Kriging system:

$$\left.\begin{aligned} \sum_j \lambda_j \sigma_{x_i x_j} - \mu &= \sigma_{Zx_i} \qquad (i = 1, \ldots\ldots, n) \\ \sum_i \lambda_i &= 1 \end{aligned}\right\} \quad I$$

Multiplying both sides of the first expression in system I by $\sum_i \lambda_i$ will produce the following expression:

$$\sum_i \sum_j \lambda_i \lambda_j \sigma_{x_i x_j} - \sum_i \lambda_i \mu = \sum_i \lambda_i \sigma_{Zx_i}$$

$$\sum_i \sum_j \lambda_i \lambda_j \sigma_{x_i x_j} = \sum_i \lambda_i \sigma_{Zx_i} + \mu \qquad (6.8)$$

Substituting this value of $\sum_i \sum_j \lambda_i \lambda_j \sigma_{x_i x_j}$ in expression (6.4) will give the minimum estimation variance referred to as kriging variance and denoted by (σ_k^2):

$$\sigma_k^2 = \sigma_Z^2 - 2\sum_i \lambda_i \sigma_{Zx_i} + \sum_i \lambda_i \sigma_{Zx_i} + \mu$$

$$= \sigma_Z^2 - \sum_i \lambda_i \sigma_{Zx_i} + \mu \qquad (6.9)$$

The Kriging system can, also, be expressed in terms of the semivariogram function. This is achieved by substituting the semivariogram values for the covariances in the first expression in system I (Journel and Huijbregts, 1978).

$$\text{i.e., } \sigma(h) = \gamma(\infty) - \gamma(h) \qquad (6.10)$$

similarly,

$$\sum_j \lambda_j [\gamma(\infty) - \gamma_{x_i x_j}] - \mu = \gamma(\infty) - \gamma_{Zx_i}$$

$$\sum_j \lambda_j \gamma(\infty) - \sum_j \lambda_j \gamma_{x_i x_j} - \mu - \gamma(\infty) = - \gamma_{Zx_i} \qquad (\text{where } \sum_j \lambda_j = 1)$$

and,

$$\sum_j \lambda_j \gamma_{x_i x_j} + \mu = \gamma_{Zx_i} \qquad (6.11)$$

Therefore, the Kriging system, in terms of semivariogram, will be in the following form:

$$\left.\begin{aligned} &\sum_j \lambda_j \gamma_{x_i x_j} + \mu = \gamma_{Zx_i} \qquad (i = 1, \ldots\ldots, n) \\ &\sum_i \lambda_i = 1 \end{aligned}\right\} \quad \text{II}$$

The same system can be expressed in the matrix form as follows:

$$[P]\,[W] = [B]$$

where [P] is the matrix of semivariograms between points (samples)

[W] is the matrix of weights and Lagrange multiplier

[B] is the matrix of semivariograms between samples and blocks.

i.e.

$$[P] = \begin{bmatrix} \gamma_{11} & \gamma_{12} & \cdots & \gamma_{1n} & 1 \\ \gamma_{21} & \gamma_{22} & \cdots & \gamma_{2n} & 1 \\ \cdot & \cdot & & \cdot & \cdot \\ \cdot & \cdot & & \cdot & \cdot \\ \cdot & \cdot & & \cdot & \cdot \\ \gamma_{n1} & \gamma_{n2} & \cdots & \gamma_{nn} & 1 \\ 1 & 1 & \cdots & 1 & 0 \end{bmatrix}$$

$$[W] = \begin{bmatrix} \lambda_1 \\ \lambda_2 \\ \cdot \\ \cdot \\ \cdot \\ \lambda_n \\ \mu \end{bmatrix} \qquad \text{and } [B] = \begin{bmatrix} \gamma_{Zx_1} \\ \gamma_{Zx_2} \\ \cdot \\ \cdot \\ \cdot \\ \gamma_{Zx_n} \\ 1 \end{bmatrix}$$

and the kriging variance, in terms of semivariograms, is expressed as follows (Sahin, 1988):

$$\sigma_k^2 = -\gamma_Z + \sum_{i=1}^{n} \lambda_i \gamma_{Zx_i} + \mu \qquad (6.12)$$

After computing the elements of matrices [P] and [B] from the model semivariogram, the linear system can be solved for λ_i's and μ. Finally, the kriged estimate for the block value can be determined using expression (6.1) and the corresponding kriging variance from the expression (6.12).

6.2.2 Point kriging

The methodology of point kriging is the same as that of block kriging. Considering the fact that the block is reduced to a point, the kriging system in terms of semivariograms, will be in the following form:

$$\sum_{j=1}^{n} \lambda_j \gamma_{x_i x_j} + \mu = \gamma_{x_o x_i} \qquad i = 1, ...n$$

$$\sum_{i=1}^{n} \lambda_i = 1$$

This linear system can be solved for λ_i's and μ using Gaussian back substitution. The kriged estimator for the point value (x_o) can be determined using the expression:

$$x_o^* = \sum_{i=1}^{n} \lambda_i x_i \qquad (6.13)$$

and the corresponding kriging variance is calculated by:

$$\sigma_k^2 = \sum_{i=1}^{n} \lambda_i \gamma_{x_o x_i} + \mu \qquad (6.14)$$

6.2.3 Kriging results on Zarghat magnesite deposit

The kriged estimates of the logarithms of MgO(%) for 25m x 25m x 1m blocks, located in the Central Hill, were carried out using KRIGE3 program (GEOSTAT computer package, 1984). This program was designed to produce kriged estimates using composited data file that contains the logarithms of MgO(%) samples and their corresponding 3-dimensional coordinates. The control file containing semivariogram parameters and various other options is, also, provided.

The X,Y and Z dimensions of the ellipsoid of influence, which were based on the values of model semivariogram ranges, were chosen to be 72m, 72m and 1m respectively. These dimensions were selected after several trials, as they provided the optimal estimates with relatively smaller number of samples (i.e., smaller computation time was required to estimate each block). Specifying search ellipsoid ensures that to krige a particular block only the samples, located within the ellipsoid centered at the block, are used.

The output generated by the kriging program includes the following information for 1714 blocks: The X, Y and Z coordinates of block center, the number of samples used to krige the block, the logarithmic kriged estimate for MgO% and the relative kriging standard deviation (σ_k/Z) for this estimate. This output was processed by BLKPLT program. (GEOSTAT computer package 1984). The options selected as such to provide the plots of

the estimated blocks on seven vertical sections parallel to N53° W direction with a horizontal spacing of 25m. An example of these plots is illustrated in Figure 6.1. The three numbers in each block represent, from left to right, the logarithimic kriged estimate, relative kriging standard deviation and number of samples used to krige the block respectively.

The kriging standard deviations depend on the semivariogram parameters and the relative geometries of the samples used in estimation and the block to be estimated. The kriging standard deviation can be used as a measure of reliability and accuracy of the corresponding kriged estimate. Assuming the normal distribution of kriged estimate, 95% confidence limits for the true block value will lie within the interval $Z^* \pm 2\sigma_k$ where Z^* is the kriged estimate and σ_k is the corresponding kriging standard deviation.

The results indicate that the relative kriging standard deviations are generally low with values ranging from 0.003 to 0.008. This implies the reliability of the kriged block estimates. Most blocks have similar values of relative kriging standard deviation, which is, of course, due to the regular nature of sampling that resulted in similar kriging plans. However, the blocks near the boundaries of the deposit have, somewhat, variable and relatively higher relative kriging standard deviations due to smaller number of samples used to estimate them.

Finally, the kriged estimates for the deposit in the Central Hill, were combined to give the the total tonnage for the whole deposit as follows:

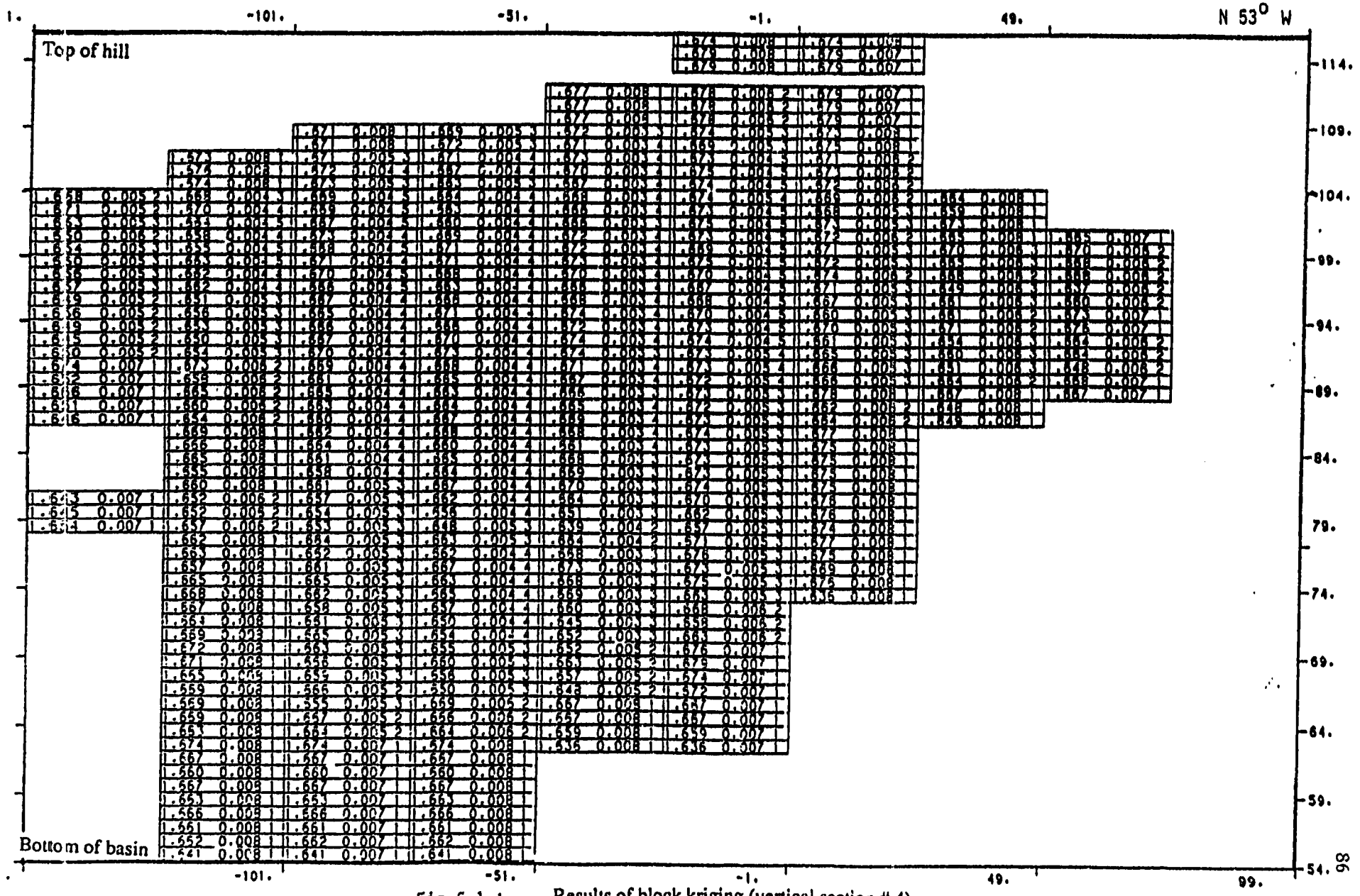

Fig.6.1 : Results of block kriging (vertical section # 4)

Total tonnage = n x s x t x d (6.15)

where:

n is the total number of kriged blocks (1714 blocks)

s is the surface area of each block (25m x 25m)

t is the thickness of each block (1m)

d is the density of magnesite ($3t/m^3$)

Substituting these values in Eq. (6.15), the total tonnage in the Central Hill was found to be about 3.2 million tonnes. The mean kriged block estimate and the kriging standard deviation values were found to be 1.665 (log %) and 0.011 (log %) respectively.

6.3 Grade - tonnage relationship

6.3.1 General

Because of variations of grade from place to place, an orebody can seldom be mined without selection. Therefore, it is more appropriate to derive the relationship between the cut-off grades and the corresponding tonnage of reserves (i.e., grade - tonnage relationship). Such relationship should be based, of course, on the distribution of selective mining units, the size of which depends on economical and technological conditions that vary with time and the nature of the deposit (Huijbregts, 1976).

To derive the grade-tonnage relationship for any selective mining unit, the following conditions must be verified:

1) The type of distribution of the selective mining units must be known.
2) The mean and the variance of the distribution of selective mining units (i.e.variance of selective mining units within the whole deposit) must be determined (Sahin 1984).

Finally, it can be concluded that for each selective mining unit, the grade-tonnage relationship gives tonnage of ore to be expected at different cut-off grades. In addition, the returns can be ealculated on the forecasted tonnage derived from the grade-tonnage curves.

6.3.2 Results on Zarghat magnesite deposit

The grade-tonnage relationship have been determined using the program REPORT of the GEOSTAT computer package (1984). This program was written for the purpose of producing grade-tonnage reports using kriged block estimates as input file. It assumes the grade distribution of the selection units to be lognormal and drives the mean of this distribution from the kriged block estimates. The variance of the distribution is estimated by combining the variances of the kriged block estimates and the dispersion variance of the grade of selection units within the block.

Considering the dimensions of selection units and kriged blocks to be 12.5m x 12.5m x 1m and 25m x 25m x 1m respectively, the grade-tonnage results have been determined. The dispersion variance of the grade of selective units within the block was computed, using the program KRIVAR (GEOSTAT package, 1984), to be 0.2434×10^{-4}.

The grade-tonnage relationship indicates the existence of the total magnesite reserves of 3.2×10^6 tons above the cut-off grade of 1.633 (log %). This tonnage, which confirms the total reserves obtained by combining kriged estimates, was based on a tonnage factor of 3 t/m^3 reported by Brosset (1978). The graphical relationship between the mean grade and the cumulative tonnage is illustrated in Figure 6.2.

6.4 Logarithmic - arithmetic transformation

The logarithmic kriged estimates and the associated kriging variances are not used in practice. Therefore their arithmetic equivalents should be determined to evaluate blocks under consideration. The following expressions are used to transform the above mentioned logarithms into arithmetic values (Journel and Huijbregts, 1978):

$$Z_a^* = 10^{[(Z^* + (\sigma_k^2/2))]} \qquad (6.16)$$

$$\sigma_{ka}^2 = (Z_a^*)^2 \, (10^{\sigma_k^2} - 1) \qquad (6.17)$$

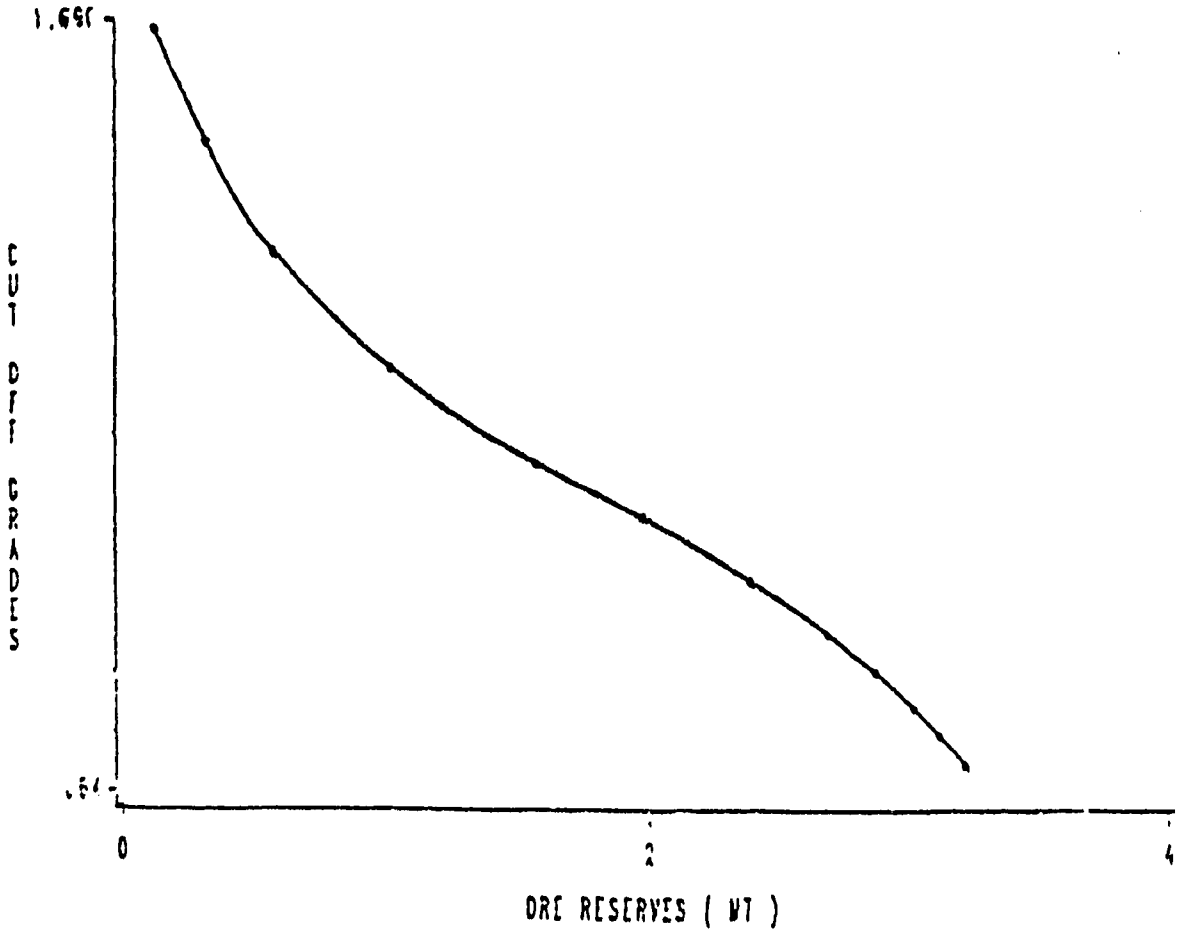

Fig. 6.2: Logarithmic grade - tonnage relationship based on 12.5 x 12.5 x 1m mining units.

Where Z^* and σ_k^2 are the logarithmic kriged estimate and its corresponding kriging variance; Z_a^* and σ_{ka}^2 are the arithmetic equivalents of these logarithmic values.

To apply the above mentioned transformation, let us consider the block with the central coordinates, Y = -13.5m and Z = 101.5m, located in the vertical section No. 4 (Fig. 6.1). This block has the logarithmic kriged estimate and kriging variance values equal to 1.675 (log %) and 4.5 X 10^{-5}, (log %)^2 respectively. Substituting these values in equations (6.16 and 6.17), the arithmetic kriged estimate and the corresponding kriging variance for this block were calculated to be 47.3 (%) and 0.23 (%)^2.

The histogram of kriging standard deviations for MgO% shown in Fig. 6.3 indicates that 82.8% of the total number of kriged blocks have been estimated with kriging standard deviation values less than 0.94 (%).

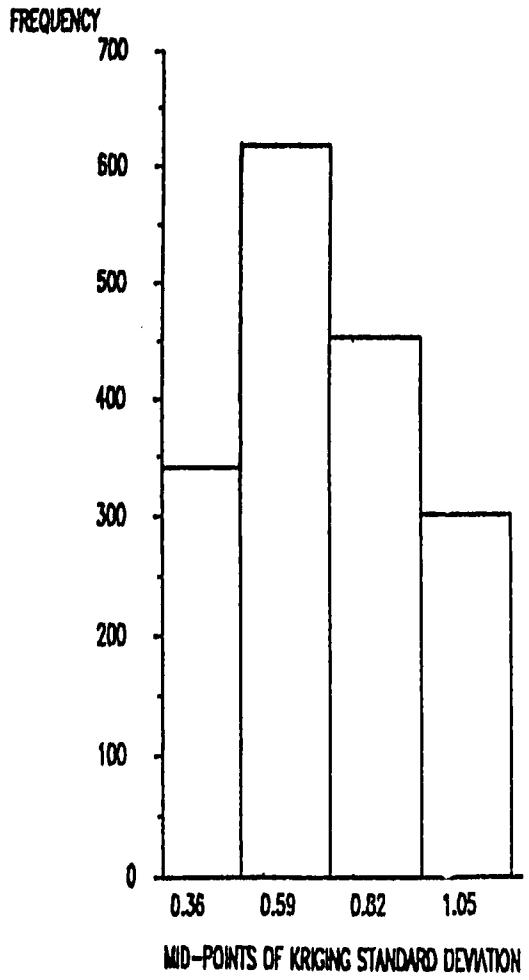

Fig. 6.3: Distribution of kriging standard deviation.

CHAPTER 7

CO-KRIGING

7.1 Introduction

As it was mentioned earlier in Chapter 4, there is a strong linear correlation ($r = -0.89$) between crude values of MgO% and CaO%. Therefore, the estimates of one of these variables can be improved using the data for both variables. The improvement in the estimates is expected due to the presence of additional information from the other variable.

For instance, to derive the estimates for MgO%, both the MgO% and CaO% sample values can be used in estimation. The method of estimation which considers the correlation between variables and makes use of the values of both variables as explained above, is reffered to as the co-kriging. To conduct co-kriging, the cross-semivariogram between the variables is required.

7.2 Cross-semivariogram

It is defined as the half of the expectation of the co-variance of the increments of two different regionalized variables. Theoretically, it can be expressed as follows (Leenaers, Okx, and Burrough, 1989):

$$\gamma_{mc}(h) = \frac{1}{2} E\{[m(x_i) - m(x_i + h)][c(x_i) - c(x_i + h)]\} \quad (7.1)$$

However, in practice it can be computed using the following equation:

$$\gamma_{mc} = \frac{1}{2n(h)} \sum_{i=1}^{n} \{[m(x_i) - m(x_i + h)][c(x_i) - c(x_i + h)]\} \quad (7.2)$$

where $m(x_i)$ and $c(x_i)$ are the values of the variables at point x_i, and n(h) is the number of data pairs separated by h.

7.3 Co-kriging

The basis idea of point co-kriging is to assign optimal weights to sample values of two different correlated variables (e.g. m and c) in order to estimate the unknown value of one of these variables. Let us assume that we want to estimate the value of variable m at a point within the deposit using several samples of variables m and c. The best possible linear estimate for m is given by:

$$m^* = \sum_{i=1}^{n} \lambda_i m(x_i) + \sum_{j=1}^{k} \upsilon_j c(y_j) \qquad (7.3)$$

where λ_i's and υ_j's are the weights assigned to m (x_i) and c (y_j) values respectively.

The main problem of co-kriging is to calculate λ_i and υ_j values which satisfy the following criteria simultaneously:

1) The estimate should be unbiased. This condition requires that

$$\sum_{i=1}^{n} \lambda_i = 1 \qquad (7.4)$$

and

$$\sum_{j=1}^{n} \upsilon_j = 0 \qquad (7.5)$$

2) The estimation variance $E[(m - m^*)^2]$ must be minimum.

After long mathematical manipulation, the co-kriging system can be expressed in terms of samivariograms and cross-semivariograms as follows (Isaak & Srivastava, 1989; Hohn, 1988; and Sahin, 1988):

$$[C][W] = [E] \qquad (7.6)$$

where [C] is the matrix containing semivariograms of both variables (i.e γ_m and γ_c) and cross-semivariograms (i.e. γ_{mc}).

[W] is the matrix of weights and Lagrange multipliers.

[E] is the matrix of the semivariograms of variable to be estimated (i.e. γ_m) and the cross-semivariograms (i.e γ_{mc}).

i.e.

$$[C] = \begin{bmatrix} \gamma_m(x_1x_1) & \cdots & \gamma_m(x_1x_n) & \gamma_{mc}(x_1y_1) & \cdots & \gamma_{mc}(x_1y_k) & 1 & 0 \\ \vdots & & \vdots & \vdots & & \vdots & \vdots & \vdots \\ \gamma_m(x_nx_1) & \cdots & \gamma_m(x_nx_n) & \gamma_{mc}(x_ny_1) & \cdots & \gamma_{mc}(x_ny_k) & 1 & 0 \\ \gamma_{mc}(y_1x_1) & \cdots & \gamma_{mc}(y_1x_n) & \gamma_c(y_1y_1) & \cdots & \gamma_c(y_1y_k) & 0 & 1 \\ \vdots & & \vdots & \vdots & & \vdots & \vdots & \vdots \\ \gamma_{mc}(y_kx_1) & \cdots & \gamma_{mc}(y_kx_n) & \gamma_c(y_ky_1) & \cdots & \gamma_c(y_ky_k) & 0 & 1 \\ 1 & & 1 & 0 & & 0 & 0 & 0 \\ 0 & & 0 & 1 & & 1 & 0 & 0 \end{bmatrix}$$

$$[W] = \begin{bmatrix} \lambda_i \\ \vdots \\ \lambda_n \\ \upsilon_1 \\ \vdots \\ \upsilon_k \\ \mu_1 \\ \mu_1 \end{bmatrix} \quad \text{and} \quad [E] = \begin{bmatrix} \gamma_m(x_10) \\ \vdots \\ \gamma_m(x_n0) \\ \gamma_{mc}(y_10) \\ \vdots \\ \gamma_{mc}(y_k0) \\ 1 \\ 0 \end{bmatrix}$$

After solving this system and determining weights, the co-kriged estimate for the point value can be determined by the expression (7.3) and the corresponding co-kriging variance can be calculated using the following expression:

$$\sigma^2_{ck} = \sum_{i=1}^{n} \lambda_i \gamma_m (x_i 0) + \sum_{j=1}^{k} \upsilon_j \gamma_{mc} (y_j 0) + \mu_1 \qquad (7.7)$$

7.4 Applications to Zarghat magnesite deposit

7.4.1 Cross-semivariogram for Zarghat deposit

The strong linear correlation between MgO% and CaO% crude values (i.e., r = - 0.89) suggested the applicability of co-kriging technique to Zarghat magnesite deposit. The isotropic (average) vertical and horizontal cross-semivariograms were computed and illustrated in Figure 7.1 and Figure 7.2 respectively. The general behavior of these cross-semivariograms is similar to the behavior of the corresponding semivariograms of individual variables.

The compound sperical model with a short range of about 7m and a long range of about 22m appears to be suitable for the vertical cross-semivariogram. As explained in section 5.3.1, the same type of models with exactly the same values of ranges have been fitted to vertical semivariograms of both CaO and MgO. However, there are considerable variations between the sill values of cross-semivariogram and semivariograms.

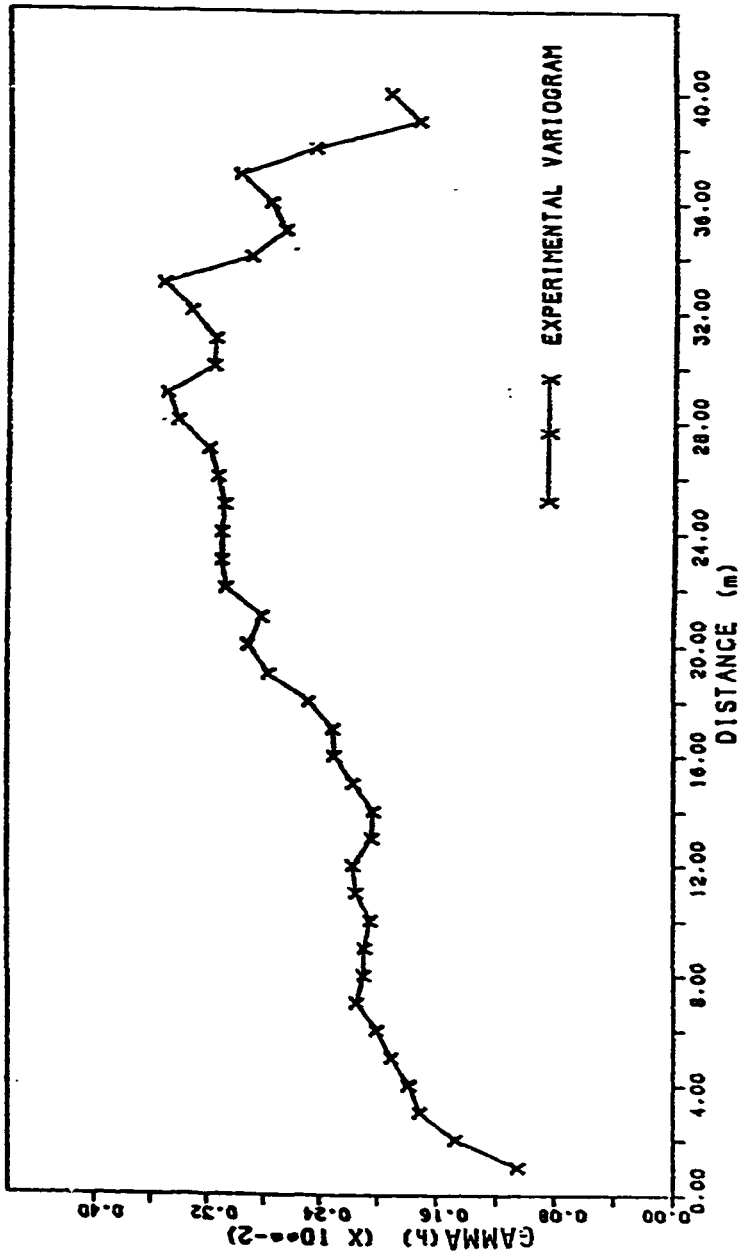

Fig. 7.1 : Average vertical Cross-semivariogram for CaO * MgO (10g%)

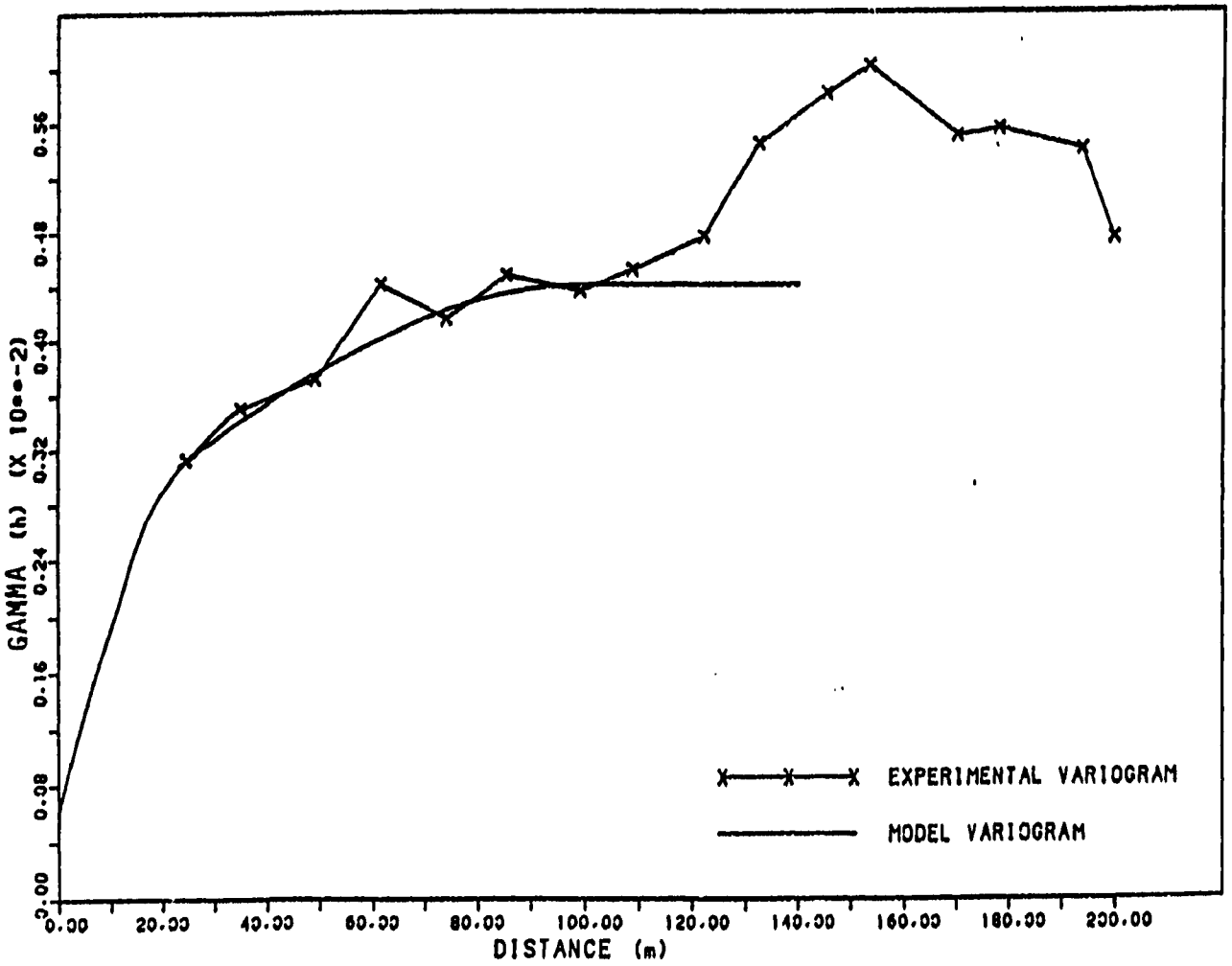

Fig. 7.2 : Isotropic horizontal Cross-semivariogram for CaO * MgO (10g%)

The isotropic horizontal cross-semivariogram and the fitted model are presented in Figure 7.2. The compound sperical model, with short range of 25m and long range of 100m, appears to give good fit as in the case of horizontal semivariograms. The model parameters, which will be used in subsequent local estimation (co-kriging) procedure, are listed as follows:

a) The nugget variance (C_0) = 0.06×10^{-2} $(\log\%)^2$

b) The first spatial variance (C_1) = 0.18×10^{-2} $(\log\%)^2$

c) The second spatial variance (C_2) = 0.20×10^{-2} $(\log\%)^2$

d) The short range (a_1) = 25m

e) The long range (a_2) = 100m

7.4.2 Comparison of kriging and co-kriging methods

A study was carried out for the purpose of comparison between the simple kriging and co-kriging estimation methods. Both the simple kriging and the co-kriging were applied to estimate the known values of MgO (log %) at 20 sampling points and the results were compared.

The search radius was restricted to 40m in both estimation methods. This restriction was imposed in order to limit the total number of samples used in estimation. This provided a maximum of 8 samples in the case of simple kriging and 16 samples in the case of co-kriging. The latter technique made use of all CaO (log%) samples in addition to MgO

(log%) samples. Both the kriging and the co-kriging estimations were performed using a FORTRAN program written for this purpose.

The results of both estimation methods together with the known (real) sample values are listed in Table 7.1. The comparison of the estimates and the sample values indicates that the co-kriging estimates are more reliable than simple kriging estimates as they are closer to the corresponding sample values. Moreover, co-kriging variances are substantially smaller than the corresponding simple kriging variances.

Finally, it can be concluded that the prediction of point values using co-kriging produces better estimates than the ones produced using simple kriging as illustrated in Fig. 7.3 and 7.4 respectively. Furthermore, co-kriging may provide reliable MgO (log %) estimates in areas where MgO have not been sufficiently sampled to provide estimates with acceptable precision. However, it should be noted that the co-kriging requires at least one sample value of the estimated variable (i.e., MgO in this case) in addition to the values of other variable as reported by Journel and Huijbregts (1978).

Table 7.1 Results of simple kriging and co-kriging procedures

Sample value	Kriging		Co-kriging	
	Estimated value	σ_k^2	Estimated value	σ_{ck}^2
MgO (log %)	MgO (log %)	$X10^{-6}$(log %)^2	MgO (log %)	$X10^{-6}$(log %)^2
1.673	1.674	128.691	1.673	128.666
1.678	1.675	128.366	1.676	128.347
1.678	1.676	129.091	1.677	129.074
1.668	1.671	128.712	1.670	128.688
1.676	1.673	128.266	1.674	128.251
1.674	1.674	128.692	1.674	128.666
1.678	1.676	128.366	1.677	128.348
1.676	1.673	129.089	1.674	129.074
1.675	1.674	128.266	1.674	128.250
1.674	1.675	128.691	1.674	128.668
1.675	1.673	128.360	1.674	128.347
1.676	1.674	129.091	1.675	129.070
1.675	1.673	128.713	1.674	128.688
1.671	1.673	129.018	1.672	129.000
1.674	1.672	128.691	1.673	128.660
1.675	1.673	128.360	1.674	128.347
1.676	1.674	129.090	1.675	129.072
1.676	1.673	128.712	1.674	128.690
1.675	1.673	129.020	1.674	129.000
1.677	1.674	128.260	1.675	128.251

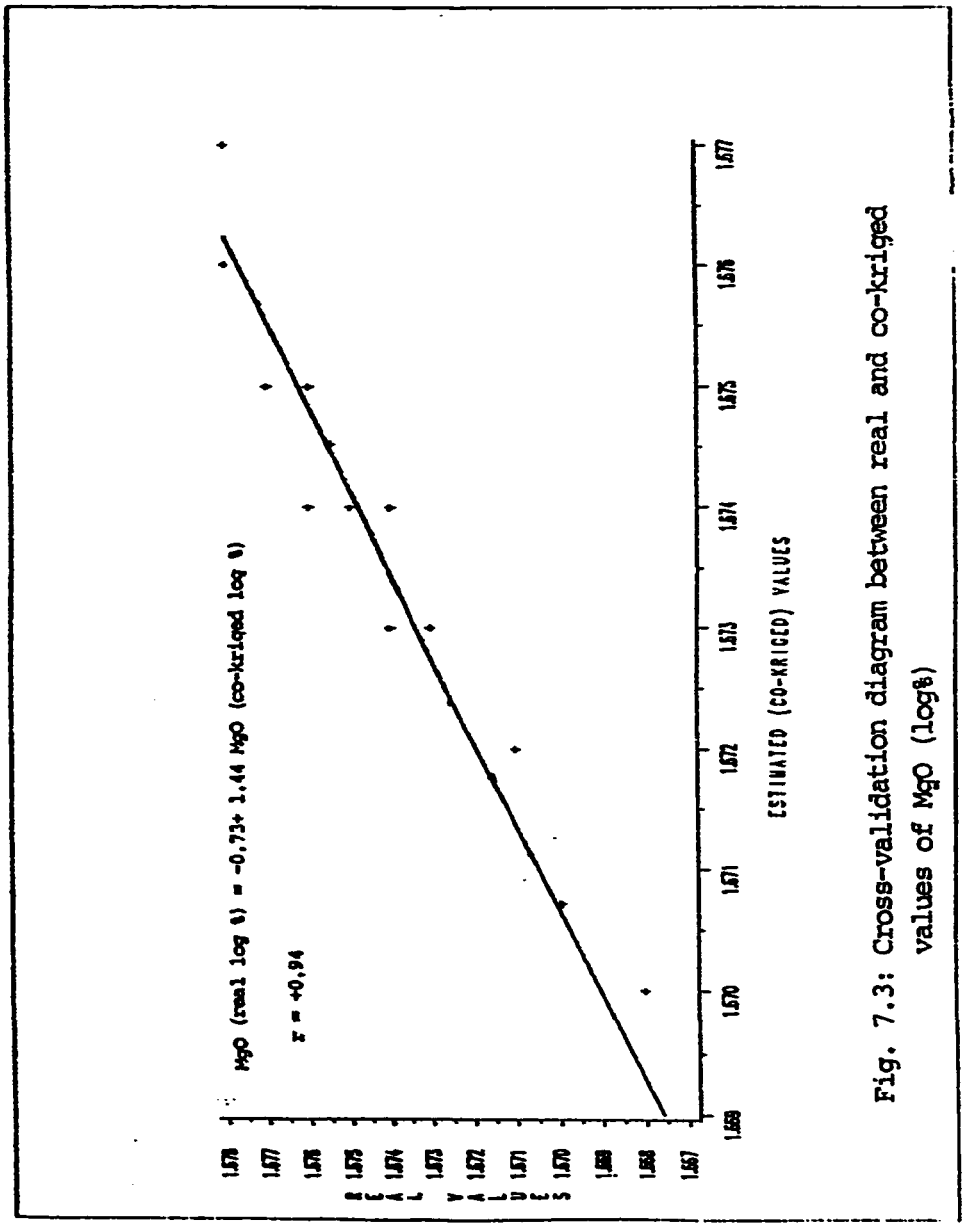

Fig. 7.3: Cross-validation diagram between real and co-kriged values of MgO (log%)

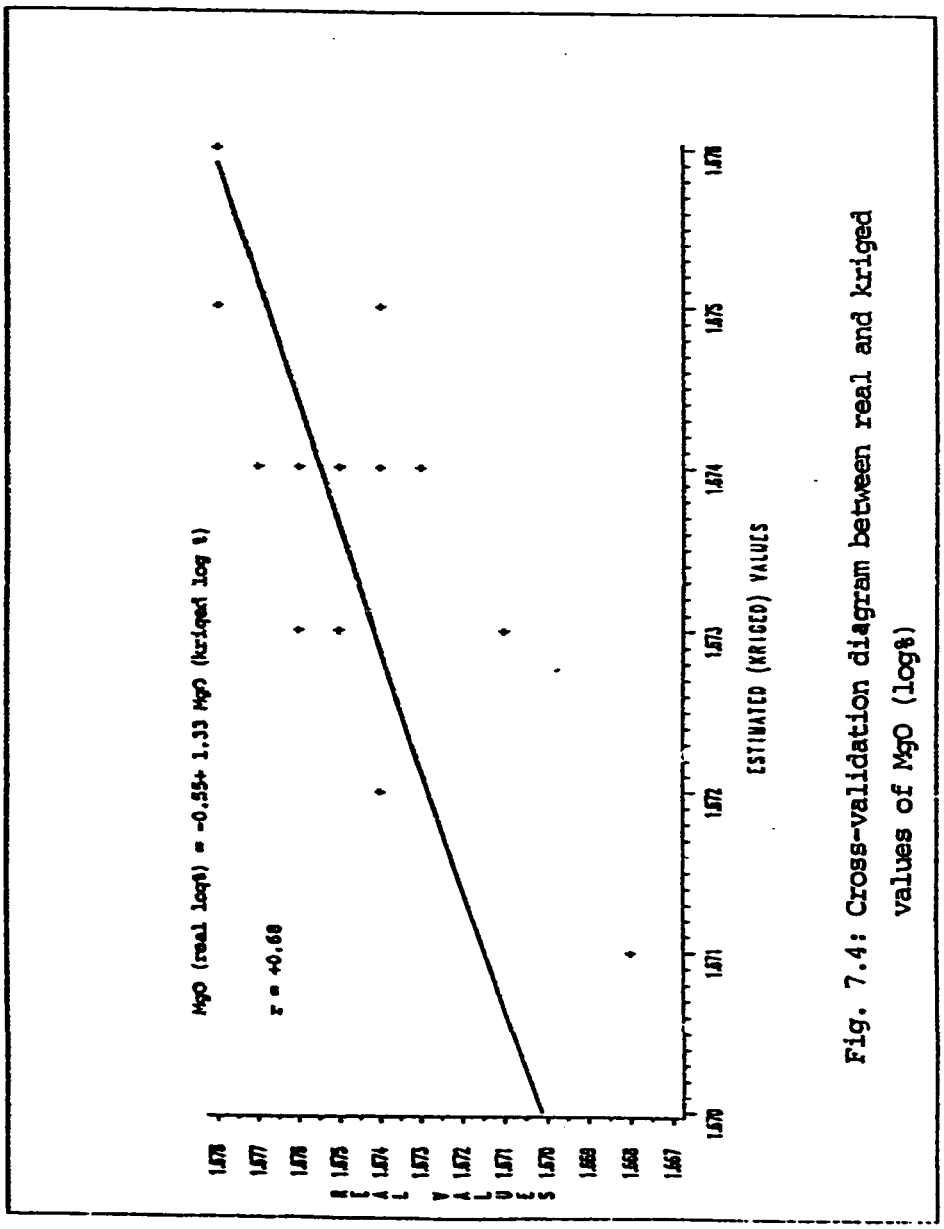

Fig. 7.4: Cross-validation diagram between real and kriged values of MgO (log%)

CHAPTER 8

CONCLUSIONS

Zarghat magnesite deposit is located in the northern part of the Arabian Shield. This deposit occurs in the form of three small hills referred to as the Central Hill, East-southest Hill and West-northwest Hill. The Central Hill is the largest among all occurrences and contains magnesite of good quality with a grade ranging from 38% to 48% MgO.

The deposit occurs in a small sedimentary basin of the Jibalah Group which is considered to be Late Proterozoic to Early Cambrian age. Zarghat sedimentary basin contains (from base to top) andesite unit, cherty limestone, dolomitic limestone, bedded dolomite and magnesite. Several structural events, which resulted in folding and faulting can be observed in the area. Previous studies have revealed that the magnesite is cryptocrystalline, massive but highly sheared and fragmented. It is, generally, intersected by dolomite veins ranging from microscopic to one meter in width. Magnesite and dolomite veins were formed as a result of the dehydration of originally precipitated hydromagnesite.

The main conclusions drawn from this study can be summarized in the following praragraphs:

The preliminary statistical analysis of the available data from the Central Hill provided means and variances for both crude and calcined values of CaO% and MgO% within the whole deposit and in individual drill-holes. The average values for crude CaO% and MgO% have been estimated to be 1.38% and 46.27% and the same values for calcined CaO% and MgO% to be 2.86% and 96.02% respectively. The comparison of means and variances for the variables in individual drill-holes indicates that considerable variations exist in various parts of the deposit.

The histograms for variables revealed the skewed nature of distributions. Both crude and calcined CaO% distributions are positively and the crude and calcined MgO% distributions are negatively skewed. This lognormal behavior of the sampling distributions has suggested that more accurate modelling and evaluation can be achived using logarithmic values.

The correlation diagrams between CaO% and MgO% illustrate the existence of the inverse relationship with Pearson's linear correlation coefficients of -0.89 and -0.85 for crude and calcined values respectively. This relationship, which may be explained by the enrichment of Mg at the expense of Ca and vice versa, suggests the suitability of co-kriging method in the local estimation of the deposit. However, the correlation diagrams between the calcined and the crude values of each variable illustrate significant positive correlation with the correlation coefficient value of + 0.97. This correlation revealed close similarities between crude and calcined values of each sample providing enough justification for the detailed study of only crude values (or their logarithms) in semivariogram modelling and subsequent estimations.

The results of semivariogram and cross-semivariogram analysis indicate that compound spherical models could appropriately be fitted to all experimental semivariograms and cross-semivariograms. The behavior of the semivariograms and cross-semivariograms near their origins indicates nugget type with average continuity. The presence of nugget variance may be explained by the presence of microstructures in the deposit such as irregular fractures and dolomitic veins, whereas the average continuity may reflect the sedimentary origin of the deposit. The analysis of semivariograms and cross-semivariograms ranges indicate the presence of small depositional basins within larger one.

The local estimation, based on MgO (log%) of 1m composite samples, has been carried out using the geostatistical procedure known as the kriging. A total of 1714 blocks having 25m x 25m x 1m dimensions were kriged using an ellipsoid of influence that has 72m x 72m x 1m dimensions. The mean grade of the kriged block estimates was found to be 1.665 (log %). The relative kriging standard deviations associated with the kriged estimates, for most of the blocks, are generally low ranging from 0.003 to 0.008 and indicating the reliability of the kriged estimates.

Based on the kriged block estimates and using selective mining units of 12.5m x 12.5m x 1m dimensions, the grade-tonnage relationship for the whole deposit was determined. This relationship indicates the existence of the total magnesite reserves of 3.2 million tonnes above the cut-off grade of 1.633 (log%). The tonnage derived from this relationship compares well with the one calculated by combining kriged blocks.

Finally, the comparison of the point estimates derived using kriging and co-kriging methods and the corresponding real sample values indicates that the co-kriging produces estimates closer to the real values than the ones produced using simple kriging. Moreover, the co-kriging variances are smaller than the corresponding simple kriging variances.

REFERENCES

Abdul-Latif, A. A., "Geostatistical Estimation of Reserves in the Abu-Tartur Phosphate Deposits, Western Desert, Egypt", M. Sc. Thesis, King Fahd University of Petroleum and Minerals, Dhahran, Saudi Arabia, 246 p., 1987.

Ali, A. Z., "Geostatistical Evaluation of Jabal Sayid Polymetallic Sulfide Deposit, Saudi Arabia", M. Sc. Thesis, King Fahd University of Petroleum and Minerals, Dhahran, Saudi Arabia, 201 p. 1986.

Armstrong, M. (Ed.), "Geostatistics", Kluwer Academic Publisher, Netherlands, Vol. 1 and 2, 1989.

Bain, G. W., "Types of Magnesite Deposits and Their Origin", Econ. Geology, Vol. 19, pp. 412-433, 1924.

Berton, Y., "Unpublished Field Notes on Zarghat Magnesite Deposit", BRGM, 1968.

Blais, R. A. and Carlier, P. A., "Application of Geostatistics in Ore Evaluation", Canadian IMM, Sp. Vol. 9, pp. 41-67, 1968.

Brosset, R., "Zarghat Magnesite Deposit", DGMR, Report BRGM 70 JED 2, 20 p., 1970.

Brosset, R., "Zarghat Magnesite Deposit - Completion Report on Drilling (ZA1-ZA26)", DGMR, Report BRGM 76 JED 20, 19 p., 1976.

Brosset, R., "Zarghat Magnesite Deposit - Completion Report on Drilling (ZA27-ZA90)", DGMR, Report BRGM 78 JED 12, 27 p., 1978.

Brown, G. F., "USGS Map 1-205A", 1963.

Brown, G. F. and Jakson, R.O., "An overview of the geology of Western Arabia", USGS report SA(IR)-250, 1978.

Calvez, J. Y., Alsac, C., Delfour, J, Kemp, J. and Pellaton, C. "Geological evolution of the western, central and eastern parts of the northern Precambrian Shield, Kingdom of Saudi Arabia", in: Pan-African Crustal Evolution in the Arabian -Nubian Shield (Proceedings of a symposium hold on 1982), King Abdulaziz Universityh, Jeddah, No. 6, PP 24-45, 1984.

Celik, M. S., "Benefication Studies on Zarghat Magnesite Ore", AJSE, Dhahran, Vol. 15, No. 2A, pp. 213-218, 1990.

Cheeney, R. F., "Statistical Methods in Geology", George Allen & Unwin Ltd., U. K., 169 P., 1983.

Clark, I., "The Semivariogram": in Geostatistics, McGraw-Hill, Inc., New York, 168 p., 1980.

Clark, I., "Practical Geostatistics", Elsevier Applied Sciences Publishers, London, 129 p., 1984.

David, M., "What happens if some remarks on useful concepts in the design of sampling patterns", Australian IMM, Sampling Symp., pp. 1-15, Sept. 1976.

David, M., "Geostatistical Ore Reserve Estimation", Elsevier Sci. Pub. Co., Amsterdam, 216 p., 1988.

Davis, J. C., "Statistics and Data Analysis in Geology", John Wiley & Sons, Inc., USA, 2nd ed., 646 p., 1986.

Delfour, J., "Preliminary Data on Zarghat Magnesite Prospect", BRGM, 2nd Annual Report 70 JED 1, 8 p., 1970.

Feugueur, L., "Problems concerning search for non-metalic minerals in Saudi Arabia", BRGM, Open-file report SG JED 66 A1, 1966.

GEOSTAT Computer Package, Geostat Systems International Inc., Montreal, 32 p., 1984.

Ghaleb, A. R., "Geological, Mineralogical, and Geostatistical Studies on Zarghat Magnesite Deposit, Saudi Arabia", M. Sc. Thesis, King Fahd University of Petroleum and Minerals, Dhahran, 142 p., 1985.

Greenfield, P., "Magnesium", Mills & Boon Ltd., London, 56 p., 1982.

Guarascio, M., "Improving the Uranium Deposit Estimation (The Novazza Case)": in Advanced Geostatistics in the Mining Industry, Proceedings of NATO Advanced Study Inst., pp. 351-367, 1976.

Guarascio, M., David, M. and Huijbregts, Ch. (ed.), "Advanced Geostatistics in the Mining Industry", NATO Advanced Study Institute Series, Reidel Publishing Company, Holland, 461 p., 1976.

Hadley, D. G., "The Taphrogeosynclinal Jubaylah Group in the Mash'had Area, Northwestern Hijaz, Kingdom of Saudi Arabia", DGMR, Mineral Resources Bulletin 10, Jeddah, 1974.

Hadley, D. G. and Schmidt, D. L., "Sedimentary Rocks and Basins of the Arabian Shield and their Evolution": in Evolution and Mineralization of the Arabian Nubian Shield, King Abdul-Aziz University, Jeddah, Vol. 4, pp. 26-50, 1980.

Hawkins, D. M., "Identification of Outliers", Cambridge University Printing House, 1980.

Hohn, M. E., "Geostatistics and Petroleum Geology", Van Nostrand Reinhold, New York, 264 p., 1988.

Huijbregts, Ch., "Selection and Grade-Tonnage Relationships": in Advanced Geos. in Min. Industry, Proceedings of NATO Advanced Study Inst., Reidel Publishing Company, Holland, pp. 113-135, 1976.

Hurlbut, C. S., "Dana's Manual of Mineralogy", John Wiley & Sons Inc., 18th ed., New York, 579 p., 1971.

Isaaks, E. H. and Srivastava, R. M., "An Introduction to Applied Geostatistics", Oxford University Press Inc., 561 p., 1989.

Jensen, M. L. and Bateman, A. M., "Economic Mineral Deposits", John Wiley & Sons Inc., 3rd ed. (revised), 593 p., 1981.

Journel, A. G. and Huijbregts, Ch. J., "Mining Geostatistics", Academic Press Inc. Ltd., London, 600 p., 1978.

Khar, V. P., "Zarghat Magnesite Occurrence", DGMR, Open-File Report, Jeddah, 1962.

Klein, C. and Hurlbut, C. S., "Manual of Mineralogy", Jhon Wiley & Sons Inc., 20th ed., 596 p., 1985.

Koch, G. S. and Link, R. F., "Statistical Analysis of Geological Data", Dover Publications Inc., New York, 438 P., 1980

Krige, D. G., "Statistical Application in Mine Valuation", J. Inst. Mine Surv., South Africa: Vol. 12, No. 2-3, 1962.

Leenaers, H., Okx, J. P. and Burrough, P. A., "Co-kriging: an accurate and inexpensive means of mapping floodplain soil pollution by using elevation data": Geostatistics, Kluwer Academic Publishers, Netherlands, Vol. 1, pp. 371-382, 1989.

Marsal, D., "Statistics for Geoscientists", Pergamon Books Ltd., 176p. 1987.

Matheron, G., "Principles of Geostatistics", Econ. Geol., Vol. 58, pp. 1246-1266, 1963.

Matheron, G., "The Theory of Regionalized Variables and Its Applications", University of Leeds (Dept. of Mining & Mineral Sciences), England, 211 p., 1971.

Montgomery, D. C., "Design and Analysis of Experiments", John Wiley & Sons Inc., Singapore, 538 p. 1984.

Morris, W. (ed.), "The American Heritage Dictionary of the English Language", Houghton Mifflin Co., Boston, 1550 p., 1981.

Parker, H., "The Volume-variance Relationship: A Useful Tool for Mining Planning": In Geostatistics, McGraw-Hill Inc., New York, 1980.

Petrucci, R. H., "General Chemistry", Macmillan Publishing Co. Inc., New York, 2nd ed., 1977.

Rendu, J. M., "An Introduction to Geostatistical Methods of Mineral Evaluation", South African Inst. of Mining and Metallurgy, Johannesburg, Geostatistics Series 2, 84 p., 1978.

Rendu, J. M., "Geostatistical Modeling and Geological Controls", IMM, APCOM, London, (18th International Symp.), pp. 467-476, 1984.

Rendu, J. M. and Readdy, L., "Geology and Semivariogram - A Critical Relationship", American Inst. of Min., Metal. and Pet. Eng. Inc., New York:, APCOM (17th International Symp.), pp. 771-783, 1982.

Royle, A. G., "Global Estimates of Ore Reserves", Transactions of Institution of Min. & Metal., London, Vol. 86, Section A, pp. A9-A17, 1977.

Royle, A. G. (et. al.), "Geostatistics", McGraw-Hill, New York, 168 p., 1980.

Royle, A. G., "Why Geostatistics": In Geostatistics, McGraw-Hill, New York, pp. 1-16, 1980.

Sahin, A., "Spatial Distribution in the Bonthe Rutile Deposits of Sierra Leone", Ph. D. Thesis, University of Leeds, 218 p., 1977.

Sahin, A., "Geostatistical Computer Programs", King Fahd University of Petroleum and Minerals, Dhahran, 1983.

Sahin, A., "Geostatistical Prediction of Grain-Size Fluctuations in Feed to Reichert Cores", Trans. of Inst. of Min. & Metal., London, Vol. 93, Section C, C1-C6, 1984.

Sahin, A., "Computer Applications in Geology - Course Notes", King Fahd University of Petroleum and Minerals (Earth Sciences Dept.), Dhahran, 1987.

Sahin, A., "Advanced Geostatistics - Course Notes", King Fahd University of Petroleum and Minerals (Earth Sciences Dept.), Dhahran, 1988.

Sahin, A., and Abo-Khodair, A. A., "Geostatistical Approach in Design of Sampling Patterns of Jabal Sayid Sulfide Deposit, Western Saudi Arabia", Journal of African Earth Sciences, Vol. 7, No. 4, pp 679-690, 1988.

Sahin, A., Ghaleb, A. and Saif, S., "Spatial Distribution in Zarghat Magnesite Deposit of Saudi Arabia", Proceedings of the First Islamic Countries Conference on Statistical Sciences, Vol. 2, pp. 796-815, Pakistan, August 1988.

Sahin, A. and Royle, A. G., "Verification and Adjustment of Geostatistical Models", Journal of King Saud University, Riyadh, Vol. 2, Sciences (1), pp. 45-57, 1990.

Saif, S. I. and Ghaleb, A. R., "Geology and Origin of Zarghat Magnesite Deposit, Saudi Arabia", AJSE, Dhahran, Vol. 12, No. 3, pp. 251-261, 1987.

Saint-Marc, P., "Arabian Peninsula", in: The Phanerozoic Geology of the World (The Mesozoic, A) by Mouliode and Nairn (ed.), Elsevier Scientific Publishing Co. Netherlands, pp. 435-462, 1978.

Scoffin, T. P., "An Introduction to Carbonate Sediments and Rocks", Blackie & Son Ltd., 274p. 1987.

Stoeser, D. B. and Camp, V. E., "Pan-African Micro-plate Accretion of the Arabian Shield", Geol. Society of America Bulletin, Vol. 96, pp. 817-826, 1985.

Tewari, D. N., "Nesquehonite, Possible Precursor in the Origin of Himalayan Magnesite Deposits", Himalayan Geol., Vol. 3, pp. 94-102, 1973.

The Economics of Magnesium Metal, Roskill Information Services, London, 3rd ed., 160 p., 1982.

Verly, G., David, M. and Journel, A. G. (ed.), :Geostatistics for Natural Resources Characterization", NATO Series (Ci22), Part 1 and 2, 1984.

Zim, H. S. and Shaffer, P. R., "Rocks and Minerals", Golden Press, New York, 160 p., 1957.

APPENDIX A

An excerpt from the master data file containing the real survey and assay values

card# (1=survey data card in GEOSTAT package)
drill-hole #
X-coord. (m)
Y-coord. (m)
Z-coord. (m)
azimuth angle
inclination angle

1	ZA12	168.7	81.5	106.9	0.0	-90.0	
3	ZA12	0.0	1.0	0.48	47.06	1.00	98.50
3	ZA12	1.0	2.0	0.53	47.22	1.10	98.23
3	ZA12	2.0	3.0	0.50	47.24	1.04	98.35
3	ZA12	3.0	4.0	0.25	47.62	0.52	99.20
3	ZA12	4.0	5.0	0.62	47.36	1.28	98.20
3	ZA12	5.0	6.0	0.31	47.38	0.64	98.95
3	ZA12	6.0	7.0	0.39	47.92	0.80	97.95
3	ZA12	7.0	8.0	0.35	47.36	0.72	98.56
3	ZA12	8.0	9.0	0.34	47.96	0.70	97.95
3	ZA12	9.0	10.0	0.36	47.54	0.74	98.00
3	ZA12	10.0	11.0	0.39	47.32	0.80	97.95
3	ZA12	11.0	12.0	0.56	47.40	1.15	97.85
3	ZA12	12.0	13.0	0.39	47.32	0.80	98.75
3	ZA12	13.0	14.0	0.50	47.24	1.03	98.23
3	ZA12	14.0	15.0	0.53	47.02	1.10	98.22
3	ZA12	15.0	16.0	0.84	47.00	1.74	97.85
3	ZA12	16.0	17.0	0.76	46.86	1.59	98.10
3	ZA12	17.0	18.0	0.62	46.76	1.29	97.84
3	ZA12	18.0	19.0	0.64	46.94	1.33	97.87
3	ZA12	19.0	20.0	0.53	47.02	1.10	98.30
3	ZA12	20.0	21.0	0.64	46.74	1.34	98.15
3	ZA12	21.0	22.0	0.42	47.70	0.88	98.75
3	ZA12	22.0	23.0	0.64	46.74	1.34	98.20
3	ZA12	23.0	24.0	0.90	46.96	1.86	97.36
3	ZA12	24.0	25.0	1.68	45.80	3.48	94.95
1	ZA13	122.5	78.8	108.3	0.0	-90.0	
3	ZA13	0.0	1.0	0.74	46.17	1.57	97.95
3	ZA13	1.0	2.0	0.56	46.60	1.18	98.07

calcined MgO%
calcined CaO%
crude MgO%
crude CaO%
to (m) * bottom of the core samples
from (m) * top of the core samples
card # (3=assay data card in GEOSTAT package)

APPENDIX B

An excerpt from the composite data file containing the rotated coordinates and logarithmic assay values

drill-hole #	bench #	X-coord. (m)	Y-coord. (m)	Z-coord. (m)	crude CaO% (log)	crude MgO% (log)
-ZA11	1	119.2	-115.9	102.3	-0.051	1.668
-ZA11	2	119.2	-115.9	101.3	0.225	1.663
-ZA11	3	119.2	-115.9	100.3	0.401	1.643
-ZA11	4	119.2	-115.9	99.3	0.425	1.644
-ZA11	5	119.2	-115.9	98.3	0.322	1.659
-ZA12	1	166.6	-85.7	106.4	-0.319	1.673
-ZA12	2	166.6	-85.7	105.4	-0.276	1.674
-ZA12	3	166.6	-85.7	104.4	-0.301	1.674
-ZA12	4	166.6	-85.7	103.4	-0.602	1.678
-ZA12	5	166.6	-85.7	102.4	-0.208	1.675
-ZA12	6	166.6	-85.7	101.4	-0.509	1.676
-ZA12	7	166.6	-85.7	100.4	-0.409	1.681
-ZA12	8	166.6	-85.7	99.4	-0.456	1.675
-ZA12	9	166.6	-85.7	98.4	-0.469	1.681
-ZA12	10	166.6	-85.7	97.4	-0.444	1.677
-ZA12	11	166.6	-85.7	96.4	-0.409	1.675
-ZA12	12	166.6	-85.7	95.4	-0.252	1.676
-ZA12	13	166.6	-85.7	94.4	-0.409	1.675
-ZA12	14	166.6	-85.7	93.4	-0.301	1.674
-ZA12	15	166.6	-85.7	92.4	-0.276	1.672
-ZA12	16	166.6	-85.7	91.4	-0.076	1.672
-ZA12	17	166.6	-85.7	90.4	-0.119	1.671
-ZA12	18	166.6	-85.7	89.4	-0.208	1.670
-ZA12	19	166.6	-85.7	88.4	-0.194	1.672
-ZA12	20	166.6	-85.7	87.4	-0.276	1.672
-ZA12	21	166.6	-85.7	86.4	-0.194	1.670
-ZA12	22	166.6	-85.7	85.4	-0.377	1.679
-ZA12	23	166.6	-85.7	84.4	-0.194	1.670
-ZA12	24	166.6	-85.7	83.4	-0.046	1.672
-ZA12	25	166.6	-85.7	82.4	0.225	1.661
-ZA13	1	136.7	-50.4	107.8	-0.131	1.664
-ZA13	2	136.7	-50.4	106.8	-0.252	1.668
-ZA13	3	136.7	-50.4	105.8	-0.310	1.669
-ZA13	4	136.7	-50.4	104.8	0.364	1.651
-ZA13	5	136.7	-50.4	103.8	0.413	1.649
-ZA13	6	136.7	-50.4	102.8	0.396	1.651

APPENDIX C

Vertical logarithmic semivariograms for some individual drill-holes

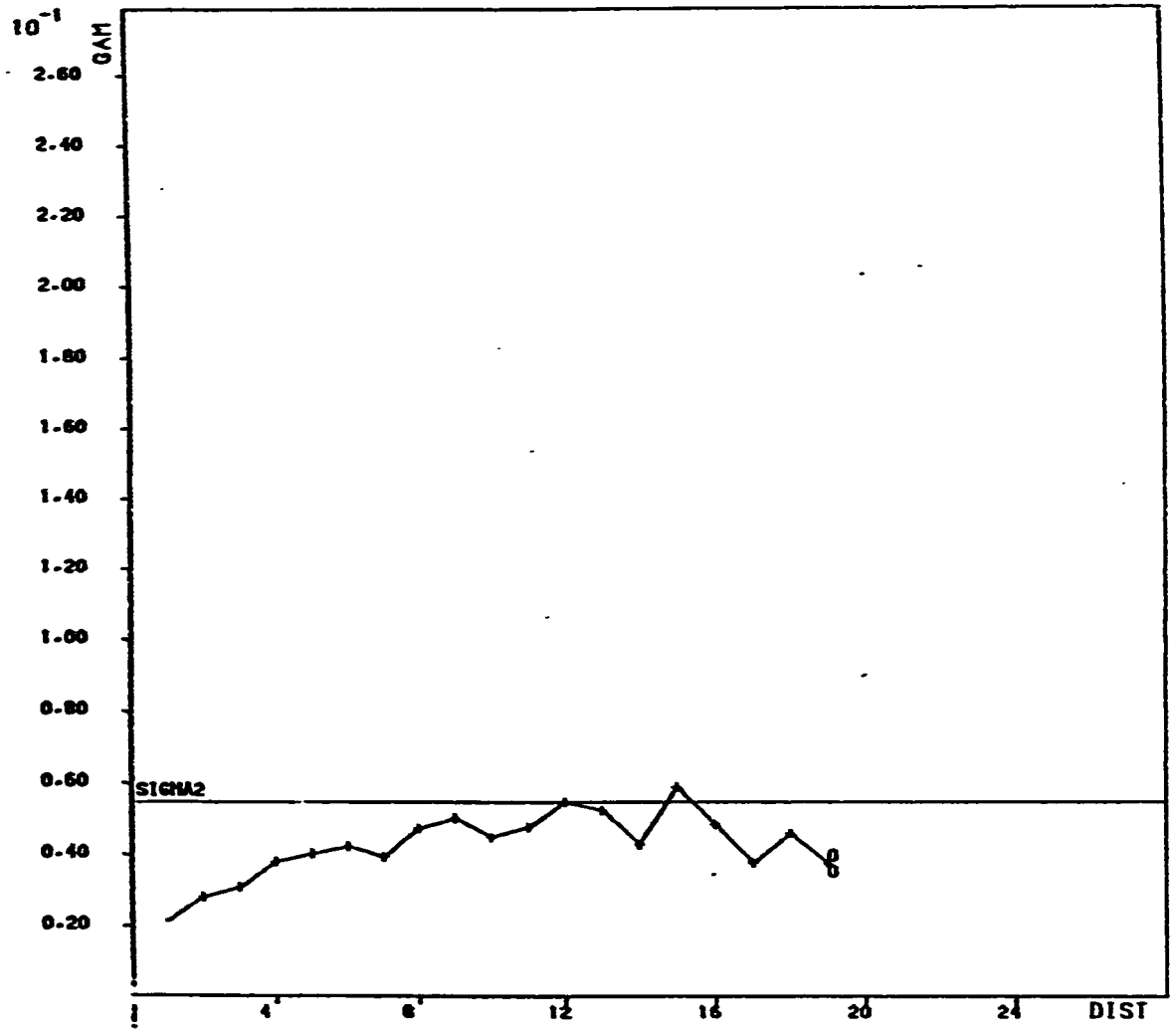

VARIABLE CAO

Fig. C.1- VERTICAL LOGARITHMIC SEMIVARIOGRAM FOR ZA-17

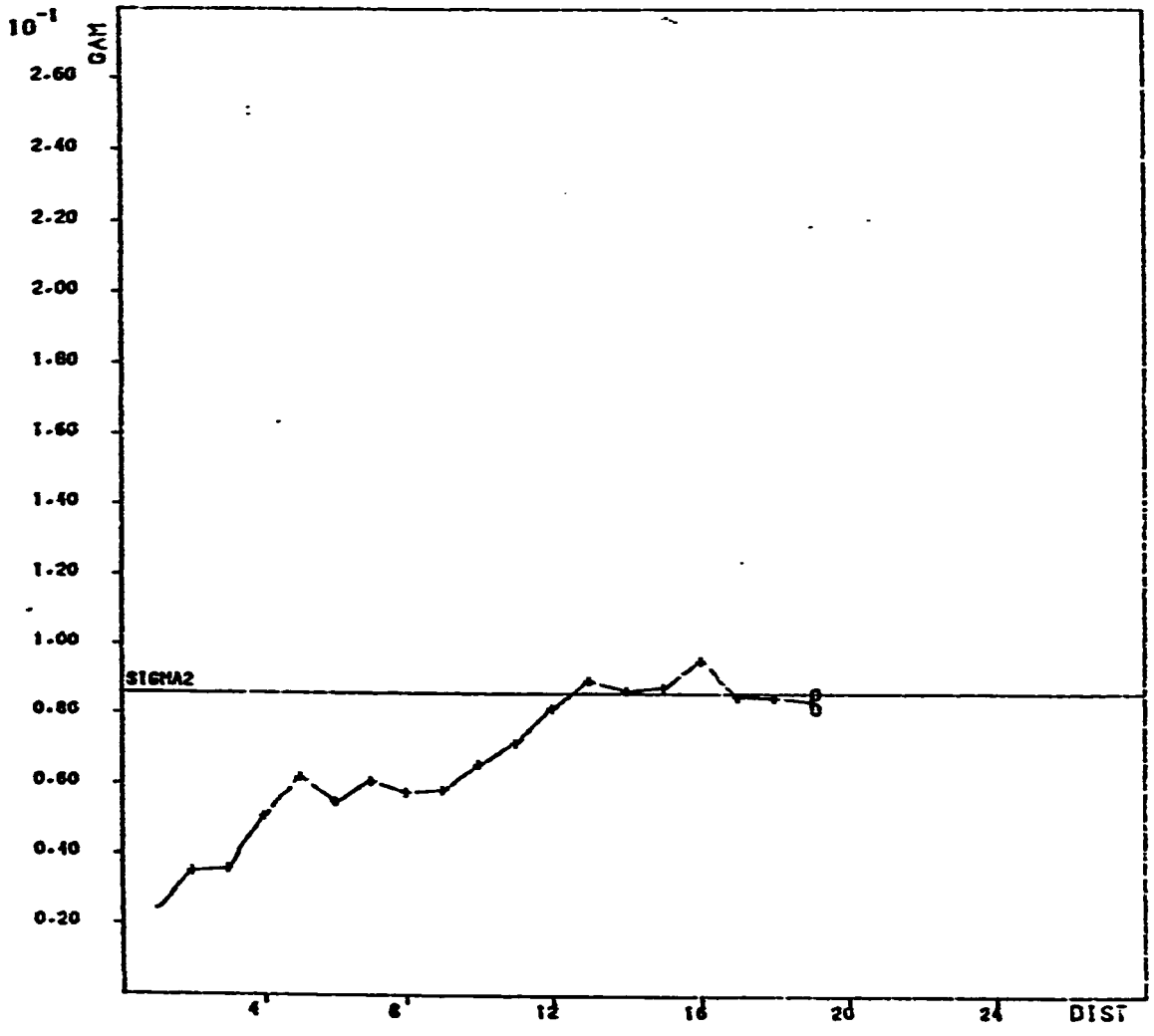

VARIABLE CAD

Fig. C.2- VERTICAL LOGARITHMIC SEMIVARIOGRAM FOR ZA-44

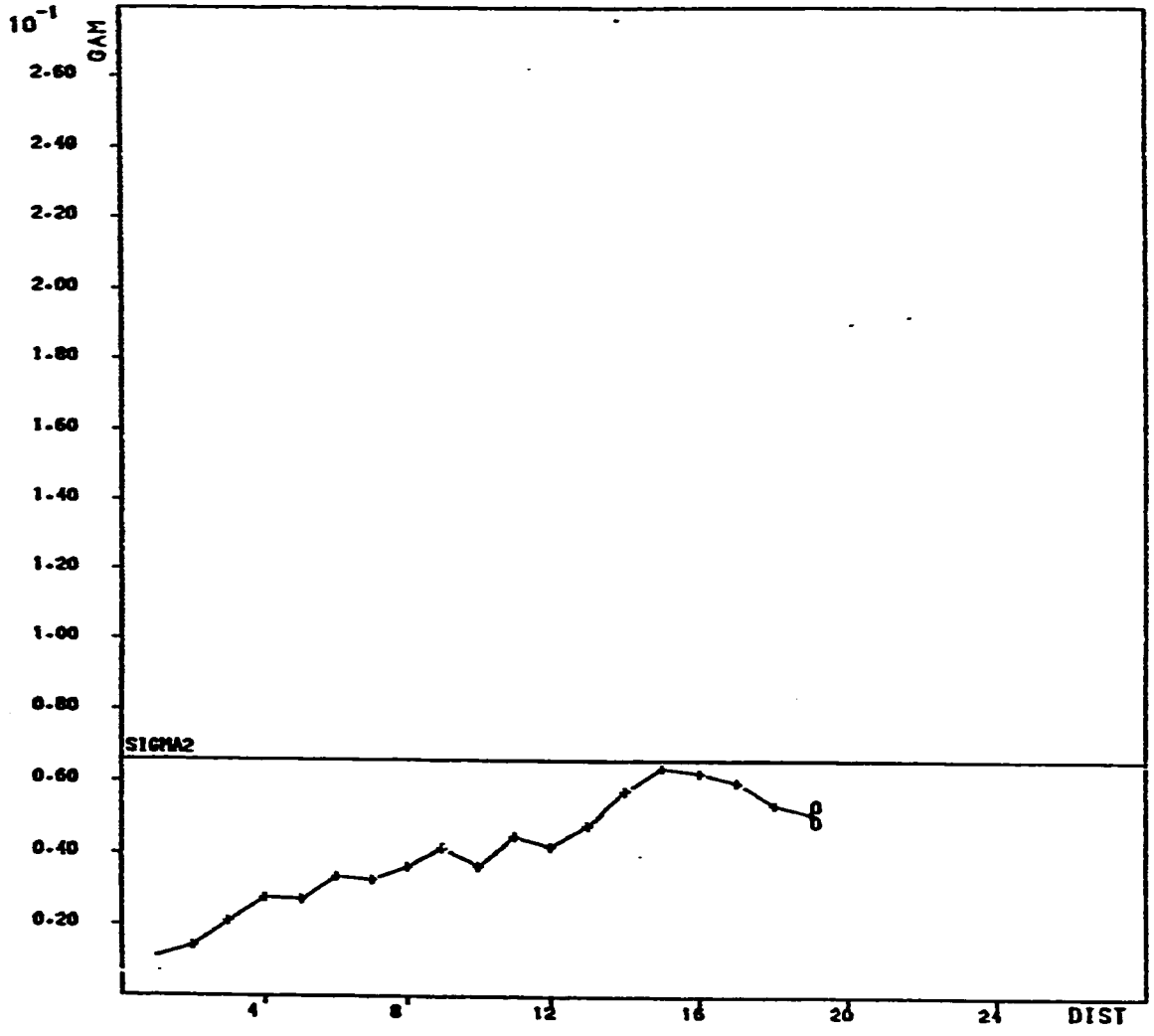

VARIABLE CAO

Fig. C.3- VERTICAL LOGARITHMIC SEMIVARIOGRAM FOR ZA-46

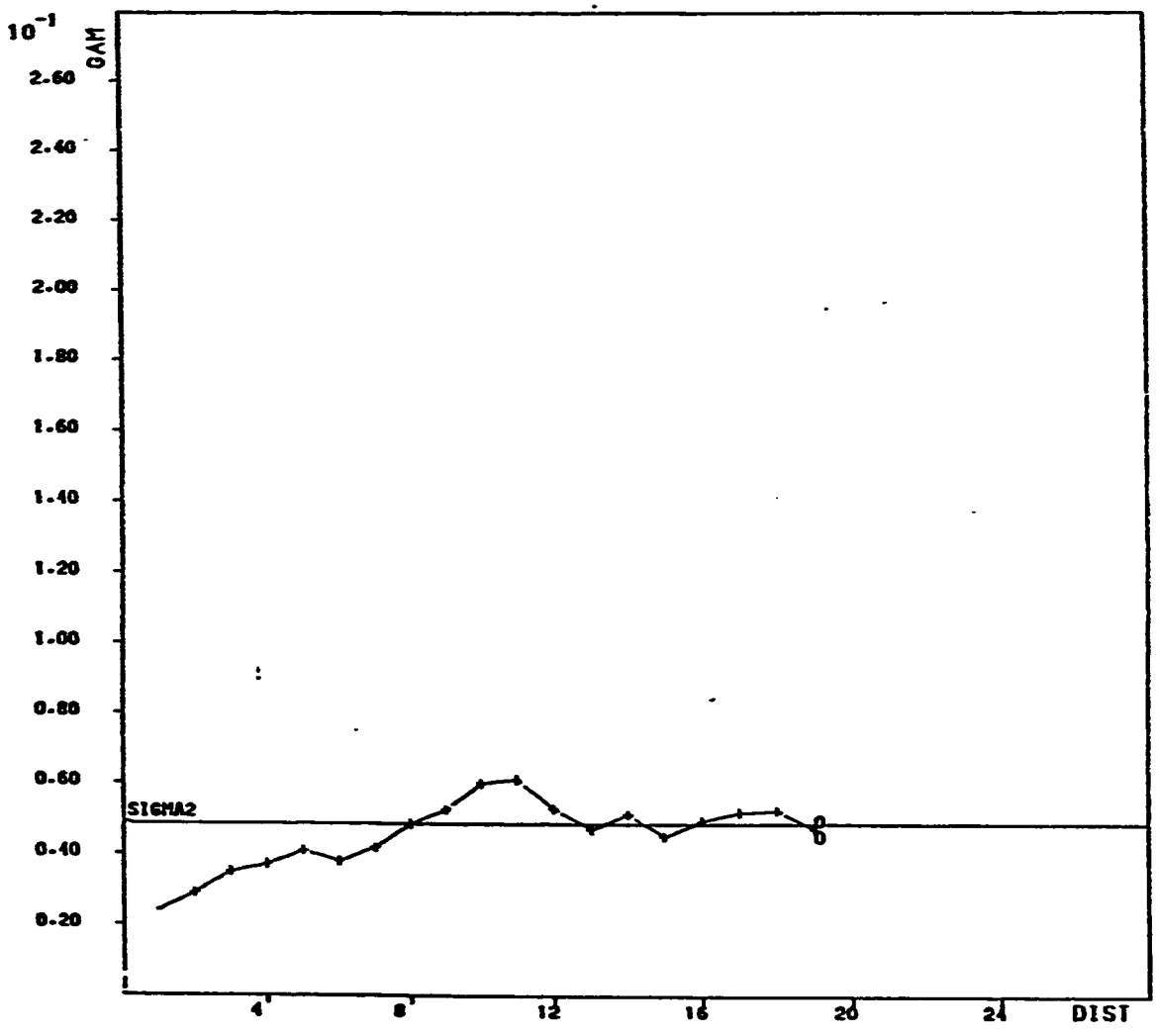

VARIABLE CAO

Fig. C.4– VERTICAL LOGARITHMIC SEMIVARIOGRAM FOR ZA-51

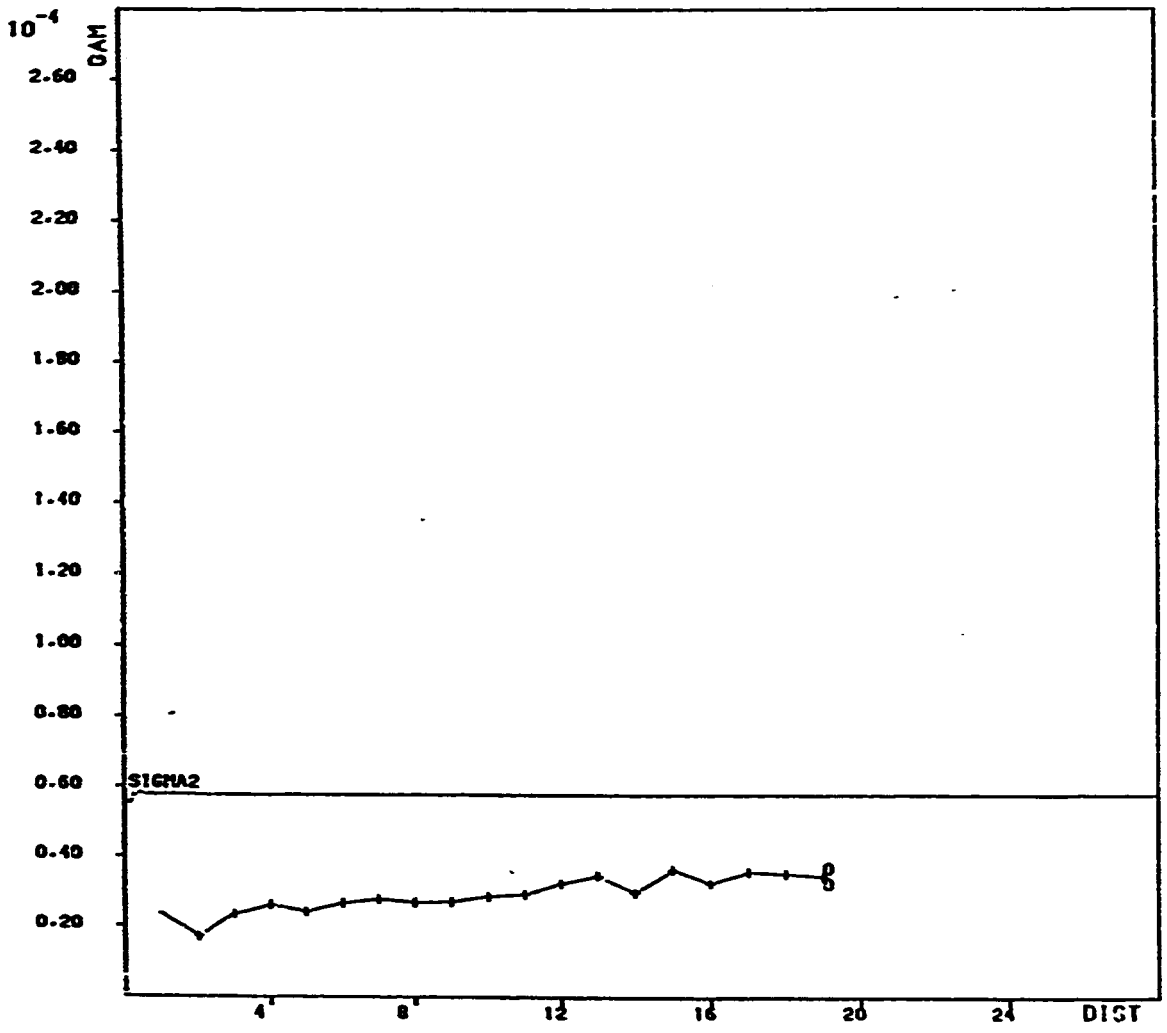

VARIABLE MCO

Fig. C.5- VERTICAL LOGARITHMIC SEMIVARIOGRAM FOR ZA-17

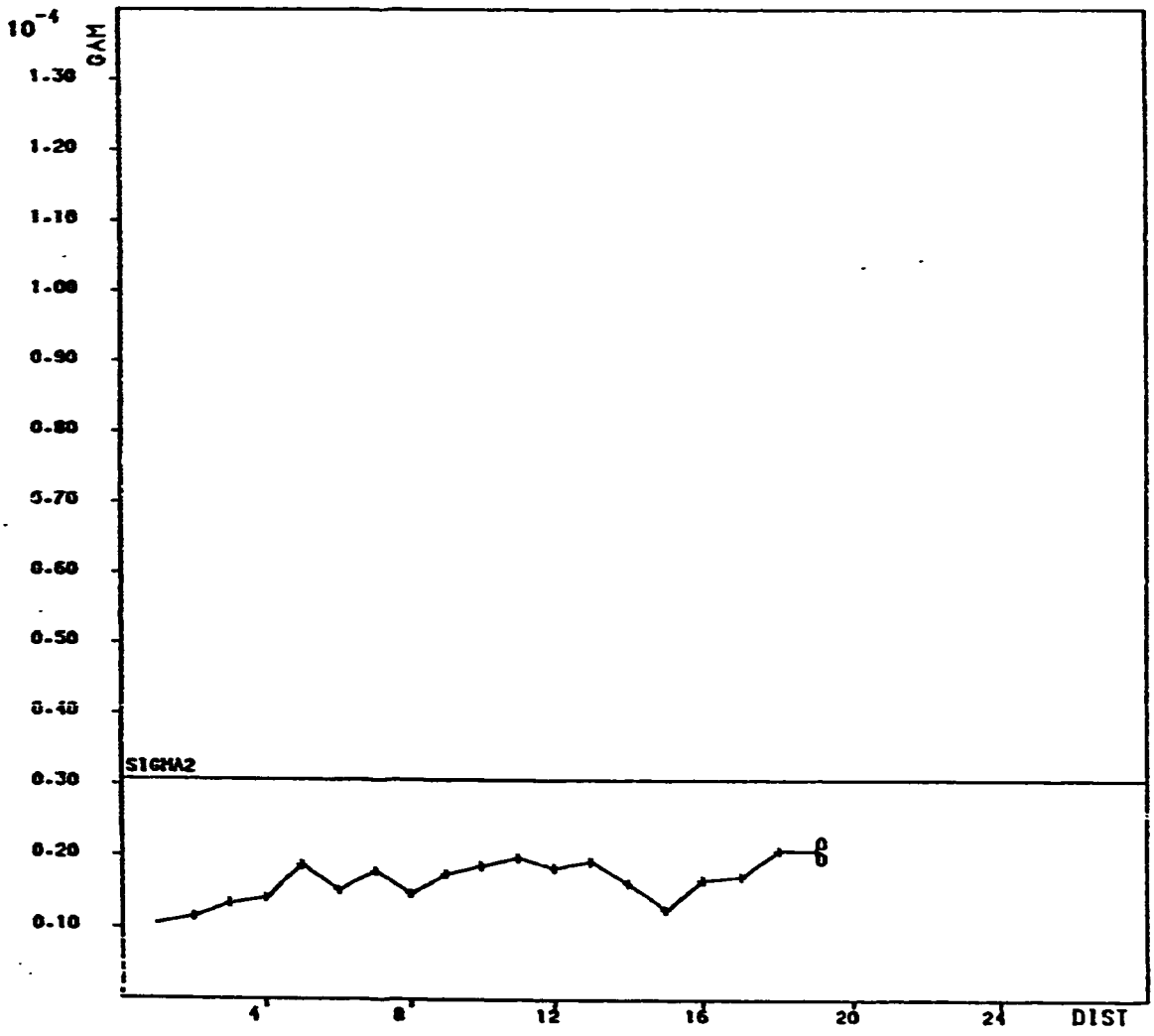

VARIABLE MGO

Fig. C.6- VERTICAL LOGARITHMIC SEMIVARIOGRAM FOR ZA-44

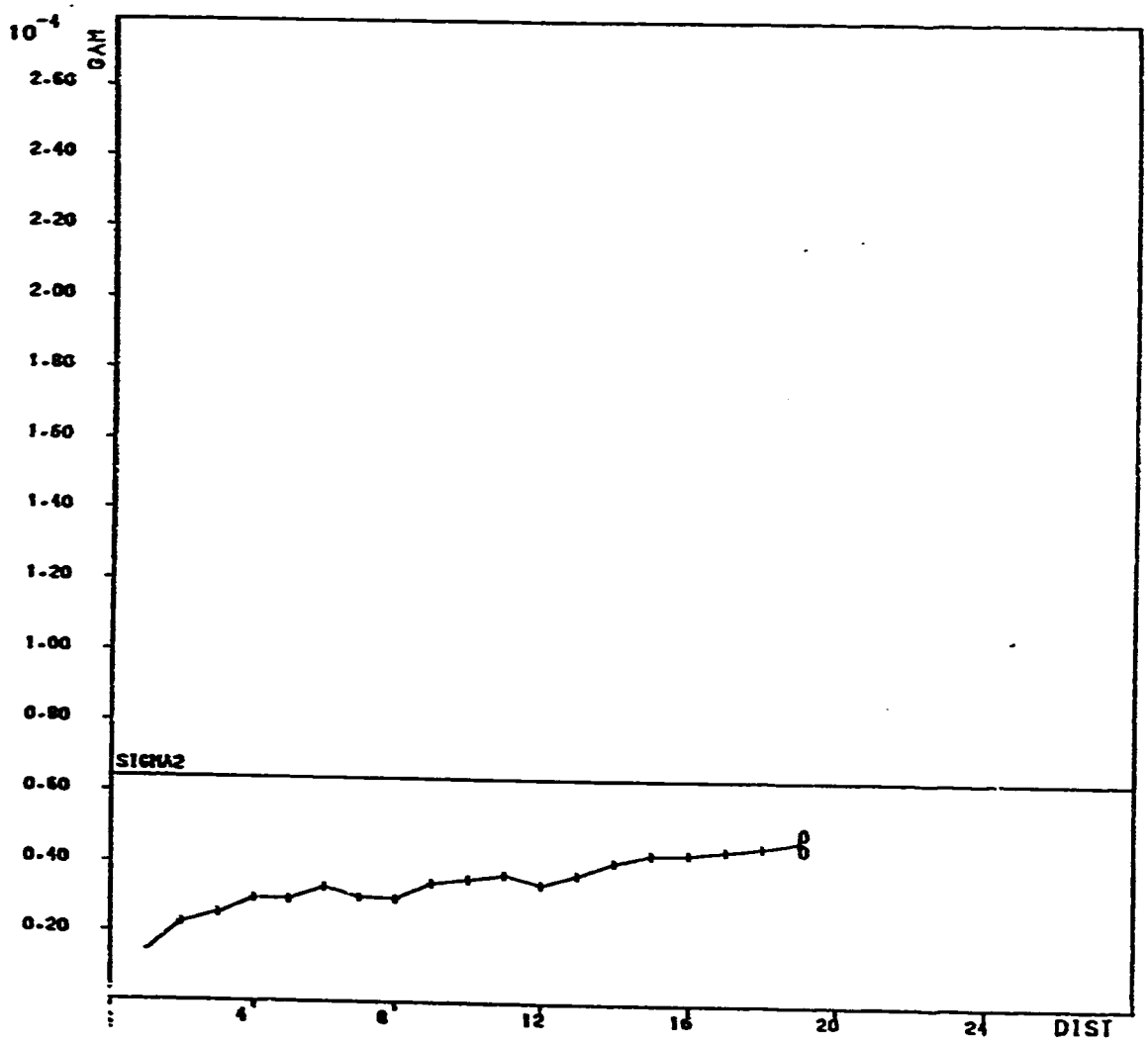

VARIABLE MGO

Fig. C.7- VERTICAL LOGARITHMIC SEMIVARIOGRAM FOR ZA-46

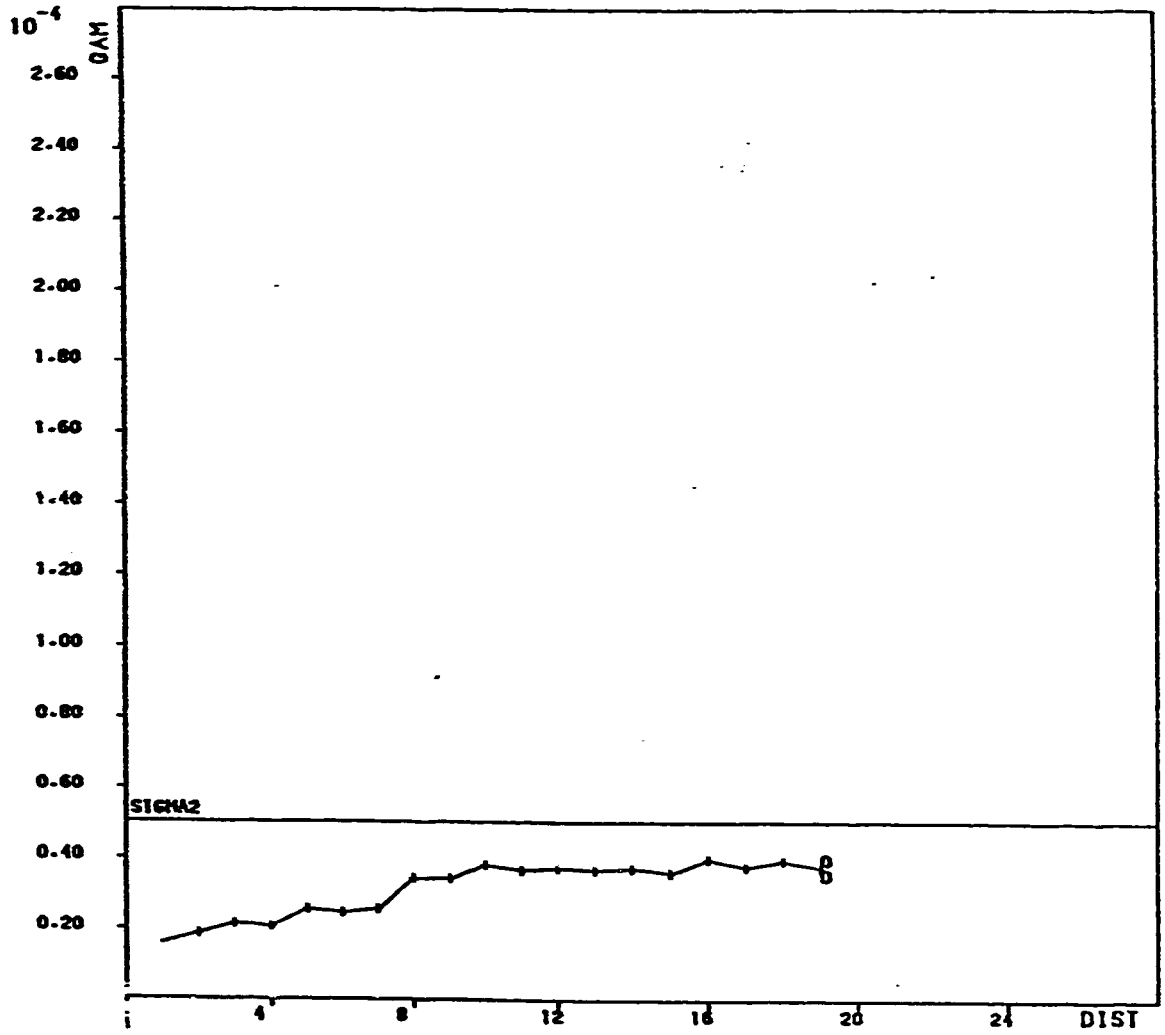

VARIABLE MGO

Fig. C.8– VERTICAL LOGARITHMIC SEMIVARIOGRAM FOR ZA-51

APPENDIX D

Directional logarithmic semivariograms for the four principle directions

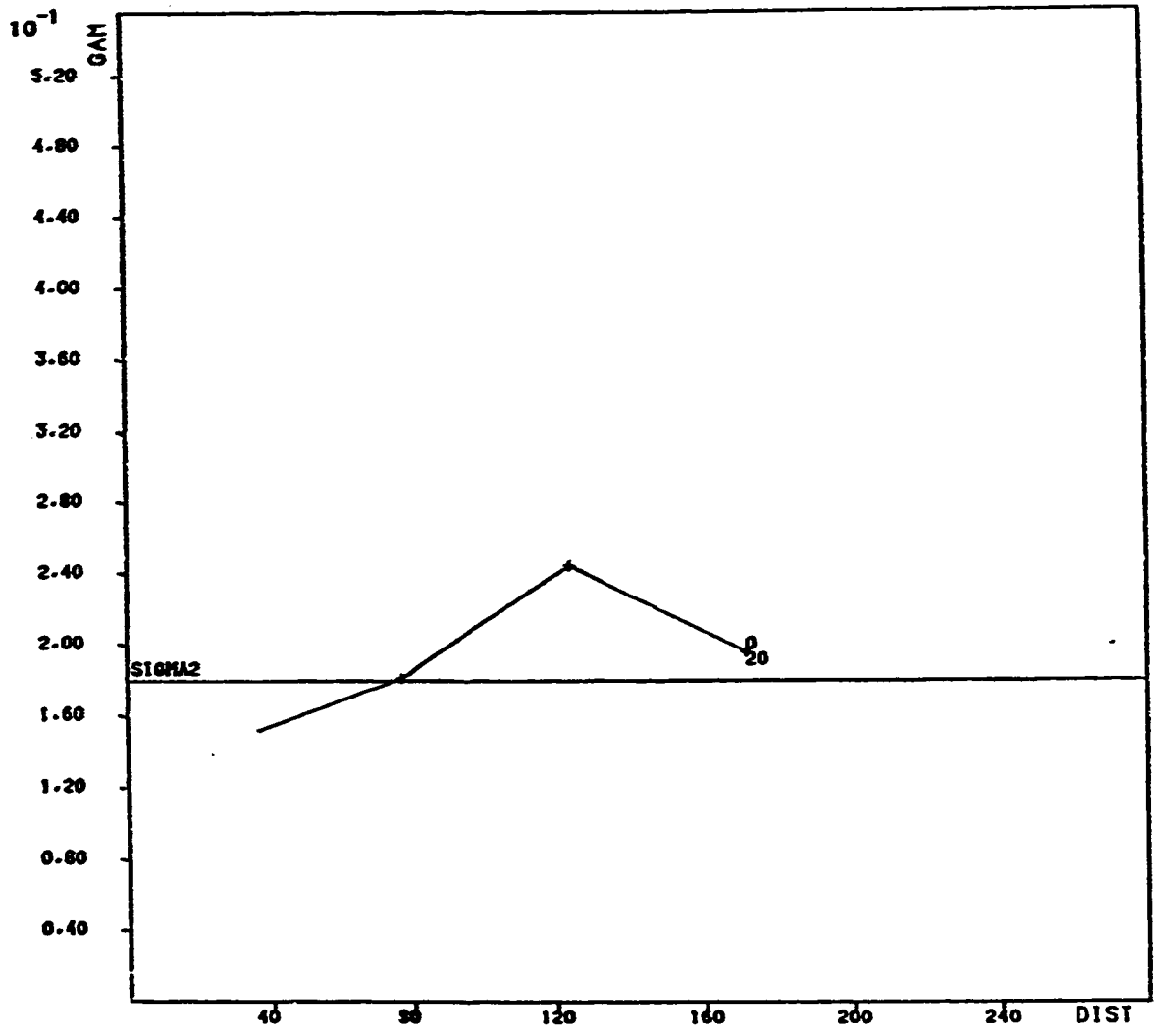

VARIABLE CAO ABSOLUTE VARIOGRAM

Fig. D.1- DIRECTIONAL LOGARITHMIC SEMIVARIOGRAM (E-W DIRECTION ••• VARIABLE:CAO%)

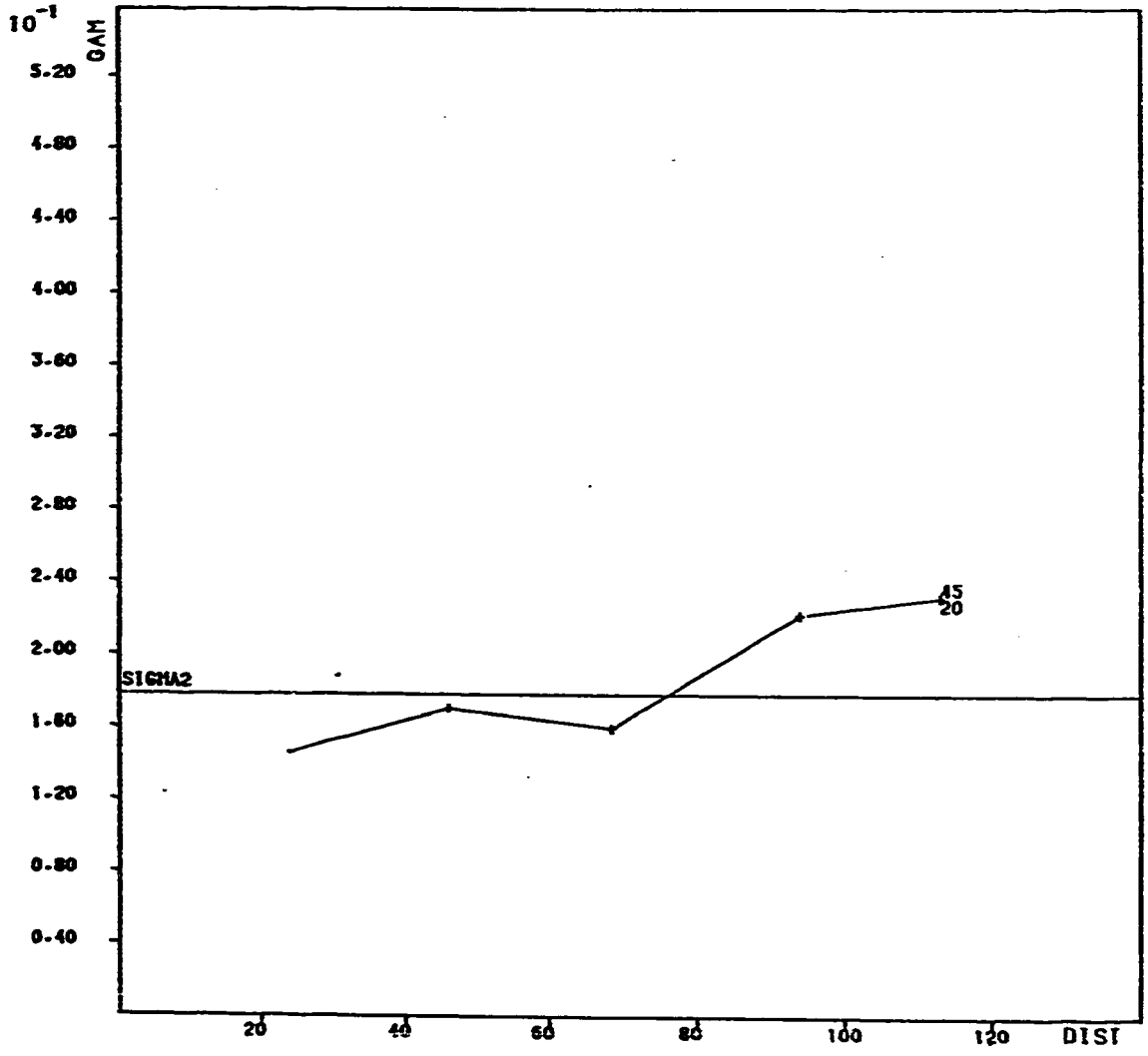

VARIABLE CAO ABSOLUTE VARIOGRAM

Fig. D.2 - DIRECTIONAL LOGARITHMIC SEMIVARIOGRAM (NE-SW DIRECTION••• VARIABLE:CAO%)

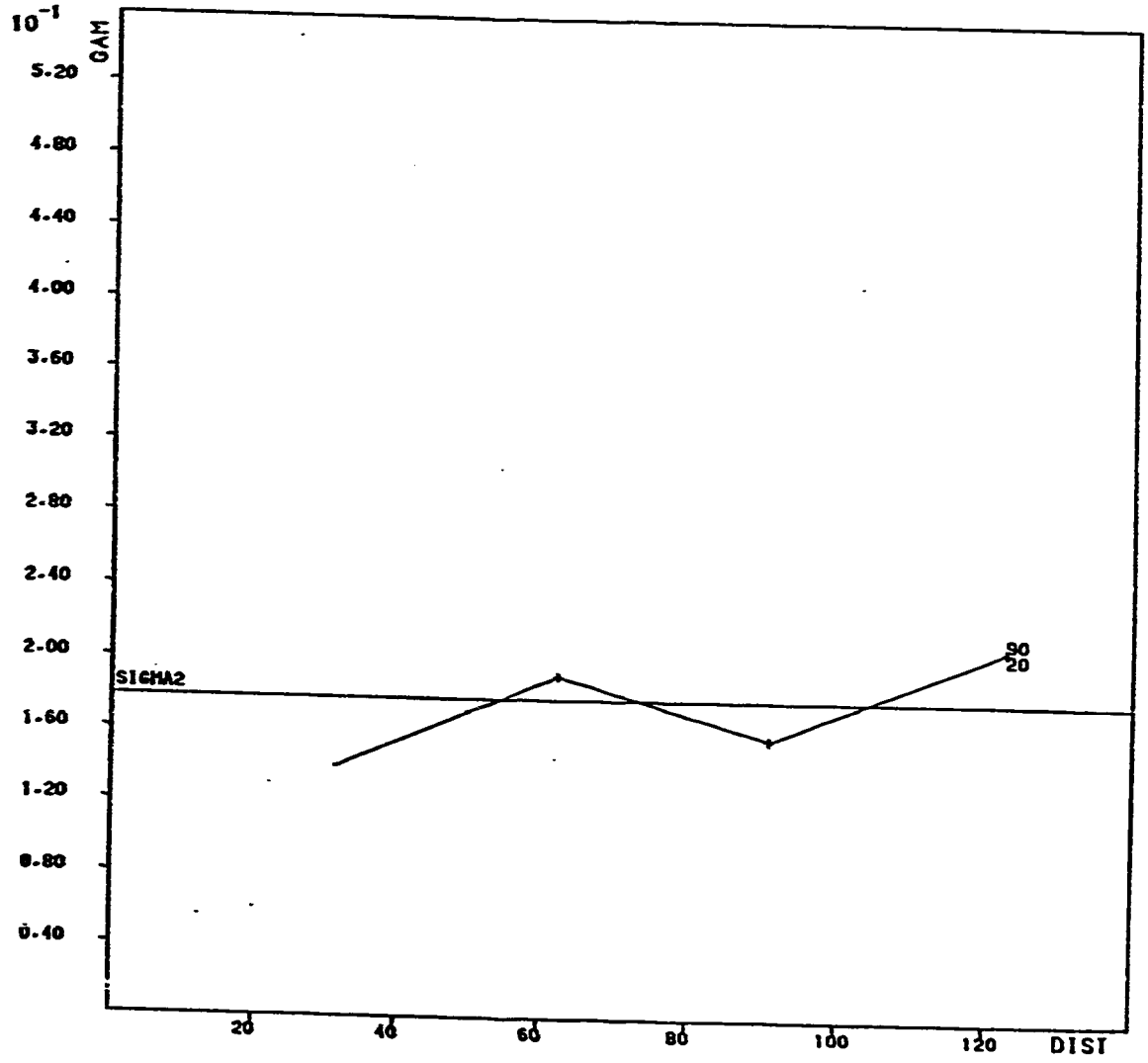

VARIABLE CAO ABSOLUTE VARIOGRAM

Fig. D.3- DIRECTIONAL LOGARITHMIC SEMIVARIOGRAM (N-S DIRECTION ••• VARIABLE:CAOX)

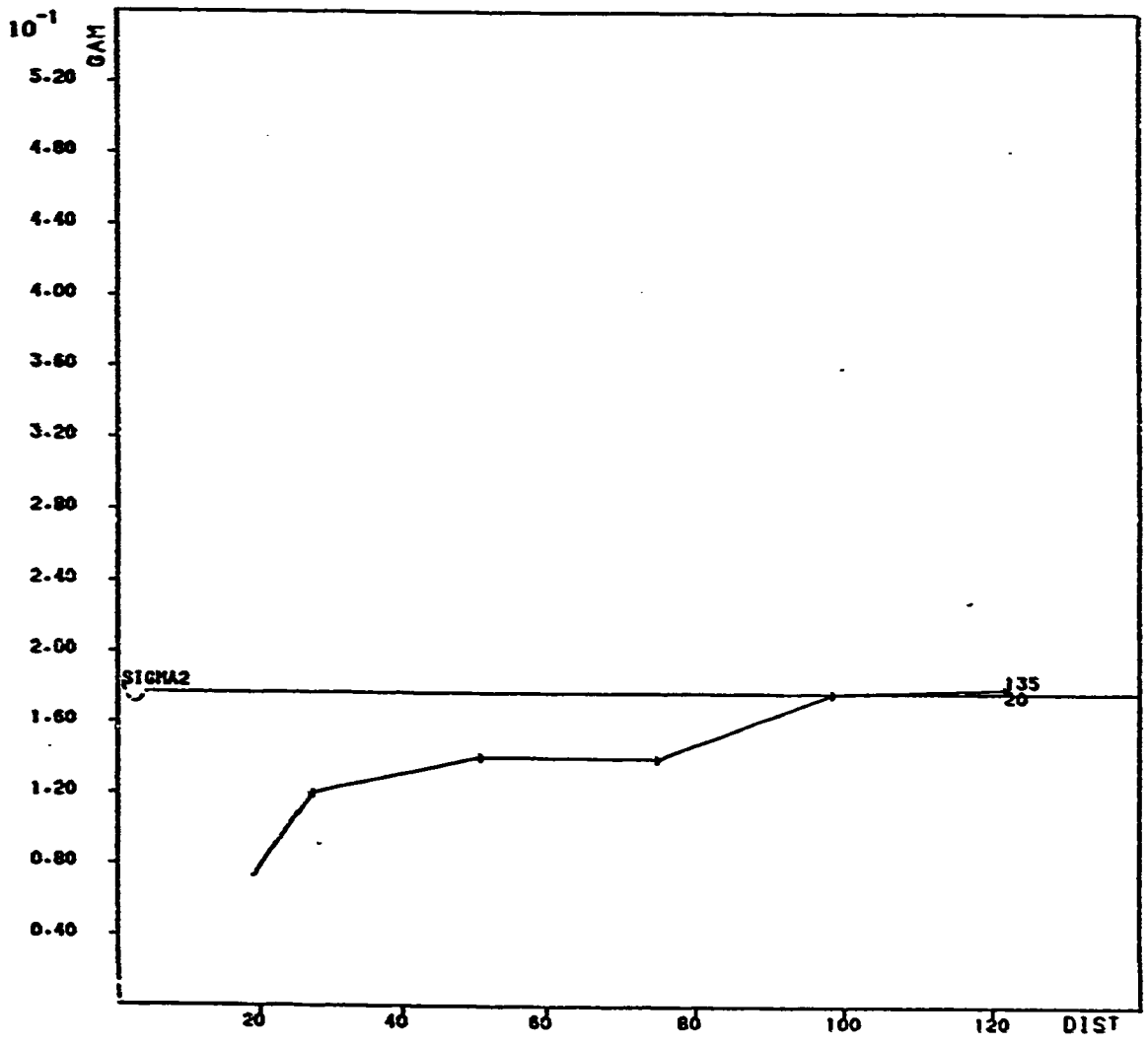

VARIABLE CAO ABSOLUTE VARIOGRAM

Fig. D.4-DIRECTIONAL LOGARITHMIC SEMIVARIOGRAM (NW-SE DIRECTION •• VARIABLE:CAO%)

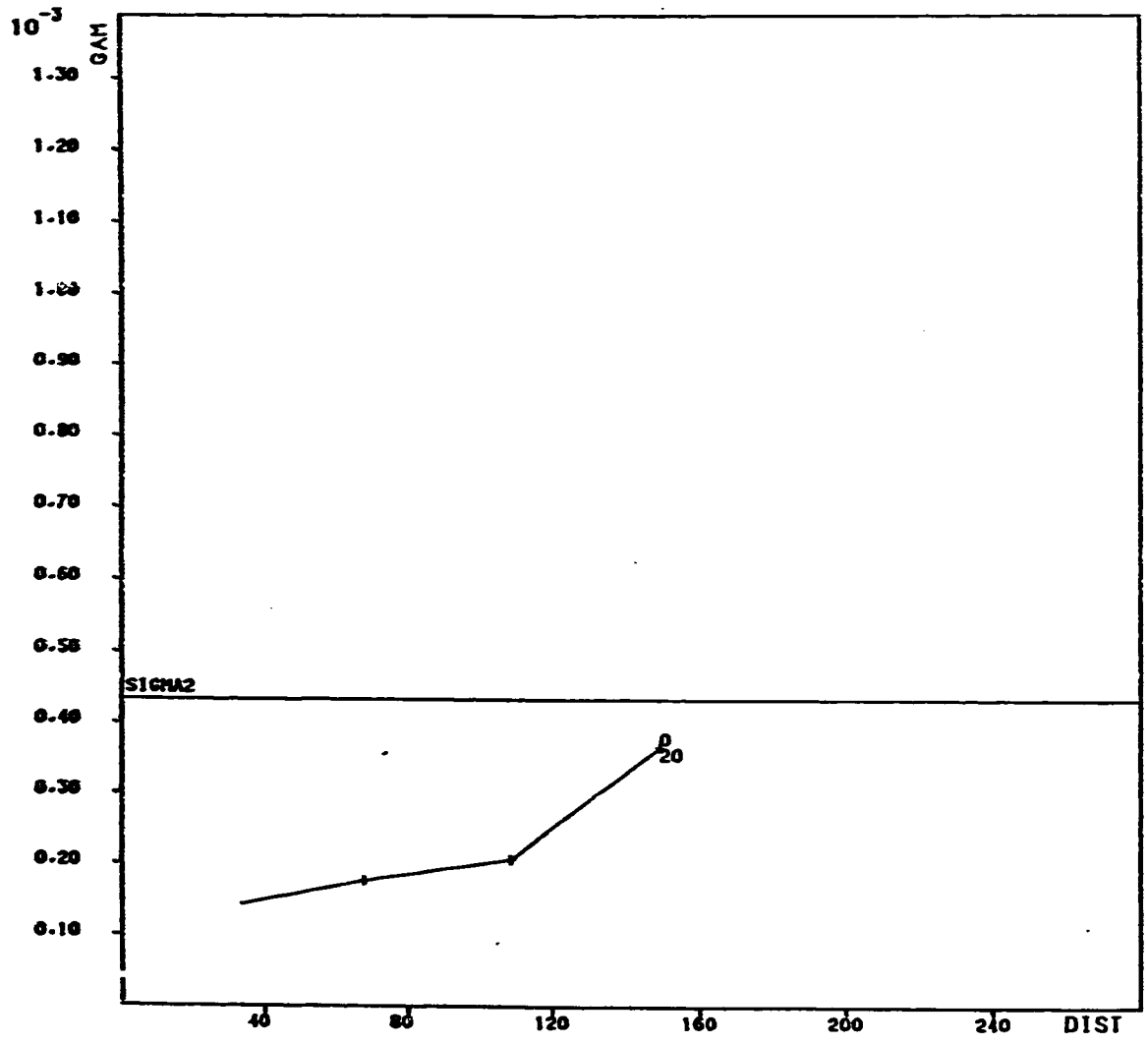

VARIABLE MGO ABSOLUTE VARIOGRAM

Fig. D.5- DIRECTIONAL LOGARITHMIC SEMIVARIOGRAM (E-W DIRECTION ••• VARIABLE:MGOX)

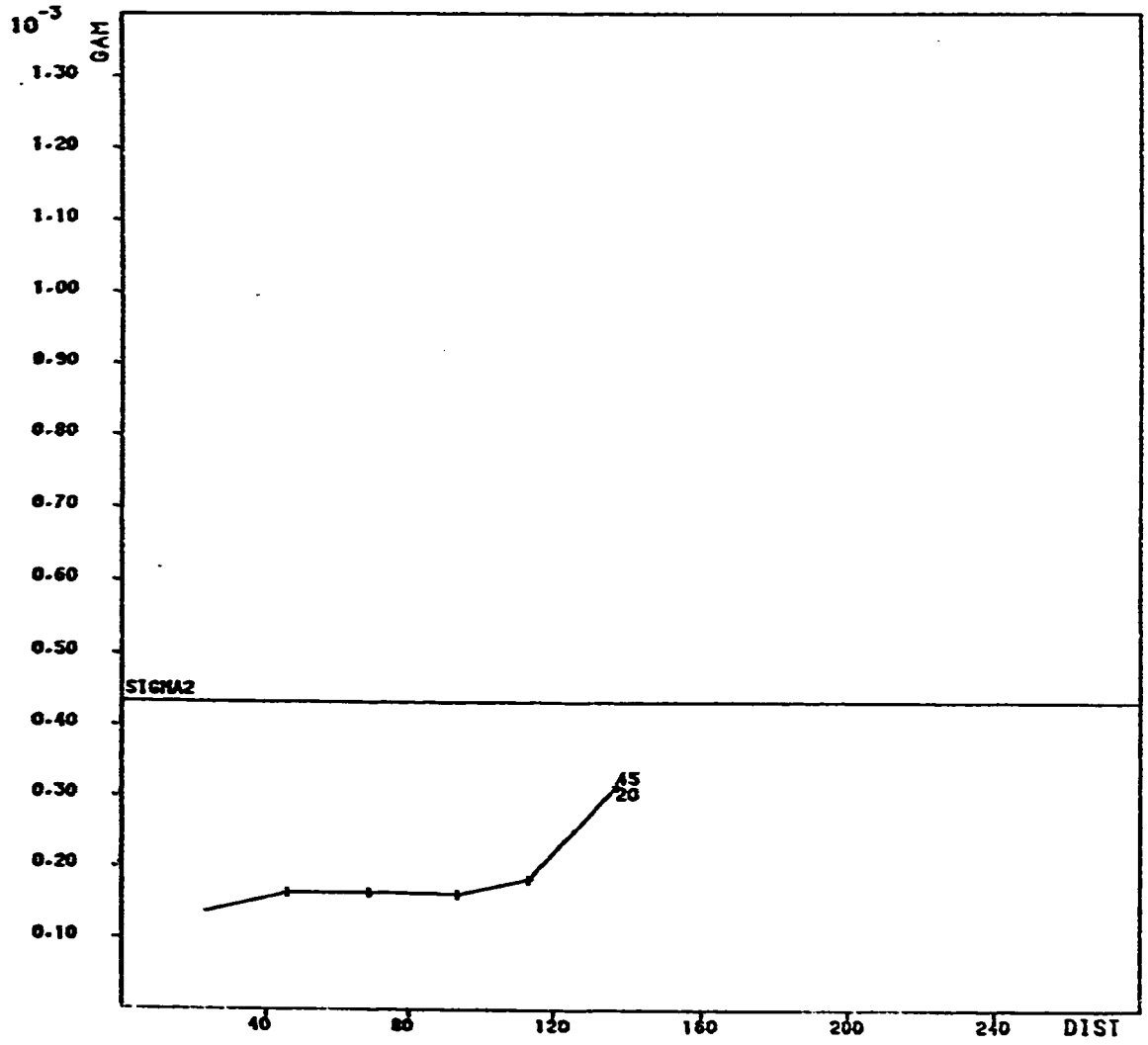

VARIABLE MGO ABSOLUTE VARIOGRAM

Fig. D.6- DIRECTIONAL LOGARITHMIC SEMIVARIOGRAM (NE-SW DIRECTION••• VARIABLE:MGO%)

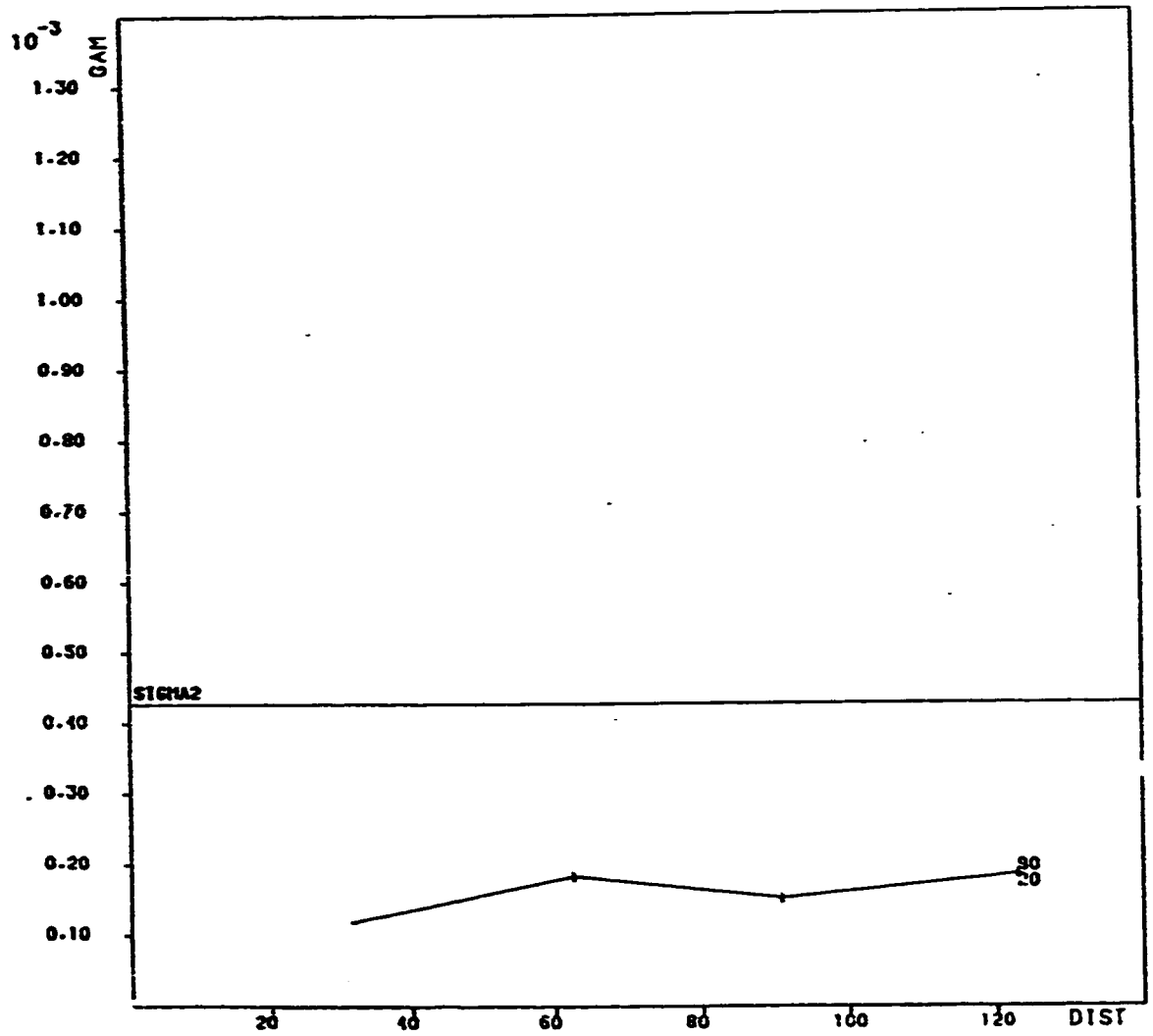

VARIABLE MGO ABSOLUTE VARIOGRAM

Fig: D.7- DIRECTIONAL LOGARITHMIC SEMIVARIOGRAM (N-S DIRECTION ••• VARIABLE:MGO%)

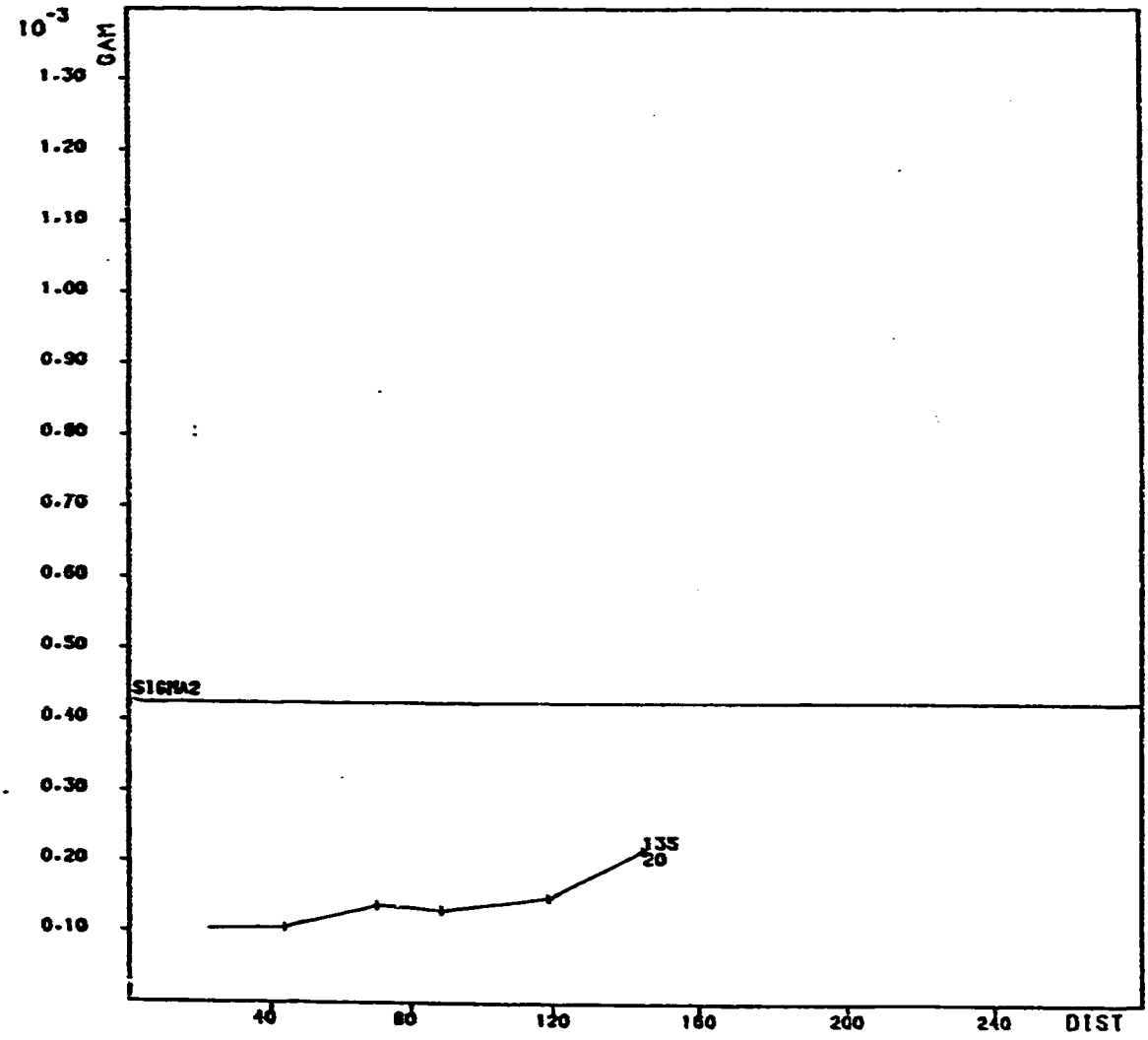

VARIABLE MGO ABSOLUTE VARIOGRAM

Fig. D.8 - DIRECTIONAL LOGARITHMIC SEMIVARIOGRAM (NW-SE DIRECTION••• VARIABLE•MGOZ)

APPENDIX E

Directional and average semivariograms for the 8 in-fill drill-holes

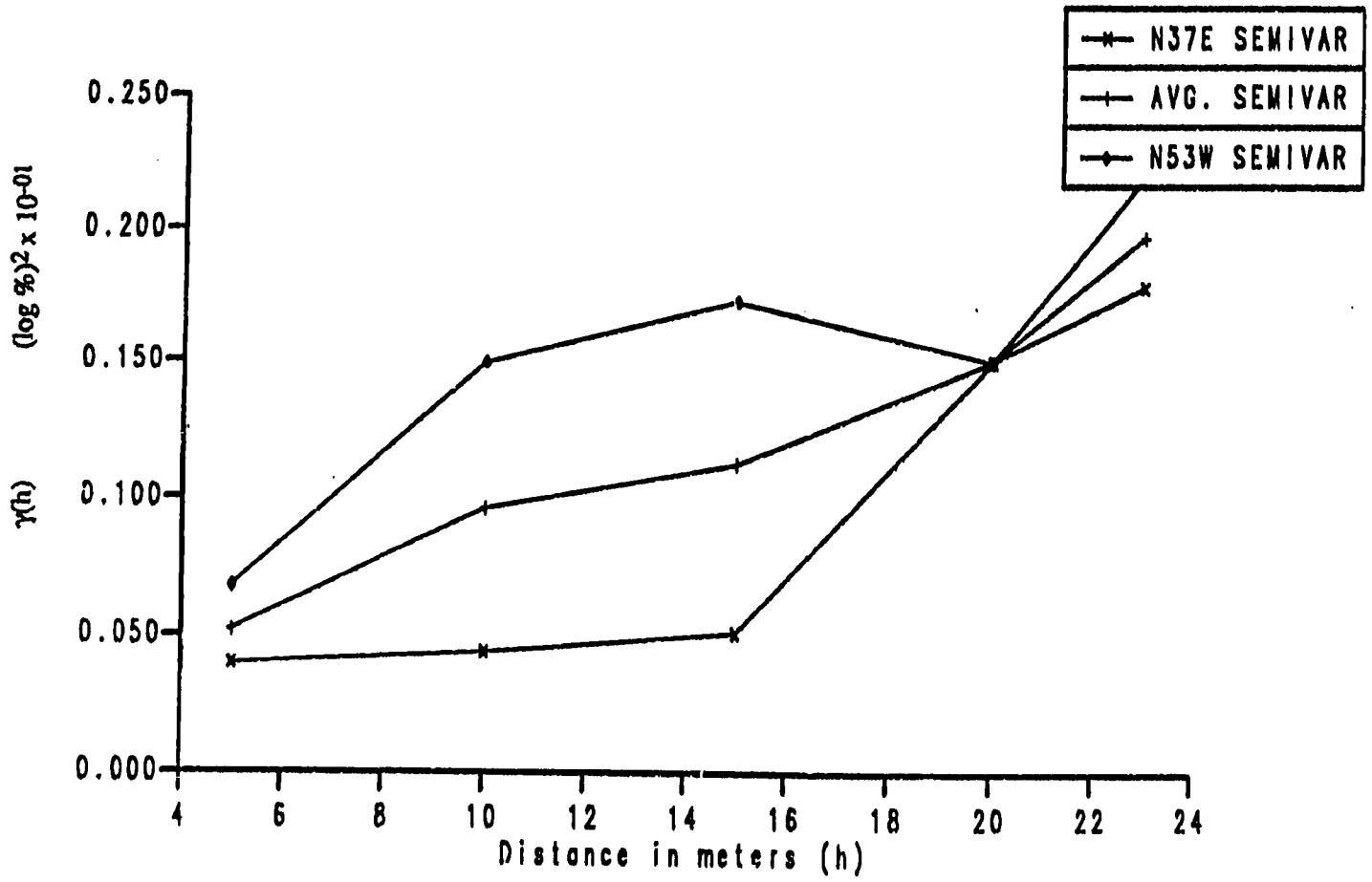

Fig. E.1- Directional and average logarithmic semivariograms for the 8 in-fill drill-holes (crude CuO%)

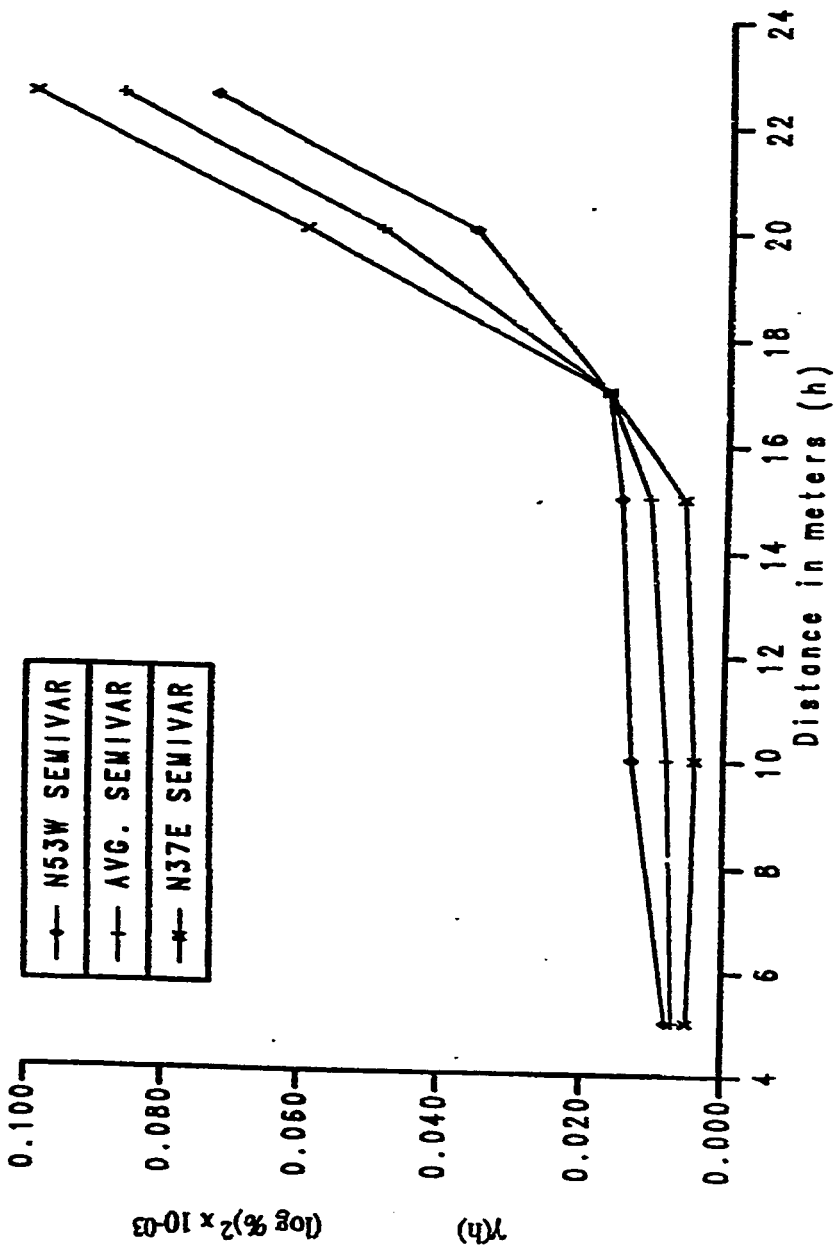

Fig. E.2- Directional and average logarithmic semivariograms for the 8 in-fill drill-holes (crude MgO%)

APPENDIX F

Testing horizontal model parameters

Block dimensions 25x25x1m

$\therefore$ L = 25m, H = 25m

(1) Verification of CaO horizontal model

Model parameters: $C_o = 0.026$

$C_1 = 0.088 \ \rho \ a_1 = 25m$

$C_2 = 0.054 \ \rho \ a_2 = 100m$

observed dispersion variance: $S^2 (O/D) = 0.177$

a) $\sigma^2(O/V) = C_o + C_1 [F(H/a_1, L/a_1)] + C_2 [F(H/a_2, L/a_2)]$
$= 0.026 + 0.088 [F(1,1)] + 0.054 [F(0.25, 0.25)]$

F - values can be read directly from Figure 5.8

$= 0.026 + 0.088 (0.66) + 0.054 (0.19)$
$= 0.09434$

b) $\sigma^2(V/D) = C_1 [1 - F(H/a_1, L/a_1)] + C_2 [1 - F(H/a_2, L/a_2)]$
$= 0.088 [1 - 0.66] + 0.054 [1 - 0.19]$
$= 0.07366$

c) $\sigma^2(O/D) = \sigma^2(O/V) + \sigma^2(V/D)$
$= 0.09434 + 0.07366 = 0.168$

(2) Verification of MgO horizontal model

Model parameters: $C_o = 0.03 \times 10^{-3}$

$C_1 = 0.065 \times 10^{-3} \ \rho \ a_1 = 25m$

$C_2 = 0.065 \times 10^{-3} \ \rho \ a_2 = 100m$

observed dispersion variance: $S^2 (O/D) = 0.166 \times 10^{-3}$

a) $\sigma^2(O/V) = 0.030 \times 10^{-3} + 0.065 \times 10^{-3} (0.66) + 0.065 \times 10^{-3} (0.19)$
$= 0.08525 \times 10^{-3}$

b) $\sigma^2(V/D) = 0.065 \times 10^{-3} (0.34) + 0.065 \times 10^{-3} (0.81)$
$= 0.07475 \times 10^{-3}$

c) $\sigma^2(O/D) = \sigma^2(O/V) + \sigma^2(V/D)$
$= 0.08525 \times 10^{-3} + 0.07475 \times 10^{-3}$